ASSESSMENT OF 21ST CENTURY CLIMATE CHANGE PROJECTIONS IN TROPICAL SOUTH AMERICA AND THE TROPICAL ANDES

A Thesis Presented

by

ROCIO B. URRUTIA

Submitted to the Graduate School of the
University of Massachusetts Amherst in partial fulfillment
of the requirements for the degree of

MASTER OF SCIENCE

September 2008

Graduate Program in Geography
Climate Change

ASSESSMENT OF 21ST CENTURY CLIMATE CHANGE PROJECTIONS IN
TROPICAL SOUTH AMERICA AND THE TROPICAL ANDES

A Thesis Presented

by

ROCIO B. URRUTIA

Approved as to style and content by:

_____

Mathias Vuille, Chair

_____

Raymond Bradley, Member

_____

Robert DeConto, Member

_____

Laurie Brown, Department Head
Geosciences

ACKNOWLEDGMENTS

for their precious help in everything, for their constant support, for being always worried about us and simply because they are amazing. Thanks to my roommate Mary too. She is a wonderful person and we have really enjoyed sharing the apartment with her.

Finally, special thanks to my loving husband, for his unconditional love and for sacrificing his career to come to the US to accompany me. Million thanks, Aldo, for always being there and for supporting me in the pursuing of my dreams. I will forever appreciate his invaluable love and support being far away from my beloved Chile, family and friends.

ABSTRACT

ASSESSMENT OF 21ST CENTURY CLIMATE CHANGE PROJECTIONS IN

TROPICAL SOUTH AMERICA AND THE TROPICAL ANDES

SEPTEMBER 2008

ROCIO B. URRUTIA, B.S., PONTIFICIA UNIVERSIDAD CATOLICA DE

CHILE

M.S., UNIVERSITY OF MASSACHUSETTS AMHERST

Directed by: Professor Mathias Vuille

The tropical Andes are one of the regions where climate change has been most evident. This is consistent with the notion that tropical high-elevation mountains will be more affected by warming. One of the main impacts of this warming is the retreat of glaciers; a process that may affect the availability of water for human consumption, irrigation and power production.

This study presents results related to the most important changes in climate that might be expected in tropical South America, but especially in the tropical Andes, at the end of the 21st century. Results are provided by the comparison of two Regional Climate Model simulations based on the Hadley Center Regional Climate Modeling System, PRECIS. A medium-high CO_2 emission scenario simulation for the period 2071-2100 (A2) is compared to a base-line mean climate state simulation for the 1961-1990 period.

In addition, some results using a low-medium CO_2 emission scenario (B2) are also presented for comparison.

Results show a clear warming trend over South America reaching up to 8º C in northeastern South America. In this same place the largest decrease in precipitation and cloud cover are found. Along the Andes warming reaches up to 7º C in Cordillera Blanca in the A2 scenario and precipitation presents a mixed pattern of increases and decreases across the Cordillera. Warming is expected to be larger at higher elevations and significant changes in temperature variability are expected along both slopes of the Andes based on the A2 scenario. In addition both scenarios (B2 and A2) show an amplification of free tropospheric warming at higher altitudes. Finally, pressure-longitude cross-sections of zonal winds and vertical velocities at the latitudes of the Altiplano and the Cordillera Blanca show weakened mid- and upper tropospheric easterlies and strengthened westerlies in the A2 scenario. This change in the atmospheric circulation is conducive to a decrease in precipitation in those areas, and consequently may negatively impact glacier mass balance.

In summary the obtained results reveal that anthropogenic climate change, as predicted with the A2 scenario, may constitute a serious threat to the survival of many tropical glaciers along the Andes Cordillera.

TABLE OF CONTENTS

LIST OF TABLES

LIST OF FIGURES

CHAPTER 1

INTRODUCTION

1.1. Climate change

During the last few years climate change has become a growing worldwide environmental concern. One of the most remarkable characteristics of climate change is the increase in temperature, so it has been mainly recognized as 'global warming'. This warming has been attributed to the enhanced greenhouse effect produced, among others, by the increased amounts of carbon dioxide from the burning of fossil fuel since the Industrial Revolution (Houghton, 2004).

According to the IPCC, "climate change refers to a statistically significant variation in either the mean state of the climate or in its variability, persisting for an extended period (typically decades or longer). Climate change may be due to natural internal processes or external forcings, or to persistent anthropogenic changes in the composition of the atmosphere or in land use" (IPCC, 2001). Thus, this definition includes both an anthropogenic and a natural component.

Another definition comes from the United Nations Framework Convention on Climate Change (UNFCCC) that defines it as: "a change of climate which is attributed directly or indirectly to human activity that alters the composition of the global atmosphere and which is in addition to natural climate variability observed over comparable time periods". Thus, this definition attributes climate change only to human activities, and not to natural causes (IPCC, 2001).

Global warming is already having noticeable consequences, and will likely lead to more devastating ones. Some of the impacts of this phenomenon on the environment and

human beings are changes in the distribution, migration and even extinction of animals and plants, the spread of diseases to new areas, and melting of glaciers and ice caps (Parry et al., 2007), with consequences for sea level rise and water availability. These impacts on ecosystems are obviously different and more or less severe depending on the region of the world. Effects, for example, could be more devastating in tropical regions, where more than 50% of the earth's surface is located (between 30º N and 30ºS) and 75% of the world population lives (Thompson, 2000). In this study the area of interest corresponds to tropical South America between 10º N and 27º S, and especially the Andes Cordillera where many tropical glaciers are located.

In this region numerous articles have pointed out the occurrence of an impressive and accelerated retreat of glaciers (Francou et al., 2000, Francou et al., 2003, Francou et al., 2004, Ramirez et al., 2001, Vuille et al., 2003, among others). The following section mainly describes some of these observed changes, the effects of different climatic conditions on these glaciers, and the main variables that are influencing their behavior according to different studies developed in that area.

1.2. Climate and tropical glaciers in South America

One of the regions where climate change has been most evident is the tropical Andes. This is consistent with the notion that high-elevation tropical mountains, extending to the mid-troposphere, will be more affected by warming, (Bradley et al., 2004, Bradley et al., 2006). One of the main impacts of this warming in the Andes is the retreat of glaciers, a process that can have profound consequences affecting the availability of water for human consumption, irrigation, mining and power generation (Vuille et al., 2008a).

According to Vergara et al., (2007) changes in hydrological conditions could affect water costs in cities such as La Paz in Bolivia and Quito in Ecuador, where glaciers provide a significant portion of the drinking water and affect the ability of these cities to maintain their economies. In addition, hydropower plants in Andean regions would see a reduction in their production if glaciers continue their retreat, with the consequent rationing and replacement costs. Finally, and beyond economic impacts, social and cultural life of Aymara and Quechua cultures, which view glaciers as important religious icons, could be affected.

In general, there is not much understanding about how climate change will affect this region and its glaciers, and today most of the future projections of glacier behavior are based on linear extrapolations of their actual retreat (Vuille et al., 2008a).

Tropical glaciers are present in three continents, America, Africa and Asia (Irian Jaya), but 99% are concentrated in the Andes with 70% in Peru, 20% in Bolivia and 10% in Ecuador, Colombia and Venezuela. These glaciers are very sensitive to climate variations, because of the absence of a season without ablation and because of their small size, which means that they react very rapidly to climate fluctuations (Francou et al., 2000). For this reason they are high elevation indicators for the early detection of climate change in regions where instrumental measurements are generally absent (Ramirez et al., 2001).

On tropical glaciers in general, seasonal mass balance variability is mainly dominated by seasonal precipitation rather than temperature, due to the absence of any major thermal seasonality. In these areas ablation occurs throughout the year and

accumulation is restricted to periods of precipitation and to the high parts of the glaciers (Kaser and Georges, 1999).

When discussing tropical glaciers it is important to differentiate between inner and outer tropics (approximately around 8 º S). In the inner tropics precipitation occurs more or less continuously during the year, and stable humidity conditions cause accumulation and ablation to occur at the same time throughout the year. In the outer tropics however, there is one wet and one dry season, and there is a marked seasonality of specific humidity, precipitation and cloudiness. The outer tropics are proposed as an intermediate area with tropical and subtropical conditions in the humid and dry season, respectively. During the dry season (April-September) there is no accumulation, and ablation is reduced due to the low melting rate (Kaser and Georges, 1999, Favier et al., 2004).

Glaciers in the tropical Andes have retreated significantly in the last decades, particularly since the late 1970's (Francou et al., 2004). The tropical glacier Chacaltaya (16º S) close to La Paz, Bolivia (0.06 Km^2 in 2000), lost 62% of its mass from 1940 to 1983 and in 1998 it was reduced to 7% of the 1940s ice volume (Francou et al., 2000). The balance was generally negative between 1991 and 1998, with an average loss of water as high as 1400 mm/year (Francou et al., 2000). The ice thickness was reduced to less than 15 m at the beginning of this century, and its complete disappearance has been predicted within a decade (Francou et al., 2003). The retreat of small glaciers, like Chacaltaya, is accelerated when they reach a certain size, below which edge effects such as the advection of warm air above the glacier acquire importance (Vuille et al., 2008a). Similarly the glacier Antizana 15, located in Ecuador (0º 28'S), experienced a negative

balance of about 600-700 mm/year in the last decade of the 20th century (Francou et al., 2000). Since glacier recession has been a coherent pattern along the tropical Andes, it is possible to assume that a large-scale climatic forcing is influencing their behavior (Vuille et al., 2003).

Although glacier melting increases runoff, the disappearance of glaciers will provoke important and unexpected changes in streamflow, mainly because of the absence of a glacial buffer in the dry season (Bradley et al., 2006). In the past decade, nearly half of the water discharge from Chacaltaya glacier was supplied by its shrinkage rather than by precipitation. The disappearance of the glacier will provoke a significant decrease of 30% in the total runoff for this basin. Retreat of glaciers modifies not only the runoff volume, but also the hydrologic regime, because of the regulating effect of glaciers compared with basins with completely pluvial runoff (Ramirez et al., 2001).

The reasons for the accelerated retreat in this area are not fully understood, but recent studies have indicated that primary causes for the glacier retreat can be the increase in near-surface temperature and humidity (Vuille and Bradley, 2000; Vuille et al., 2003). Other mentioned causes for this retreat, at least in the Bolivian Andes, are an increase in humidity, and decreased precipitation and cloudiness (Wagnon et al., 2001).

Cloud cover and precipitation are important since they influence the net short- and longwave radiation (cloud cover), and the absorption of incoming solar radiation through changes in albedo (precipitation). Despite their importance, changes in the amount of precipitation and cloud cover in the second half of the 20th century were found to be minor in most regions and it is thus unlikely that these elements have influenced retreat (Vuille et al., 2003). Another important element that may have a certain influence on a

negative glacier mass balance is an increased humidity content near the surface that increases melting and reduces sublimation, leading to higher ablation rates (Wagnon et al., 1999, Kaser, 1999). This melting process caused by an increase in relative humidity close to the surface is only important in the ablation zone and only when temperatures are at or above freezing. However on a large-scale, snowfall accumulation is associated with an increase of relative humidity in the troposphere (Vuille et al., 2008b).

In relation to the humidity content, it is important to note that variations in air humidity have different consequences in humid and dry areas. In the dry season of the outer-tropics, an increase of air humidity might reduce sublimation and increase the long-wave radiation contributing to mass loss. On the contrary, in a humid area, a negative mass balance might be produced by a decrease in air humidity and the related effects of increased insolation and decreased precipitation (Wagnon, 1999). According to Kaser, (2006) increased atmospheric water vapor will lead to enhanced accumulation only if it is associated with a significant increase in precipitation. Otherwise increased air humidity can produce a net mass loss, in particular in very dry areas where sublimation is relevant. In general, increased humidity is more beneficial for glacier mass balance in the humid inner tropics.

In addition, warming in the tropical troposphere has also been related to a negative glacier mass balance due to an increase in glacier melt (Thompson, 2000) and to the presence of rainfall rather than snow contributing to a lower albedo especially in the inner tropics (Francou et al., 2004). According to the study by Francou et al., (2003) cloud cover, albedo that controls the net short-wave radiation, humidity, and precipitation are all involved in the seasonality of the annual mass balance observed on Chacaltaya

glacier. In the annual mass balance, precipitation appears as one of the most important variables, mainly because it influences albedo, which is a key factor of the energy balance (Francou et al., 2003).

Tropical Andean glaciers are sensitive to variations in tropical Pacific sea surface temperature (SST). It has been observed that tropical Andean glaciers are closely related to the climate of the tropical Pacific and that they react to SST changes with a very short time-lag. The SST signal in the tropical Pacific shows a thermal and hydrological response in the tropical Andes. Cold and wet events such as La Niña, act in favor of glacier mass balance and warm and dry events such as El Niño cause glaciers to retreat (Vuille et al., 2003). This response has been reported for the Antizana glacier in Ecuador, where the glacier has reacted very quickly with positive or negative changes in mass balance. Highest ablation rates were registered during El Niño events of 1995, 1997/1998 and 2001/2002 and a positive balance was observed from mid-1998 until mid-2000 coincident with La Niña 1998-2000 (Francou et al., 2004). According to this study, in general El Niño periods are characterized by higher melting rates, produced by rainfall rather than snow due to higher temperatures, and by the deficit in precipitation. Both factors contribute to a lower albedo. In addition, a significant reduction in cloudiness in El Niño periods has an influence on the amount of incoming shortwave radiation, especially during the equinoxes. On the other hand, La Niña events are characterized by cold temperatures, high snowfall amounts and to a lesser degree constant winds and high humidity in the troposphere. These elements increase albedo and sublimation, thereby decreasing the amount of melting during La Niña years (Francou et al., 2004).

To understand more about the total setting in which the Andes are immersed, the next section presents a description of the climate in tropical South America.

1.3. Climate in tropical South America

Atmospheric phenomena in South America are strongly influenced by topography and vegetation patterns over the continent. The Andes Cordillera constitutes a strong barrier for tropospheric flow, and acts as a wall with dry climate conditions to the west and wet conditions to the east in the tropics/subtropics. It also promotes tropical-extratropical interactions especially to the east (Garreaud and Aceituno, 2007). On the other hand, the large area of landmass at low latitudes (10º N-20ºS), that leads to an intense convective activity, allows the development of the world's largest rain forest in the Amazon basin (Garreaud and Aceituno, 2007).

According to McGregor and Nieuwolt (1998), the Andes Cordillera divides tropical South America in three climatic regions: a narrow coastal area to the west of the Andes, the Andes highlands, and the area to the east of the Andes.

In the narrow area of the coast two main features determine the climate, one is the Humboldt-Peru ocean current, that provides cool water up to the equator, and the other is the Andes cordillera that leaves only a narrow portion of lowlands on the coast. Both features play a role maintaining the ITCZ out of this area, as far as north as latitudes between 3º and 8º N throughout the year. Because of that, a permanent wet area can be found between about 8º N and the equator, an intermediate region with some rainy months between the equator and 2º S, and finally an entirely dry area to the south (McGregor and Nieuwolt,1998).

In the wet area precipitation can annually reach 5000 mm, and the dry season is mainly concentrated around December-January and July-August in the northern and southern part of the region, respectively. Temperatures in this region remain without large variations throughout the year (McGregor and Nieuwolt,1998).

In the transition zone located around the gulf of Guayaquil, the dry season develops from July and can continue up to December. Its main causes are the strong high pressure cell over the ocean at that latitude and the somewhat cool ocean waters. Such long dry seasons are a feature characteristic of areas just along the coast, because the interior western slopes of the Andes receive rainfall throughout the year due to orographic lifting. An exception to these long dry seasons is produced in El Niño years when the ITCZ moves southward as far as 5-7º S (McGregor and Nieuwolt,1998).

The southern part corresponds to a coastal desert zone, that is one of the driest areas in the world because of the strong subtropical high pressure cell and the deflection of the south-south-east winds by the Andes cordillera (McGregor and Nieuwolt,1998).

In the Andes highlands, elevation and exposure mainly control climate conditions. In most of the Andes, precipitation increases with altitude, but only up to approximately 1200-1500 m.a.s.l. Above that it decreases slowly because remnants of the subtropical trade wind inversion reduce the capacity of clouds to produce rain above this altitude. In relation to the exposure, easterly winds are dominant in the region. Thus, eastern slopes receive more precipitation than western ones. This factor also influences the altitude of the snowline, which is lower on the east-facing slopes. Another important factor is the exposure to the sun at high altitudes. As the west-facing slopes receive more sun during

the afternoon, these are generally warmer than other areas at the same altitude (McGregor and Nieuwolt,1998).

The area to the east of the Andes is generally flat with a depression in the center that corresponds to the Amazon basin. Mountains are present to the north and south-east, but their altitudes do not surpass 1000 m.a.s.l (McGregor and Nieuwolt,1998). Climatic conditions in this region are mainly dominated by seasonal variations of precipitation and related winds. From April to October rainfall is concentrated between about 1º and 9º N while south-easterlies occupy most of the tropical area south of the equator (McGregor and Nieuwolt,1998). From December to March the convective activity migrates to a position around 15ºS and another area of convergence is formed around 10 ºS. North of these convergence areas dry north-easterlies dominate, especially on the east coast of Brazil (McGregor and Nieuwolt,1998).

According to these seasonal modulations of convective activity, a permanently wet climate, with a mean annual rainfall over 1500 mm and mainly produced by the equatorial air masses, is present near the equator throughout the year. On the other hand, a type of climate with one dry season is present at some distance from the equator, where north- and south-easterlies help maintain seasonally dry conditions (McGregor and Nieuwolt,1998) . The permanently wet climate is present over the Amazon basin, in the Guyanas and the east coast of Brazil. This climate is mainly produced by surface conditions, such as the abundance of rivers and swamps and the presence of well-developed vegetation that produce large amounts of water vapor. Local convection and orographic lifting along the coast and in the Andes are then responsible for producing high precipitation (McGregor and Nieuwolt,1998) .

The climates with one dry season are present to the north and south of the wet zone. In the northern region the wet season corresponds to April to September, when southerly winds bring humid and unstable air masses from the Amazon basin. In the rest of the year a dry season is present, mainly produced by the stabilization of the north-easterlies winds (McGregor and Nieuwolt,1998) . In the southern region the dry season is present from March to October and it is mainly produced by stable south-easterly winds that prevail in that season. During the wet season north-easterly winds, blowing from the equator are dominant (McGregor and Nieuwolt,1998) .

This climatic pattern is disrupted by three exceptions. One is located along the coast of Venezuela and corresponds to a dry climate. The second one corresponds to a dry zone in the north-eastern Brazil and the third one to a wet coastal strip along the south-east coast of Brazil (McGregor and Nieuwolt,1998) .

An important component of the South American climate and especially of the continental warm season precipitation regime in this area is the South American Monsoon System (SAMS). Over much of tropical and subtropical South America more than 50% of the annual rainfall is produced in summer related to the establishment of the monsoon (Vuille and Werner, 2005). Monsoon circulation systems develop in general over low-latitude areas, mainly in response to seasonal changes in thermal contrasts between land and oceans. Both North and South America are characterized by such a monsoon system (Vera et al., 2006a).

Convection in South America starts to develop in September. At this time of the year convective activity migrates from Central America and the onset of the wet season starts in the equatorial Amazon, spreading later on to the east and southeast, and arriving

at the mouth of the Amazon by the end of the year. The onset and withdrawal of the Amazon rainy season is lead by an increase in the frequency of northerly and southerly equatorial flow over South America, respectively. The monsoon withdrawal starts in the southeast and then spreads to the north, being slower than the onset (Marengo et al., 2001, Vera et al., 2006a).

During late November through late February, the mature phase of the SAMS is reached, and the main convective activity is located in central Brazil and associated with a band of cloudiness and precipitation that extends southeastward from southern Amazonia to southeastern Brazil and the Atlantic Ocean. This band, a particular feature of the SAMS, is known as the South Atlantic convergence zone (SACZ). Other areas that are reached by heavy rainfall are the Altiplano and the southern Brazil highlands (Vera et al., 2006a).

The SACZ evolves in space and time. Thus, in December it is located further to the east and is associated with high precipitation over much of Brazil. In January it moves to the west, and in February as the northwesterly moisture flux decreases, rainfall also decreases. As convection retreats to the north, the demise of the SAMS continues through fall (Nogues-Paegle et al., 2002). During its decay phase deep convection related to the ITCZ in the Atlantic Ocean is not strong (Vera et al., 2006a).

At the upper-level in summer, a well defined anticyclonic circulation, the Bolivian High at 15ºS, 65ºW characterizes the region. Moreover, a trough near the coast of northeastern Brazil is also developed. At low levels and to the east of the Andes, the Chaco low develops as a response to the strong convective heating over the central Amazon (Vera et al., 2006a). In addition, a continental-scale gyre carries moisture

westward from the Atlantic Ocean to the Amazon basin, and then southward to the mid latitudes. A regional intensification of this gyre occurs to the east of the Andes due to the South American low-level jet (SALLJ, Vera et al., 2006a). This low-level jet develops in the lower troposphere and plays a fundamental role transporting moisture from the Amazon to La Plata basin. Its strongest winds are present near Santa Cruz de la Sierra in Bolivia (18ºS, 63ºW), and it is present throughout the year (Nogues-Paegle et al., 2002, Vera et al., 2006a, Vera et al., 2006b).

In terms of diurnal variability in austral summer in the SAMS area, afternoon and evening convective activity is fairly common over the Altiplano, in two parallel bands over central Amazonia and along the northeast coast of South America. On the other hand, nighttime and early morning convective activity is more dominant along the eastern slope of the Andes and over the subtropical plains (Garreaud and Aceituno, 2007, Vera et al., 2006a). Some mentioned causes for diurnal changes in moisture are diurnal oscillations of the SALLJ, convective instability and land and sea breezes (Nogues-Paegle et al., 2002).

In relation to intraseasonal variability, the most important feature is a dipolar pattern of rainfall anomalies with wet and dry anomalies over tropical and subtropical eastern South America. High precipitation over the SACZ is associated with decreased rainfall in the subtropical plains, and the opposite situation is produced when increased transport of moisture from the Amazon provokes increased precipitation in the subtropical plains (Nogues-Paegle et al., 2001, Vera et al., 2006a). Mentioned causes of this dipolar pattern are changes in the position and intensity of the Bolivian high, and changes in low-level zonal westerlies and easterlies that cause active or inactive SACZ

and divergence and convergence over southern South America, respectively. Another hypothesis postulates that wave trains in the South Pacific link convective activity in the South Pacific Convergence Zone (SPCZ) and SACZ provoking both phases of the dipole pattern (Liebmann et al., 2004, Vera et al., 2006a).

In addition, Liebmann et al., (2004) found an opposite pattern in the phase of the Madden-Julian Oscillation (MJO) that could be associated with this dipolar pattern. The MJO is a planetary-scale oscillation characterized by tropical waves moving eastward with a periodicity of 40-50 days (Madden and Julian, 1972). According to Liebmann et al., (2004) precipitation events in southeastern South America more likely occur two days after the peak in MJO convection, while rain events in the SACZ region tend to occur 26 days after the peak. Vera et al., (2006a) on the other hand stated that this dipole pattern was controlled by the interaction among different intraseasonal fluctuations.

In relation to the interannual variability of the SAMS, Vera et al., (2006a) point out that previous studies have considered five factors that affect it: SST anomalies in the Pacific and Atlantic Oceans, regional forcings associated with land surface conditions, the position and strength of the tropical convergence zones, moisture transport by the SALLJ, and large scale circulation anomalies. Moreover, variability in South American rainfall on decadal and longer time-scales has also been reported. Marengo (2004) in his analyses of rainfall trends in the Amazon basin, recognized the precipitation regime change in 1975-1977 related to a climate shift in the Pacific. This shift was associated with negative rainfall anomalies in most of the Amazon basin, and positive anomalies in southern Brazil and northern Argentina. This shift was also associated with an increase of

SALLJ activity that provoked an increase in precipitation over southeastern South

America (Vera et al., 2006a).

In general, climate in tropical and subtropical South America is strongly

influenced by sea surface temperatures in the tropical Pacific, and particularly by the El

Niño-Southern Oscillation (ENSO) phenomenon. In the case of the climate along the

eastern coast of South America, it is highly influenced by sea surface temperatures in the

Atlantic Ocean (Garreaud and Aceituno, 2007).

El Niño episodes are regularly associated with below normal precipitation in the

north-northeastern part of South America (northeastern Brazil, French Guiana, Surinam,

Guyana and Venezuela,), and wet conditions in the southeastern part of the continent

(southern Brazil, Uruguay, southern Paraguay and northeast Argentina). The opposite

pattern is observed in La Niña years (Ropelewski and Halpert, 1987). In the Andes of

Colombia droughts characterize El Niño years and flooding conditions La Niña events.

This climate anomaly is caused by reduced convection in that area due to a weakened

temperature contrast between land and oceans and enhanced convection in the eastern

tropical Pacific during El Niño years (Garreaud and Aceituno, 2007).

One well known effect of El Niño episodes is the flooding along the coastal areas

of southern Ecuador and northern Peru. Here floods develop from around December to

May, coinciding with the rainy season (Garreaud and Aceituno, 2007). The strong

convection in this area is caused by above average sea surface temperatures in the eastern

tropical Pacific (Horel and Cornejo-Garrido, 1986).

In the Central Andes, and especially on the western side of the Altiplano, drier

than normal wet season conditions occur during El Niño episodes (Vuille, 1999). These

drier conditions are consistent with stronger subtropical westerlies (subtropical jet) over the Altiplano that inhibit the advection of moisture from the Bolivian lowlands. On the contrary, wetter than normal conditions are common during La Niña episodes (Garreaud and Aceituno, 2007).

In northeastern Brazil El Niño episodes are also characterized by droughts. However, this area is also influenced by SST, surface winds and convection patterns in the tropical Atlantic. Warm sea surface temperatures to the north of the equator are conducive for stronger than normal subsidence and drought over NE Brazil. The opposite occurs when warm SST anomalies are present to the south of the equator, and the ITCZ is displaced southward (Garreaud and Aceituno, 2007).

After having provided a general description of the main characteristics of South American climate, the next section will focus on the climate setting along the Andes Cordillera.

1.4. Climate in the tropical Andes

One of the areas that have been studied in more detail in the Andes is located in the Andes of Ecuador (1º N- 4º S). At this latitude coastal areas and the lower parts on the western slopes are influenced by air masses coming from the Pacific. The eastern part on the other hand is influenced by moist easterly winds coming from the Atlantic and Amazon basin (Hastenrath 1981, cited by Vuille et al., 2000a). The valleys that are between the western and eastern cordillera are influenced by air masses coming from the ocean and the continent in a different way (Vuille et al., 2000a). This area has two rainy seasons (February-May and October-November) and two dry periods (June-September and December), the first one being more pronounced than the second one. Precipitation

amounts in the inter-Andean valleys range between 800 and 1500 mm/year (Vuille et al., 2000a).

Relationships between sea surface temperature anomalies (SSTA) in the tropical Pacific and Atlantic Ocean, and precipitation and temperature anomalies in the equatorial Andes have been detected and show different behaviors depending on the location in the Andes. Thus, a strong relationship has been found between precipitation and ENSO in the northwestern part of the equatorial Andes, with the strongest signal in DJF (the peak phase of ENSO), but also during JJA and SON. El Niño events are characterized by below-average precipitation, being the opposite in La Niña years. The eastern Cordillera also shows negative precipitation linked to El Niño years especially during the dry season (JJA). However, precipitation in the eastern Andes is more strongly related to SSTA in the tropical Atlantic than in the Pacific. During most of the year and especially during the boreal spring (MAM) precipitation over this area is related to a dipole-like correlation structure in the tropical Atlantic, where positive correlations exist with south Atlantic SSTA (south of the ITCZ) and negative correlations with tropical north Atlantic SSTA. The Pacific influence in this case can not be discarded, because El Niño events are linked to North Atlantic warm events that can result in decreased Andean precipitation (Vuille et al., 2000a). The only region in the equatorial Andes that shows a positive correlation between precipitation and ENSO (increased precipitation associated with El Niño events) is located along the western Andean slope between 1º and 3º S, presenting a similar behavior as the lowlands coastal areas (Vuille et al., 2000a).

Finally, temperature variability in this region can be best explained by SSTA in the tropical Pacific. Temperature follows SSTA in the Niño-3 and 3.4 regions with a one-

month lag. El Niño-3 corresponds to the region between 5º N-5 º S and 90º -150º W, and El Niño 3.4 to the region between 5 º N-5º S and 120º-170º W (Trenberth, 1997). The northernmost part of the Andes (north of 0.5º N) is the only one that is more closely related to SSTA in the tropical North Atlantic area (Vuille et al., 2000a).

Another important and well studied area in the Andes is the Cordillera Blanca (8º 30` to 10º S), the most densely glaciated area hosting one quarter of all tropical glaciers. It is a pronounced barrier to the easterly atmospheric flow, separating the dry western from the humid Amazon side. Precipitation ranges from approximately 150 to 700 mm on the Pacific side to more than 3000 mm/year on the eastern slope. Precipitation in this region is related to the southward expansion of the upper-tropospheric easterlies during the intensification of the monsoon. Up to 90% of the annual precipitation amount falls between October and May (Kaser and Georges, 1999, Vuille et al., 2008b). In this Cordillera there is a pronounced hydrologic seasonality, and within short distances humid tropical conditions prevail on the eastern side during the wet season, and subtropical conditions are dominant on the western side during the dry months, clearly representing outer tropical conditions (Kaser and Georges, 1999).

South of the Cordillera Blanca is the interandean plateau or Altiplano (14º S-22º S) which has an average elevation of 3700-4400 m. In this area the Andes separate into an eastern and western Cordillera. The eastern part is influenced by a thermal heat low that develops during the summer months and by warm and humid conditions in the lower troposphere. The western part on the other hand is characterized by dry and stable conditions produced by the Southeast Pacific Anticyclone and cold SSTs. Annual

precipitation ranges between less than 200 mm/year in the southwestern part and above 800 mm/year in the northeastern area (Vuille et al., 2000b).

In the Altiplano most of the precipitation (50-80% of the annual precipitation) is concentrated in the austral summer months DJF. This rainfall is associated with convective cloud cover over the Central Andes and the southwestern part of the Amazon. In the austral winter months, precipitation is not very common and the recorded amounts are low (Vuille and Ammann, 1997). In the summer months, the destabilization of the boundary layer produced by intense solar heating of the surface induces deep convection and moist air advection from the east (Vuille et al., 1998). Locally over the Altiplano, water vapor availability in the boundary layer is the feature that controls the occurrence of deep convection (Garreaud, 2000).

The temporal distribution of precipitation in the wet season is characterized by rainy days that tend to cluster in episodes that can last 1-2 weeks and that are interrupted by somewhat longer dry periods (Garreaud, 2000, Nogues-Paegle et al., 2002). According to Garreaud (1999) rainy and dry episodes are related to continental-scale anomalies in convection activity and upper and mid-level circulation. Hence, rainy episodes coincide with a well-defined upper-tropospheric anticyclonic anomaly over the subtropical area (at 25º S) conducive for easterly winds over the Altiplano. On the other hand, dry conditions are present when a cold core upper-air cyclone and westerly winds prevail over the Central Andes. These anomalies act to reinforce or weaken the Bolivian High and appear to be forced by low frequency, planetary waves from the extratropics.

As it was mentioned before, it is important to note that in the austral summer months the Bolivian High, an anticyclonic vortex centered at 15º S-65º W, develops in

the upper troposphere (Vuille, 1999, Garreaud and Aceituno, 2007). This system has been identified as a dynamical reaction to the warming in the upper atmosphere due to convective activity in the Amazon (Figueroa et al., 1995, Garreaud and Aceituno, 2007). During summer precipitation events, an intensification and southward shift of this system can be observed. During dry periods this system is weaker and displaced northward (Vuille, 1999).

According to the study by Vuille et al., (2000b) in the Central Andes, temperature variability is closely related to ENSO, following SSTA in Niño3 and 3.4 regions. Tropical Pacific sea surface temperatures lead temperature anomalies by 1-2 months. Moreover, precipitation variability in the austral summer months (DJF) is also connected to SSTA in the tropical Pacific. This pattern is however different depending on the area of the Altiplano. In the eastern part of the Altiplano correlations with ENSO are weak, because convection and precipitation in this area are not modulated as strongly by westerly winds. On the other hand, in the western part of the Altiplano the connection with ENSO is stronger since moisture advection from the east is dampened during El Niño and increased during La Niña years. The interannual precipitation pattern in the west features a clear decadal –scale oscillation characterized by an above-average rainfall from the late 1960s to the mid 1970s and a dry period in the late 1970s and 1980s. This signal is associated with the climatic shift in the tropical Pacific in the late 1970s, characterized by an increased number of occurrences of El Niño rather than La Niña events. Finally in the northern part of the Altiplano a strong opposite signal is produced 8-12 months following an El Niño and La Niña event. This signal is related to the internal

development of the tropical Pacific SSTA that quickly changes from one state to the other (Vuille et al., 2000b).

It is important to mention that no influence of the SSTA in the tropical Atlantic on precipitation in the Altiplano has been reported. On the contrary, especially during March, SSTAs in the tropical NE Atlantic region off the coast of NW Africa are affected by heating and convection over the Altiplano through an upper air monsoonal return flow (Vuille et al., 2000b).

Surface temperature in the area located between 1º N and 23º S (Andes of Ecuador, Peru, Bolivia and northernmost Chile) has increased in the last 60 years. A study considering 268 stations in the tropical Andes indicates that mean annual temperature increased 0.1-.0.11º C/decade since 1939. This study also reported that warming more than tripled in the last 25 years (0.32-0.34º C/decade, Vuille and Bradley, 2000). It was also found that the major warm anomalies were related to El Niño events, and that major cold periods were related to La Niña events. During El Niño years the warming of the tropical troposphere causes a strong westerly flow up-stream over the Central Andes that produces drier than normal conditions in this area (Garreaud et al., 2003). Vuille and Bradley (2000) also found that temperature trends varied with elevation, showing a reduced warming with high altitude. Despite this reduced warming, there was still a trend toward increased temperatures that was significant at 95% even for the highest elevations. On the western side of the Andes the decrease in warming ranged from 0.39ºC per decade below 1000 m to 0.16 ºC per decade above 4000 m, showing an almost linear trend. This pattern of significant warming in the highest elevations is not consistent with recent observations from radiosondes and microwave sounding unit

(MSU) that report decreasing lower-tropospheric temperatures in the tropics after 1979. This inconsistency has been mainly attributed to differences in temperature and trends between high elevation surface conditions and measurements in the free atmosphere (Vuille and Bradley, 2000).

Vuille et al., (2003) also reported on a new analysis for observed temperatures that used more stations and was developed for the 1950-1994 period. In this analysis they found an average warming of 0.09-0.15ºC /decade, with most of the warming present after the mid 1970s. A recent update of this study up to 2006 showed that the warming has been of 0.10ºC/decade and that the total increase has been of 0.68ºC since 1939. In addition, only 1996 and 1999 were below the 1961-1990 average in the last 20 years (Vuille et al., 2008a).

According to Vuille et al., (2003) the greatest warming affected the lowest elevations in the western Andes, while a moderate or even negative warming below 1000 m was found in the observational data and CRU 05 data set in the eastern Andes, respectively. Higher elevations presented a warming of approximately 0.05-0.20ºC / decade with a trend that slightly decreased with elevation above 3500 m. Due to a lack of instrumental data, temperature trends in the higher regions (above ~4000m) are not known.

According to Vuille and Bradley (2000) and Vuille et al., (2003), stations located on the eastern side of the Andes showed a lower warming, with trends close to zero or insignificant at the lowest elevations. This was in contrast with the strongest and most significant warming in the Pacific side of the Andes. Vuille et al., (2003) reproduced these observed spatial differences with the ECHAM4 GCM. This east-west difference

was attributed in part to the warming of the central equatorial Pacific. On average near 50%-70% of the observed temperature change in the Andes can be considered a consequence of the temperature increase in the tropical Pacific (Vuille et al., 2003).

In addition to the mentioned studies that looked at mean temperatures, Quintana-Gomez (1997) analyzed daily temperature records from seven stations in the central Andes of Bolivia. This analysis showed that minimum and maximum temperatures increased in the period 1918-1990, and that minimum temperature increased in a higher rate especially after the 1960s, thereby decreasing the diurnal temperature range. This pattern was reproduced in a study developed in Colombia and Venezuela using 11 stations in the 1960-1990 period (Quintana-Gomez, 1999), and in Ecuador using 15 stations between 1961 and 1990 (Quintana-Gomez, 2000). Another study from Vincent et al., (2005) for the 1960-2000 period in South America, found that the percentage of cold nights decreased while the contrary happened with warm nights. These changes were more evident during the austral summer and fall (DJF-MAM) and due to the nighttime warming the diurnal temperature range over the continent decreased.

In an analysis of changes in freezing level height over the American Cordillera and the Andes, using NCEP-NCAR reanalysis data, Diaz et al., (2003) found and increase of this height of 53 m (1.17 m/year) between 1958 and 2000. They concluded that nearly half of the rise in the freezing level was due to the increase of the tropical Pacific SST associated with the ENSO phenomenon, in agreement with what was found by Vuille et al., (2003).

A commonly used data set to assess changes in cloud cover is outgoing longwave radiation (OLR) emitted by the surface and atmosphere, and monitored by polar orbiting

satellites since 1974. Observational data from the last decades in the tropical Andes indicate some significant changes in the surface climate of this area. OLR data revealed that convective cloud cover increased somewhat during summer months (DJF), especially in the inner tropics during the period 1979-1998, as reflected by the decrease in OLR. The most important increase, however, occurred during austral summer (DJF) in some limited areas to the east of the Andes. In the outer tropics (south of 10ºS) significant positive trends in OLR for JJA were found. This pattern has a more difficult interpretation because OLR in this area is only a good record for cloud cover during the wet season (DJF). Nevertheless, a significant OLR increase in DJF suggests a trend toward less cloud cover in that area (Vuille et al., 2003).

An important aspect pointed out by Vuille et al. (2003) is that the observed increase in convective cloud cover to the east of the Andes may have reduced the near-surface warming due to a decrease in the amount of incoming shortwave radiation. This feature is more apparent in JJA when the largest increase in total cloud cover occurs in an ECHAM model simulation and the east-west difference in temperature is most apparent. Since simulated temperature trends are positive everywhere, it is probable that cloud cover may have reduced the warming trend especially to the east, but it does not explain the general warming trend (Vuille et al., 2003).

Based on an analysis of 42 precipitation station records between 1950 and 1994, Vuille et al., (2003) detected a tendency for increased annual precipitation north of 11ºS, in Ecuador and northern and central Peru. This pattern was similar for the DJF wet season. In contrast, a tendency for decreased precipitation in southern Peru and along the border with Bolivia was found. Even though this pattern was coherent, the trends were in

general statistically insignificant. Vuille et al., (2003) found positive and negative trends at different elevations between 0 and 5000 m. The only period of the year that presented a trend to wetter conditions with elevation was JJA. However, in general precipitation trends were not significant and they did not show any elevation-dependence (Vuille et al., 2003).

Different studies developed on a regional scale have reported about positive precipitation trends along the eastern slope of the Andes, or even the lowlands to the east between Ecuador and NW Argentina (Vuille, 2008a). The reported changes in precipitation and cloud cover suggest that the inner tropics are becoming wetter and cloudier, while the outer tropics are getting drier and less cloudy (Vuille et al., 2008a). A possible explanation for this pattern could be the intensification of the meridionally overturning tropical circulation (regional Hadley circulation). This behavior is characterized by an intensified vertical ascent (convective activity) with moister conditions in the tropics (between 10º N and ~10ºS), and enhanced subsidence (less cloudiness) and drier conditions in the subtropics (10ºS and 30ºS) (Chen, 2002, Vuille, 2008a). In the inner tropics changes are characterized by pronounced low-level convergence and upper level divergence, that enhances upward motion, and consequently convective activity and humid conditions; the opposite trend characterizes the outer tropics (Vuille, 2007). Although a strengthening of the tropical circulation has not been observed in rawinsonde data nor reproduced in general circulation models, in-situ observational data, satellite information and reanalysis data confirm that such a strengthening is already occurring (Vuille et al., 2008a).

In addition, Vecchi et al., (2006) found that the Walker circulation in the tropical Pacific weakened during the 20th century, showing a weaker zonal sea level pressure (SLP) gradient that has lead to a shift of the mean conditions toward more El Niño-like conditions.

Finally, according to Vuille et al., (2003) coincident with the increase in temperature, relative humidity (determined using CRU05 gridded 0.5º x 0.5º data based on station observations) also showed a positive trend in the near-surface level of 0-2.5% /decade in the 1954-1994 period, especially in northern Ecuador and southern Colombia. In southern Peru, western Bolivia and northernmost Chile the increase was less pronounced (0.5-1%/decade). Trends were similar for all the seasons and to the east of the Andes the trends were lower or even negative. Given the significant increase in temperature and in relative humidity in the Andes, it follows that specific humidity increased too (Vuille et al., 2008a). Increasing humidity levels might have an influence on the increasing melt rates affecting the retreat of glaciers (Vuille et al., 2003). However, these latest results should be interpreted cautiously since the gridded CRU05 data set over South America, from which the trends were obtained, is partly interpolated from synthetic data estimated using predictive relationships with primary variables (precipitation, mean temperature and diurnal temperature range, New et al., 2000). As a result long-term humidity trends are difficult to assess, because no continuous records exist until now. Recently remote sensing techniques have provided tropospheric water vapor data sets, but they are too short to develop any long-term analysis (Vuille, 2007).

1. 5. Assessment of changes

1.5.1. Global climate models and regional climate models

One important tool to determine future changes and potential impacts of climate change are climate models. A general circulation model (GCM) is a mathematical portrayal of the climate system that takes into account the physical properties, interactions and feedbacks of its components (Jones et al., 2004). GCMs are generally based on a horizontal resolution of approximately 200-300 km, and a vertical resolution of 20 levels. Thus, GCMs make projections at a relatively coarse resolution, presenting limitations in terms of regional analyses, where they do not adequately capture the regional scale responses to forcing, or local feedbacks, and they are not very suitable in regions with complex topography or diverse land cover (Jones et al., 2004; Solman et al., 2007). To address these limitations, regional climate models (RCMs) are currently being used for weather forecasting and climate prediction. A RCM is a tool to introduce temporally and spatially small-scale information to the coarse-scale projections of a GCM, and the information developed in the RCM is based on the large-scale resolution information of a GCM. RCMs are comprehensive physical models that frequently incorporate atmosphere and land surface components, and the representation of important processes within the climate system (Jones et al., 2004). These models have the ability of solving meso-scale features that are not evident in global models, and are especially useful in places with complex topography, such as the Andes, being the only models capable of deciphering the geographic complexity of this area. There is a general agreement among different studies that regional climate models can offer a better estimation of South American climate in comparison with GCMs, even though

improvements are needed (Roads et al., 2003; Pal et al., 2007). The area covered by RCMs is typically 5,000 x 5,000 km, with a typical horizontal resolution of 50 km (Jones et al., 2004).

Due to the Andes complex topography and the steep climatic gradients, regional climate models can add a significant improvement to solve the complexity of the regional climate compared to GCMs.

1.5.2. Emission scenarios

The future evolution of greenhouse gases depends on the interaction of different complex systems that are determined by forces such as demographic, socio-economic and technological development, among others. The future evolution of these forces is uncertain; therefore scenarios constitute different alternatives of probable future conditions and a suitable tool to analyze how driving forces may influence future emission effects and the associated uncertainties (IPCC, 2000). SRES refers to the scenarios described in the IPCC Special Report on Emission Scenarios (IPCC, 2000).

Four different storylines were developed to illustrate the association between emission driving forces and their evolution and add some context for the scenarios. Each storyline symbolizes different demographic, social, economic, technological and environmental situations, and each scenario constitutes a specific quantitative interpretation of one of four storylines (IPCC, 2000).

The four storylines are A1, A2, B1 and B2 and each one constitutes a set of scenarios called families. There are six scenario groups under the four families. A2, B1 and B2 have one group each one, and A1 has three, characterizing alternatives for energy technologies. A1F1 (fossil fuel intensive), A1B (balanced) and A1T (predominantly non-

fossil fuel). The total of Special Report on Emissions Scenarios (SRES) scenarios have been developed using six different modeling teams, being all of them equally valid and without any assigned probability of occurrence (IPCC, 2000).

The A1 scenario family describes a world with a very fast economic growth, a global population that peaks in the middle of the century, and the introduction of new and more efficient technologies. It is also characterized by the convergence among regions, capacity building, decrease in regional differences in income and increased cultural and social relationships.

The A2 family describes a very heterogeneous world with a continuously increasing population. It is characterized by self-reliance and protection of local identities. Economy is mainly regionally oriented and economic growth and technological development are more fragmented and slower than in other families.

The B1 family illustrates a convergent world with the same global population growth that in A1, but with rapid changes in economic structures, reductions in the use of material, and introduction of cleaner and more efficient technologies. The B1 storyline is focused on global solutions to economic, social and environmental sustainability, with a strong emphasis on improving equity, but without further climate proposals.

Finally, the B2 family illustrates a world where local solutions to economic, social and environmental sustainability are very important. Population growth in this scenario increases, but at a rate lower than A2, and intermediate levels of economic development and slower and more diverse technological development than in the B1 and A1 storylines characterize this scenario family. This storyline focuses on local and regional levels, and is also directed toward environmental protection and social equity.

1.5.3. Future projections for tropical South America

Until now, there are not many studies of future climate predictions using climate models in South America, and most that have been developed have used GCMs instead of RCMs. Studies developed using RCMs have primarily included intercomparison between models and model validation, (Roads et al., 2003, Fernandez et al., 2006, Rauscher et al., 2007, Seth et al., 2007, among others), but rarely actual future climate projections (e.g. Fuenzalida et al., 2007; Garreaud and Falvey, 2008; Cook and Vizy, 2008).

Such projections up to now are mostly based on GCMs. Boulanger et al., (2006) for example focused on changes in surface temperature, showing that tropical South America will experience a warming of about 4ºC in the SRES A2 scenario, with larger amplitudes over the coasts of Peru and Chile, the central Amazon and the Colombia-Venezuela-Guyana region. Another interesting finding is that the amplitude of the seasonal cycle would be reduced, because the simulated warming in winter and spring is stronger than in summer and fall south of the equator. In addition, this study also found that three different scenarios (A2, A1B, and B1) showed similar patterns, and that only the amplitude was different. A1B and B1 reached about 80-90%, and 50-60% of A2's amplitude, respectively.

A projected scenario for free-tropospheric temperature using seven GCMs with 2x CO_2 levels indicates a temperature increase of >2.5º C for the mountains from 10º S in Peru to 40º S in Chile/Argentina by the end of the 21st century (Bradley et al., 2004). Moreover, results from the mean of eight different general circulation models of future climate in 2090-99 in a high emission (A2) scenario, predict that the rate of warming in

the lower troposphere will increase with altitude and maximum temperature increases are projected for the high mountains in Ecuador, Peru, Bolivia and northern Chile (Bradley et al., 2006).

A global study of regional precipitation for different periods of the 21st century, using an ensemble of 20 global model simulations and three different scenarios (A2, A1B, B1), found that only small precipitation changes would be present over the Amazon (10º N-20º S, Giorgi and Bi, 2005a). The same authors (Giorgi and Bi, 2005b) in a study about interannual variability for the April-June period in the same area, found small precipitation changes and a large and positive trend in the coefficient of variation for precipitation (increase in precipitation variability). These changes were calculated for 21 year periods through 1960-2099 with respect to the 1960-1980 period. Eighteen Atmosphere-Ocean General Circulation Models (AOGCM) under the A2 scenario were used.

Vera et al., (2006c) performed a study over South America using seven IPCC-Fourth Assessment Report (AR4) models to evaluate changes in precipitation during the 2070-2099 period, compared to the 1970-1999 period. According to their results, most of the models predict an increase in precipitation in the wet season and a decrease in the dry season for the tropical area under the A1B scenario. However intramodel differences are in general larger for precipitation than for temperature.

Boulanger et al., (2007), also analyzed changes in annual and seasonal precipitation using IPCC simulations for South America. Their analysis consisted of one simulation for the A2, A1B and B1 scenarios using seven Atmosphere-Ocean Global Climate Models. According to their results, under the A2 scenario, models converged in

projecting weaker annual precipitation in northern South America and stronger

precipitation over the coast of Ecuador and in the La Plata basin. However, a divergence

was found between the mean projection of all models and the one given by an ensemble

that gives more weight to the models that best represent present climate. The weighted

model ensemble predicted a decrease in precipitation in the Amazon basin, while the

mean projection had a value close to zero. As in Boulanger et al., (2006), A2, A1B and

B1 scenarios presented the same pattern, only differing in their amplitude. A1B and B1

reached approximately 90% and 50% of the A2 amplitude at the end of the 21st century.

Their results also indicate that precipitation might increase in austral summer and

decrease in winter in northern South America. During austral summer, the South

American Monsoon would be weaker. In NE Brazil precipitation is lower in austral

summer, but higher in winter and spring (Boulanger et al., 2007). These results partially

match with Vera et al., (2006c) in the increase of summer precipitation in the northern

Andes, but not in the decrease of precipitation for most of the continent in winter.

In general all climate models provide good simulations for temperature patterns

and their amplitudes, but results for precipitation are much more uncertain. The models

produce errors in present-day precipitation fields, and show diverging results for

precipitation changes during the 21st century (Boulanger et al., 2007).

1.6. Objectives

The main objective of this study is to provide a robust assessment of predicted

changes in climate in tropical South America, by comparing the results of a regional

climate model simulation for the end of the 21st century with a control run from the end

of the 20th century. This simulation will provide a baseline for estimating future climate

change impacts in a medium-high (A2) emission scenario. In addition, mainly for temperature change assessments, a medium-low (B2) scenario will also be considered for comparison. The next step in this NSF funded project, of which this thesis forms part, will couple the output from these simulations to a tropical-glacier climate model (Juen et al., 2007) to simulate glacier response to projected future climate changes. A special emphasis will therefore be given to the analysis of variables known to affect glacier energy and mass balance, such as temperature, precipitation amount and timing, cloud cover and the atmospheric circulation aloft, among others (e.g. Francou et al., 2003, 2004).

The study will be subdivided into separate assessments of changes in surface climate (e.g temperature, precipitation, specific and relative humidity) and changes in different levels of the free troposphere (e.g. temperature, wind field, geopotential height, cloud cover, etc.). Because of the special emphasis on the Andes region, topographic controls will be examined to assess whether certain changes in climate are elevation-dependent and whether this elevation dependence (e.g. temperature lapse rate) is a robust feature of the climate system or will change under varying greenhouse gas scenarios. These analyses will take a look at predicted climate change separately along the eastern and western Andean slopes, as observational studies indicate significant differences in current climate trends (Vuille and Bradley, 2000).

Finally a major goal of this study is to provide climate change predictions beyond just a simple description of the mean climate state, by including analyses of changes in variance (e.g. probability density functions of temperature change), the seasonal cycle (e.g. changes in magnitude of the monsoon precipitation) and the atmospheric circulation

(e.g. changes in summer circulation aloft the tropical Andes). All these analyses will be based on comparisons of output from the PRECIS regional climate model using simulations of climate at the end of the 20th century (1961-1990) and the end of the 21st century (2071-2100).

CHAPTER 2

GENERAL METHODOLOGY

2.1. Study area

The study area is South America between approximately 13º N-30º S and 89º W-41º W. This corresponds to the complete RCM domain, but after removing the grid cells where adjustments between the GCM and regional model take place, the actual study area was reduced to approximately 10º N-27º S and 86º W-44º W. (Figure 1). The analysis was mainly focused on the Andes region to detect and assess climatic changes that could potentially have an impact on tropical glaciers in that area.
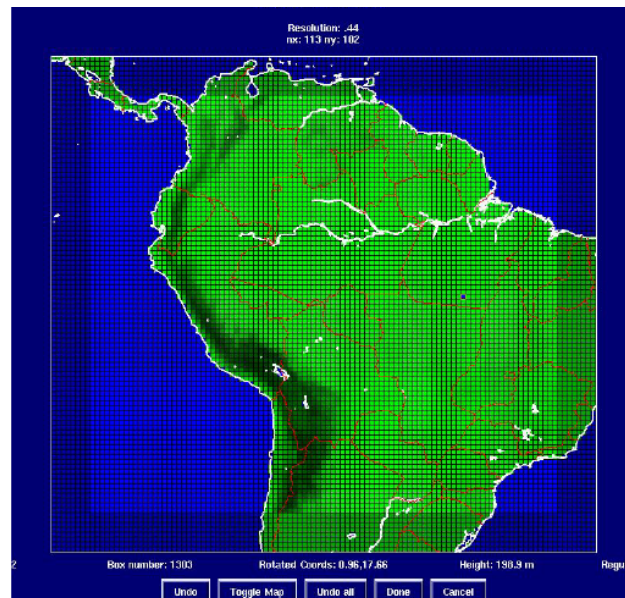
Figure 1. Study area as depicted by the Regional model PRECIS at 50 x 50 km resolution.

2.2. Climate Model

In this study the Hadley Centre Regional Climate Modeling System, called PRECIS, was used to assess changes in climate between today and the end of the 21st century. This model is "a regional modeling system that can be run over any area of the globe on a relatively inexpensive, fast PC to provide regional climate information for impacts studies" (Jones et al., 2004). It is an atmospheric and land surface model which is applicable for use over limited areas in any part of the world. In this study the model was run in 0.44º lat. x 0.44º lon. (~50 x 50 km) resolution.

PRECIS is based on the third generation Hadley Centre Regional Climate Model (HadRM3) that is driven by the latest GCM (HadCM3). This nesting scheme implies that errors which occur in the climate prediction made by the GCM may be transferred to the RCM. This RCM model encompasses 19 levels in the atmosphere from the surface to approximately 30 km in the stratosphere. Different processes such as dynamical flow, atmospheric sulphur cycle, clouds and precipitation, radiative processes, land surface and deep soils are described (Jones et al., 2004). The model requires surface and lateral boundary conditions. Lateral boundary conditions are required to provide the necessary meteorological information at the latitudinal and longitudinal boundaries of the model domain (Jones et al., 2004).

Meteorological flow and thermodynamics are simulated and special attention is given to the modifying effect of mountains. The distribution and life cycle of sulphate aerosol particles is simulated throughout the atmosphere, and convective clouds and large-scale clouds are considered separately in their formation, precipitation and radiative effects. In terms of the radiative processes, these are modeled to be dependent on

temperature, humidity, and concentrations of active gases, sulphate aerosols and clouds. The seasonal and daily cycles of incoming solar radiation are also considered, and the model has a vegetated canopy which interacts with the flow, incoming radiation and rainfall, and supplies fluxes of heat and moisture to the atmosphere and precipitation runoff. Deep soil temperature and water content are also simulated.

Other important features of this model are that the portrayal of large-scale circulation (e.g. the Bolivian High) and the capacity of resolving small-scale features such as the steep NW-SE gradient in specific humidity are improved. This last feature is represented neither in the HadCM3 GCM, nor in NCEP/NCAR reanalysis data (Kalnay et al.,1996; Lenters and Cook, 1997).

In this study three simulations were analyzed. The first simulation (RCM 61-90) involves a thirty year (1961-1990) period that serves as a control run and provides the base-line for comparison with the projected greenhouse gas emission scenarios. It is important to note that an essential step in the process of predicting climate using such a model is its validation based on observational climate records. This step, however, has explicitly been excluded from this study, as it is being developed in parallel at the Climate System Research Center of the University of Massachusetts (Vuille, in progress).

The second simulation, the projected greenhouse scenario (RCM SRES-A2) is based on a medium-high emission and high population-growth scenario (15 billion people and 850 ppm of CO_2 concentration by 2100) run for the 2071-2100 period (Giorgi and Bi, 2005). In the third simulation (RCM SRES- B2), the projected greenhouse scenario corresponds to a lower emission and population growth (10.4 billion people and 550 ppm by 2100) and it is also a simulation for the 2071-2100 period (IPCC, 2000).

37

These scenarios are part of the four IPCC Special Report on Emissions Scenarios (SRES) families: A1, A2, B1 and B2 that capture the range of uncertainties associated with different driving forces (IPCC, 2000). Output of different variables for the control, B2 and A2 runs was obtained from PRECIS. The output was converted into a different format to be manipulated in Matlab 6.0, the software of choice to develop all the analyses, figures and plots.

2.3. Methods

Methods are divided in two sections: the assessment of changes at the surface and the assessment of changes in the free troposphere.

2.3.1. Changes in surface climate

Analyses of surface variables were mainly focused on determining the differences between the A2 and control run in terms of temperature, precipitation, relative humidity, and specific humidity for the whole study area. Thus for example, in the case of temperature, output of annual mean values were obtained from PRECIS and manipulated in Matlab to obtain mean annual temperature maps for the 30 year period under each scenario. The difference in mean annual temperature was determined by subtracting annual temperatures of the control scenario from the ones of the A2 run. Results related to changes in this variable using the B2 scenario were also discussed. In addition, the difference in seasonal temperature for austral summer (DJF) and austral winter (JJA) were determined for the 30 year period. In all cases maps were developed for the whole study area in South America.

In addition, changes between control run and A2 scenario were also determined for the surface variables temperature, precipitation, relative and specific humidity, as a function of altitude (from 100 to 5000 m.a.s.l) in the Andes. In this case the eastern and western slopes were considered separately. To perform this analysis, the highest grid cell was chosen at each latitude along a N-S transect throughout the Andes Cordillera, effectively dividing the Andes into an eastern and a western side. The eastern and western slopes included all grid cells to the east and west of this dividing line respectively, as long as they were within 10 grid cells (~500 km) of the Andean crest. Only grid cells over land (>100 m) were included in this analysis, and in the case of the eastern slope a minimum altitude of 400 m was considered to remove grids located over lowlands to the east.

This procedure allowed calculations and patterns to be examined exclusively for the eastern and western slopes of the Andes. Elevation-dependent analyses also included an assessment of changes in the freezing level (0°C isotherm) and the model surface area ('mountain tops') which remains above this line in the control run, A2 and B2 scenarios respectively.

In all cases a two-tailed Students t-test considering unequal variances and 95% confidence levels was performed. This t-test was developed in Matlab (ttest2 tool) and basically allowed determining if mean values (annual or seasonal) were significantly different between both scenarios for the 30 year-period. Values of 1 and 0 indicated that means were significantly different or not, respectively.

Another analysis that was developed in this study corresponds to the Probability Density Function applied to temperature in the control, A2 and B2 scenarios for the

eastern and western slopes of the Andes. This analysis was performed to assess if there will be any change in the width and amplitude of the distribution between different scenarios. This analysis also reveals whether there will be any overlap between scenarios (e.g. if the warmest years in a control run provide an analogue for the coldest years in an A2 or B2 scenario) and whether there will be an increased likelihood for extreme outliers in future climate scenarios (e.g if the variability is much larger in a future greenhouse climate than it is today). Similar analyses by Schaer et al., (2004), for example, have revealed that the European summer heat wave of 2003 might provide a useful analog for the average climatic conditions at the end of the 21st century. Altitudes above 100 m along the western and 400 m along the eastern slope were considered for the three scenarios, and altitudes above 4000 m were considered just for the control and A2 to compare changes at all elevations and only at high altitudes. In addition, annual mean values for the 30 year-period in the different scenarios were plotted in order to see their actual distribution in the PDF.

Finally, a dynamic analysis of precipitation (reflecting monsoon behavior) was developed by means of a time-latitude diagram (Hovermuller Diagram). This diagram was obtained averaging precipitation values over longitude 50º-70º W in order to see changes in the intensity and seasonality of the monsoon system, and compare the results with the ones obtained by Vuille & Werner (2005) for approximately the same area. In addition precipitation values were also averaged over longitude 64º -70º W to assess changes in the Central Andes.

2.3.2. Changes in the free troposphere

Besides surface temperature, annual and seasonal (summer and winter) changes in mean temperature in the free-troposphere were also analyzed for both the A2 and B2 scenarios. In each case latitudinal transects showing temperature changes at different altitude levels were created. To draw these figures, only the highest grid points along this transect and their immediate neighbors to the east and to the west were considered. The average value from these three grid cells was used to plot the free-tropospheric temperature above that altitude. As temperature is directly related to pressure in the database, but not to altitude, a polynomial function was used to obtain the temperature at different elevation levels using the geopotential height.

Besides the analyses of free-tropospheric temperature, plots of summer geopotential height in South America for the control and A2 run, and differences between the two, were analyzed for 850 mb, 500 mb, and 200 mb, to see changes relatively close to the surface, in the mid-troposphere and in the upper troposphere, respectively. In addition, zonal and meridional winds were analyzed in combination with geopotential height in order to see changes in wind strength and direction between both scenarios. An additional variable of interest that was analyzed was the vertical motion at 500 hPa, a key variable to detect changes in the regions of large-scale ascent and subsidence.

To determine probable future changes in cloud cover and their relation with expected changes in precipitation, the total annual and seasonal fractional cloud cover was also assessed for the control and A2 scenarios.

Of special relevance for climate and precipitation in the Andes is the upper-tropospheric zonal flow aloft (Garreaud et al., 2003). This study therefore also included

an analysis of a latitudinal cross section of zonal wind and vertical velocity from the

Pacific to the Amazon basin across the Central Andes (at approximately 16ºS) and

considering longitudes between 55º and 85ºW. Such an analysis can help assessing the

dynamic mechanisms responsible for the simulated changes in Andean precipitation. It is

also useful to test whether the premise put forth by Garreaud et al. (2003) that

precipitation in this region is dynamically tied to the zonal wind aloft, still holds in a

future greenhouse world. The same analysis was also developed for the Cordillera Blanca

(at approximately 9º S) to assess probable changes in the upper tropospheric flow in that

area and their effect on the precipitation regime in the most highly glaciated tropical

mountain range in the world.

3.1. Analysis of surface climate

3.1.1 Analysis over the entire domain

3.1.1.1. Temperature at the surface

To assess future changes in surface temperature, Figure 2 shows maps of the

mean annual temperature in a) control run and b) A2 scenario.
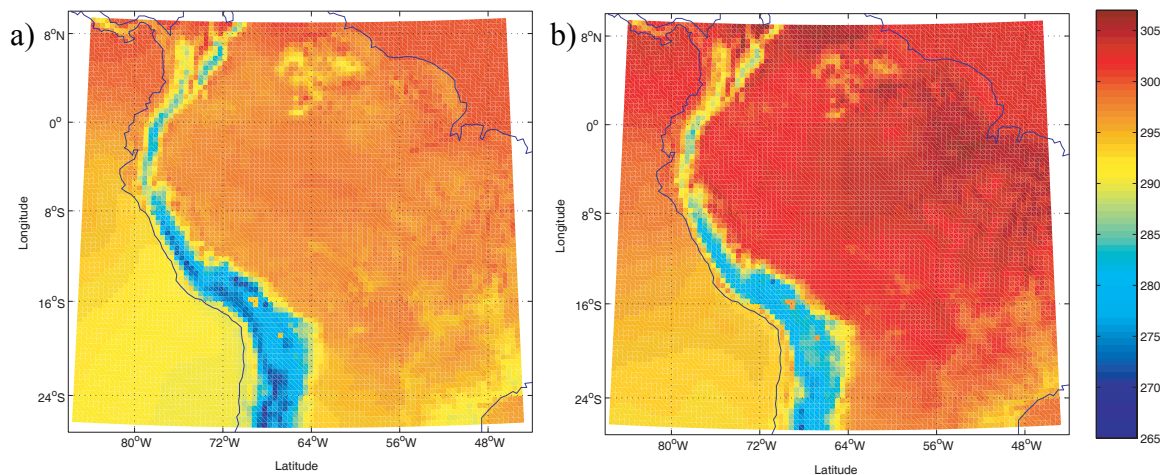
Figure 2. a) Mean annual temperature (K) in the control scenario b) The same as a), but
for the A2 scenario.

Higher temperatures are present in the northeastern and northern part of South

America in both scenarios, while in the Andes temperature is the lowest. In general there

is an increase in temperature in all areas in the A2 scenario compared to the control run.

The highest temperatures in the control run are mainly located in northern and

northeastern South America, the Atlantic Ocean and the northern equatorial Pacific,

while in the A2 scenario they are also mainly located in northern and northeastern South

America but not over the oceans, demonstrating that warming will be stronger over land than in oceans at the end of the 21st century. Warming in general is less over the ocean than over land because of the enormous heat capacity of the deep-mixing ocean, which leads to a slower rate of warming (NOAA, 2007).

Figure 3 shows maps of the temperature difference between the A2 and control scenario for the annual mean as well as for austral summer and winter seasons. From here onward, seasons will always be referred to with respect to the southern hemisphere. Thus, summer is considered as December, January and February (DJF), and winter as June, July, August (JJA).
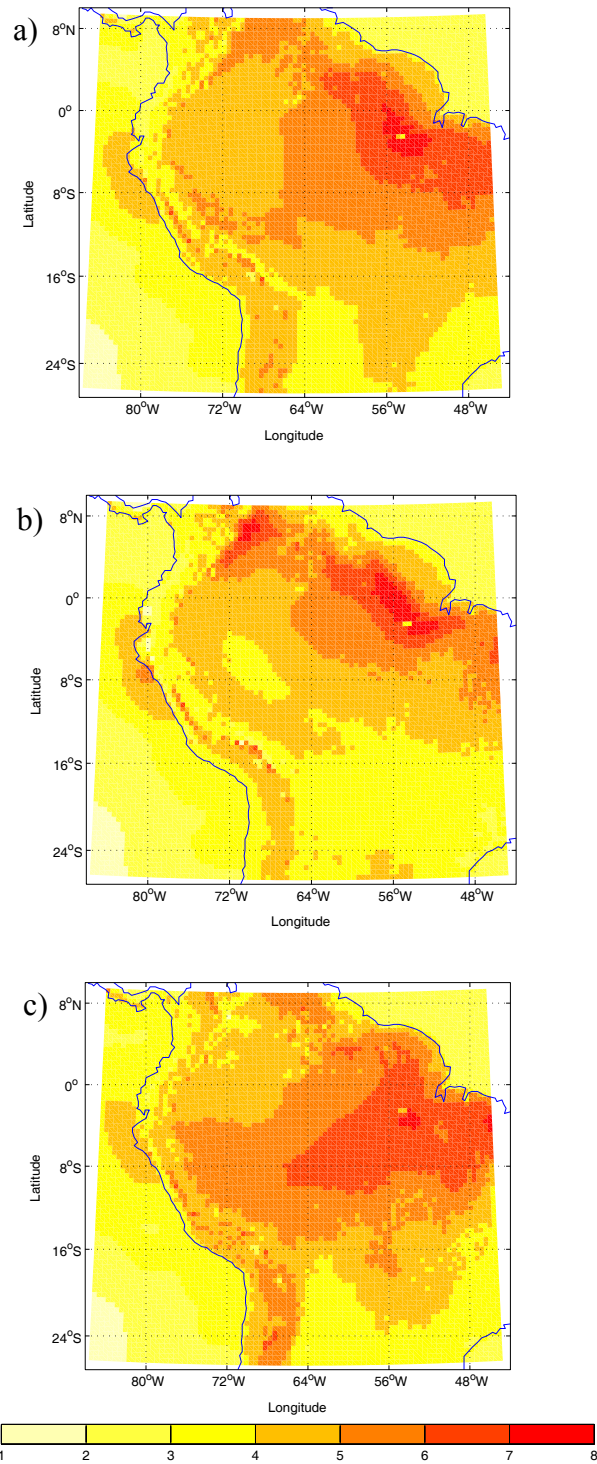
Figure 3. a) Difference in mean annual temperature between A2 and control scenario. b) Difference in mean summer temperature (DJF) for the same period and scenarios as in a) c) Difference in mean winter temperature (JJA) for the same period and scenarios as in a).

In order to focus the attention toward patterns of change in the Andes Cordillera, this area was analyzed separately by extracting the highest elevation at each latitude and the ten nearest points to the east and to the west of this highest position. Only altitudes above 400 m.a.s.l were considered along the eastern slope. Hence, to see in more detail patterns of change in the Andes, Figure 4 represents an example of mean annual temperature differences between the A2 and control scenario.
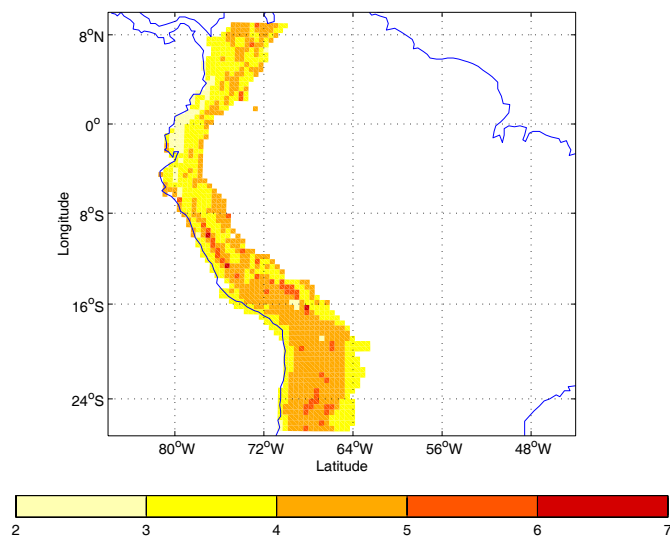
Figure 4. Difference in mean annual temperature between the A2 and control scenario for both slopes in the Andes.

As can be seen in Figure 3 a) the warming between control and A2 scenario ranges from 1º C to more than 7º C, with the largest warming located in the Amazon basin. A major temperature increase of more than 7º C is simulated for the eastern Amazon basin, relatively close to the mouth of the Amazon River in Brazil. Warming is less pronounced (between 3º and 4º C) in the Andes of Colombia, Ecuador and northern Peru, but it is more evident south of 8º S, with a warming between 4º and 5ºC, and in some cases even higher than that. The largest warming (mostly above 4º C) in the Andes

is apparent in Cordillera Blanca in Peru (approximately between 8º and 12 ºS), in parts of the Altiplano and along the western slope in the Cordillera Real of Bolivia (near 15-17 ºS). Warming in Cordillera Blanca reaches more than 6º C (Figure 4), posing a real threat to the most highly glaciated tropical mountain area in the world. The largest warming over the oceans (also between 4º and 5ºC) is located along the coast of Ecuador and Peru between approximately 3º and 10ºS.

Based on Figure 3b it can be appreciated that in summer the pattern of major warming is concentrated in two areas, the northern part of the study area (Colombia and Venezuela) and the northeastern region covering part of the Amazon in Brazil. On the other hand, in winter (Figure 3c) major warming is evident in northeastern Brazil, but it spreads more to the western and southwestern side of the continent. In winter warming is also more evident and stronger than in the summer in most parts of the Andes.

Monthly difference maps (not shown) indicate that the summer pattern is representative of all three months that compose this season (December, January and February), while in the case of winter the observed pattern is more representative of what occurs in July and August only.

A t-test reveals that mean annual, summer and winter temperatures are all significantly different between the A2 and control scenario throughout the entire domain.

Figure 5 presents maps of seasonal differences between austral summer (DJF) and austral winter (JJA) temperature in control and A2 scenarios, which allow an assessment of changes in the seasonal cycle of temperature.
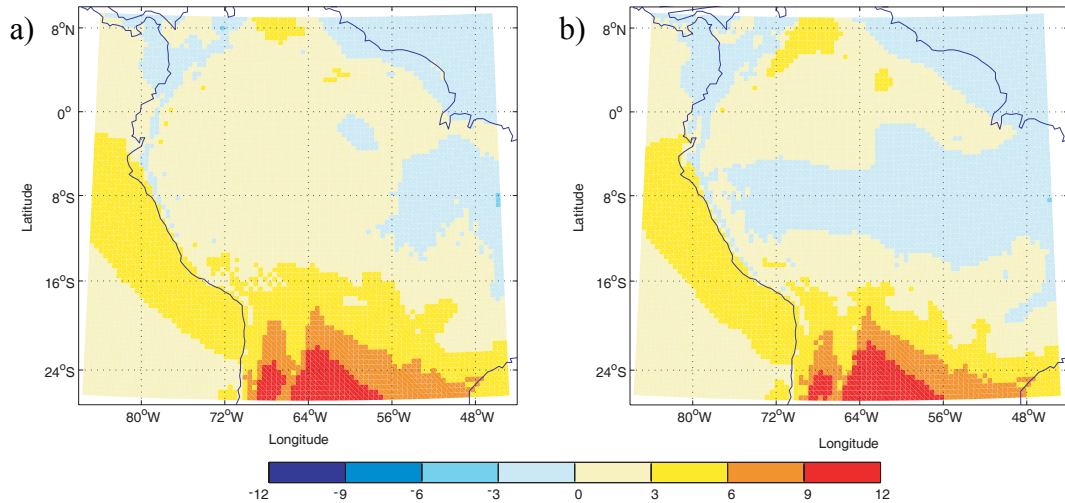
Figure 5. a) Difference between austral summer and winter mean temperature in the control scenario b) The same as a), but for the A2 scenario.

Large positive differences between summer and winter temperatures occur mostly south of 16º in both scenarios, indicating much warmer temperatures in summer than in winter, especially south of 20º S (differences between 9º and 12º C). Warmer temperatures in summer (between 3º and 6ºC) are also present along the Pacific Ocean and coastal areas south of approximately 4ºS. The most evident change between both scenarios is the seasonal temperature reversal with temperatures that have become warmer in the winter in the A2 scenario between 4 ºS and 12 ºS. The increase in winter temperature mainly in the outer tropics would be indicating a smaller amplitude in the seasonal cycle, which might possibly be conducive to endemic diseases in those areas (such as Dengue, Boulanger et al., 2006). Another important change is the increase in temperatures in summer in northern South America, especially in Venezuela and parts of Colombia.

3.1.1.1.1. Comparison of annual mean surface temperature change in A2 and B2 scenarios

Figure 6 presents the difference in mean annual temperatures between the A2 and control (a)) and the B2 and control scenarios (b)). This figure helps to determine differences in the pattern and magnitude of changes between different emission scenarios.
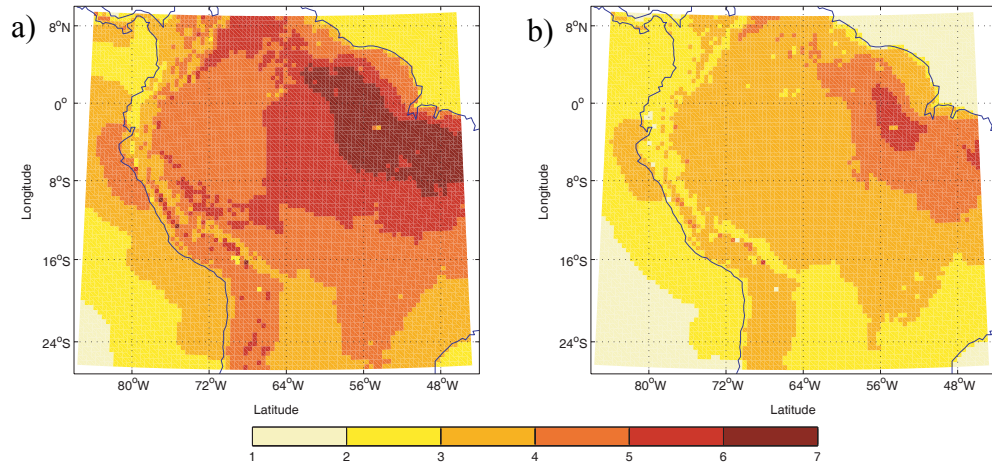
Figure 6. a) Difference in mean annual temperature between the A2 and control scenarios. b) The same as a), but using the B2 instead of the A2 scenario.

The spatial pattern of temperature change is almost the same in both cases, but the magnitude varies. The warming is up to 3° C larger in A2 than in the B2 scenario. Extreme warming is also more widespread in A2 than in B2. This can clearly be seen in northeastern South America.

There is a close coupling between ELA and the 0° C isotherm in the tropics (Greene et al., 2002). It is therefore of interest to see how large of an area might be affected by a future rise of this freezing line. Table 1 presents the total area with temperatures below the freezing level in the control, A2 and B2 scenarios for the annual mean and the summer and winter seasons.

Table 1. Area with temperature below 0º C (273.15º K) in km^2

	Control	A2	B2
Annual	95,000	5,000	10,000
DJF	22,500	0	5,000
JJA	285,000	55,000	82,500

As expected areas with temperature below freezing are largest in winter and smallest in summer. In fact areas below 0º C will disappear entirely during the summer months under the A2 scenario, with significant ramifications for glaciers in the tropical Andes. However, it should be kept in mind that the RCM grid resolution does not sufficiently resolve the highest peaks in this region of complex topography and that this estimate is therefore an underestimation of the true area above the freezing line.

3.1.1.2 Precipitation

Changes in precipitation between the A2 and control scenario were again determined for annual and seasonal periods. Both absolute (in mm) and relative changes (in percent) were analyzed. Figure 7 shows the absolute and relative difference in annual precipitation between the A2 and control run as well as their significance. In the case of relative change in precipitation the scale was capped at 250% to allow for a clear representation of smaller changes.
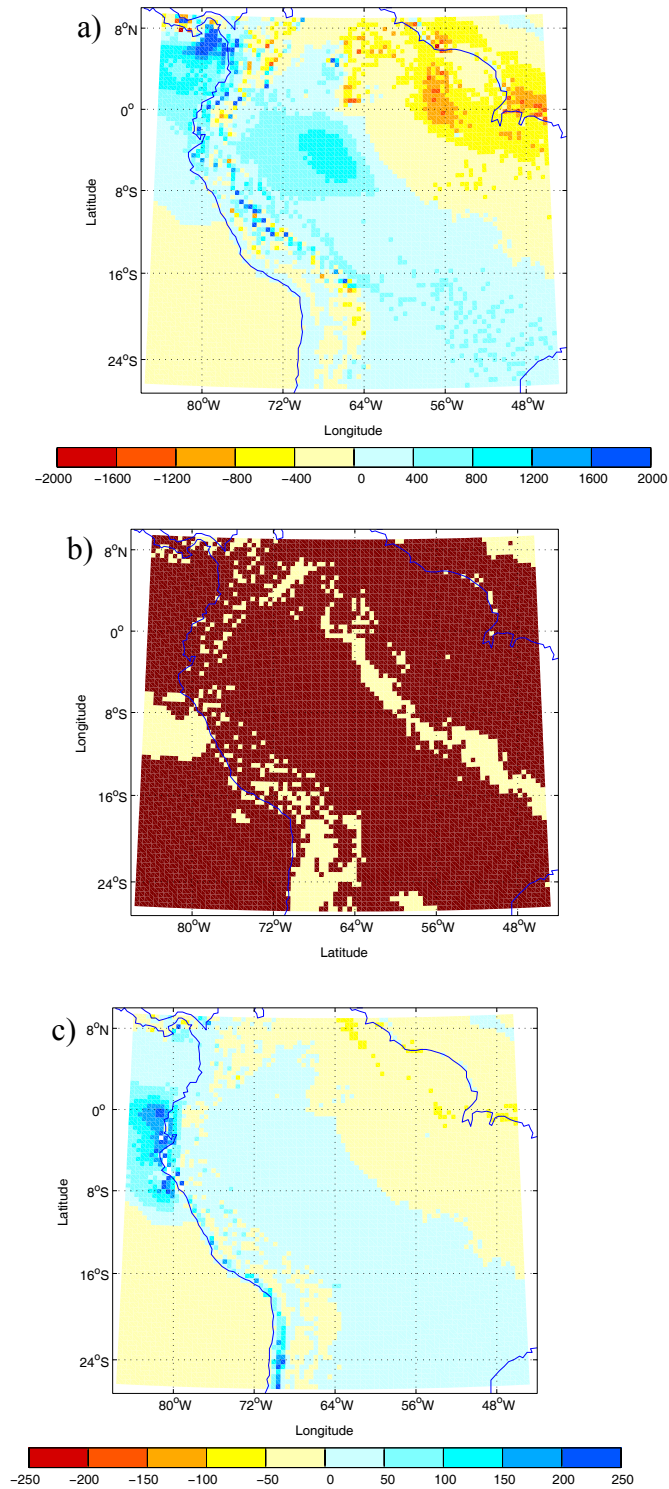
Figure 7. a) Absolute difference in mean annual precipitation between A2 and control scenario. b) Map showing where annual mean precipitation values are significantly different between both scenarios. Areas in dark red are significantly different at 95% of confidence. c) The same as a), but for relative difference (percentage).

The largest increase in precipitation in absolute terms occurs in the northern tropical Pacific off the coast of Panama and Colombia, and in the coastal area of the latter (more than 2000 mm). In relative terms the largest increase in rainfall is located over the Pacific Ocean and along the coast of Ecuador and Northern Peru (between 0º and 8ºS approximately), but also along the coast south of 0ºS. The largest decrease is manifested in northeastern South America and the adjacent Atlantic Ocean. This decrease in precipitation reaches more than 50% in some areas. In the central part of South America along a NW-SE diagonal there is a general increase of precipitation of less than 50%, and in the Andes region there is a mixed pattern with both increasing and decreasing precipitation ranging from -50 to 250%. (the highest values occur along the coast and are significant up to 22º S). A decrease in precipitation of less than 50% is apparent in the Altiplano and most of the Andes south of 16ºS, in Cordillera Blanca and in the Andes of Colombia and Venezuela. However, this decrease in precipitation, especially south of 16ºS, is mostly insignificant. In addition, areas bordering the limit between increase and decrease in precipitation in the NW-SE diagonal, present annual means that are not significantly different between the two scenarios.

Figure 8 shows the difference in summer precipitation in absolute and relative terms between the A2 and control scenario. A map indicating where summer mean precipitation values are significantly different between both scenarios is also presented.
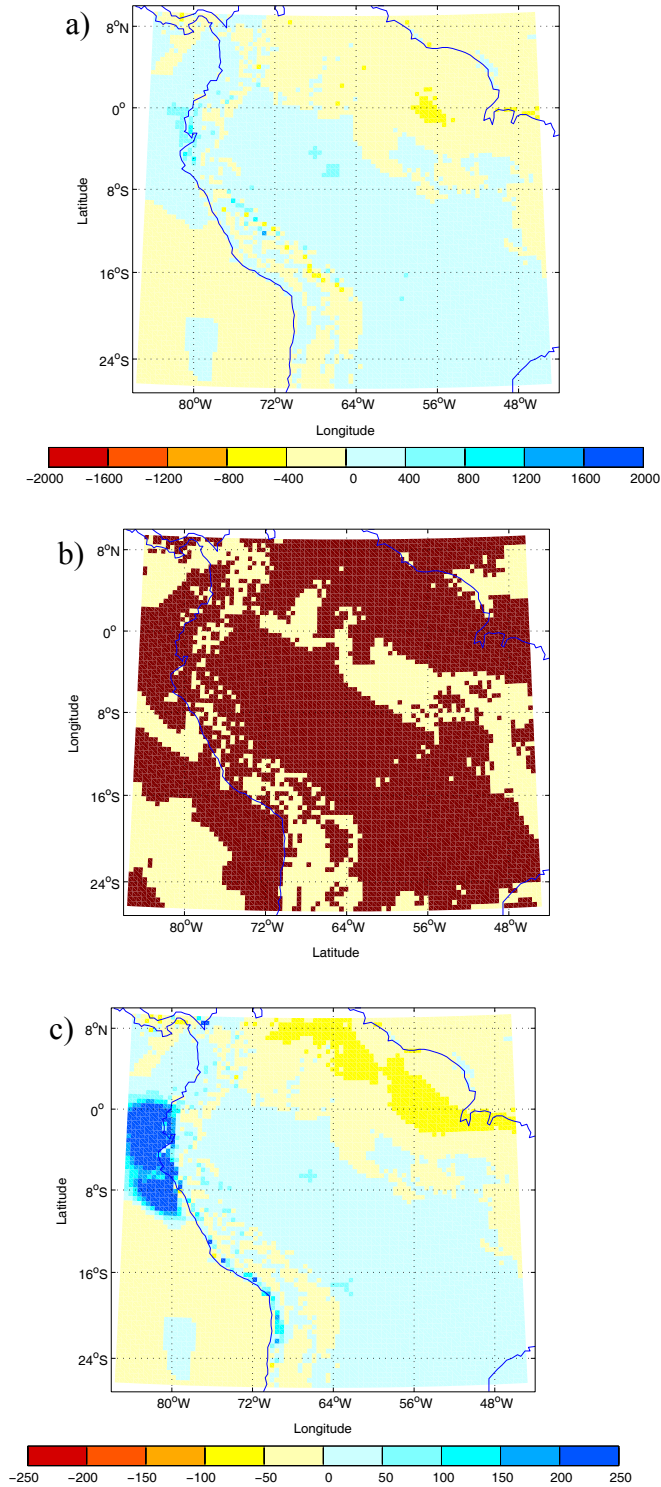
Figure 8. a) Difference in summer precipitation (in absolute values) between A2 and control run b) Map showing where summer mean precipitation values are significantly different between both scenarios. Areas in dark red are significantly different at 95% of confidence c) The same as a), but for relative difference (percentage).

The difference in summer precipitation is very similar to the annual difference pattern of this variable, because in most of the study area precipitation occurs during the summer months. The largest relative increase takes place over the ocean and coastal area of Ecuador and northern Peru (between approximately 0º and 8-9º S) and along the western coast of South America south of this area, but north of 22º S. The major relative decrease in precipitation is located in the north-northeastern area, including a big part of Venezuela and Colombia. This decrease in precipitation in the north-northeast matches the region of largest warming in summer (Fig. 3b). Based on this projection it appears that the monsoon area will experience increased summer precipitation at the end of the century. Figure 9 presents the same plots as in Figure 8, but for the winter season.
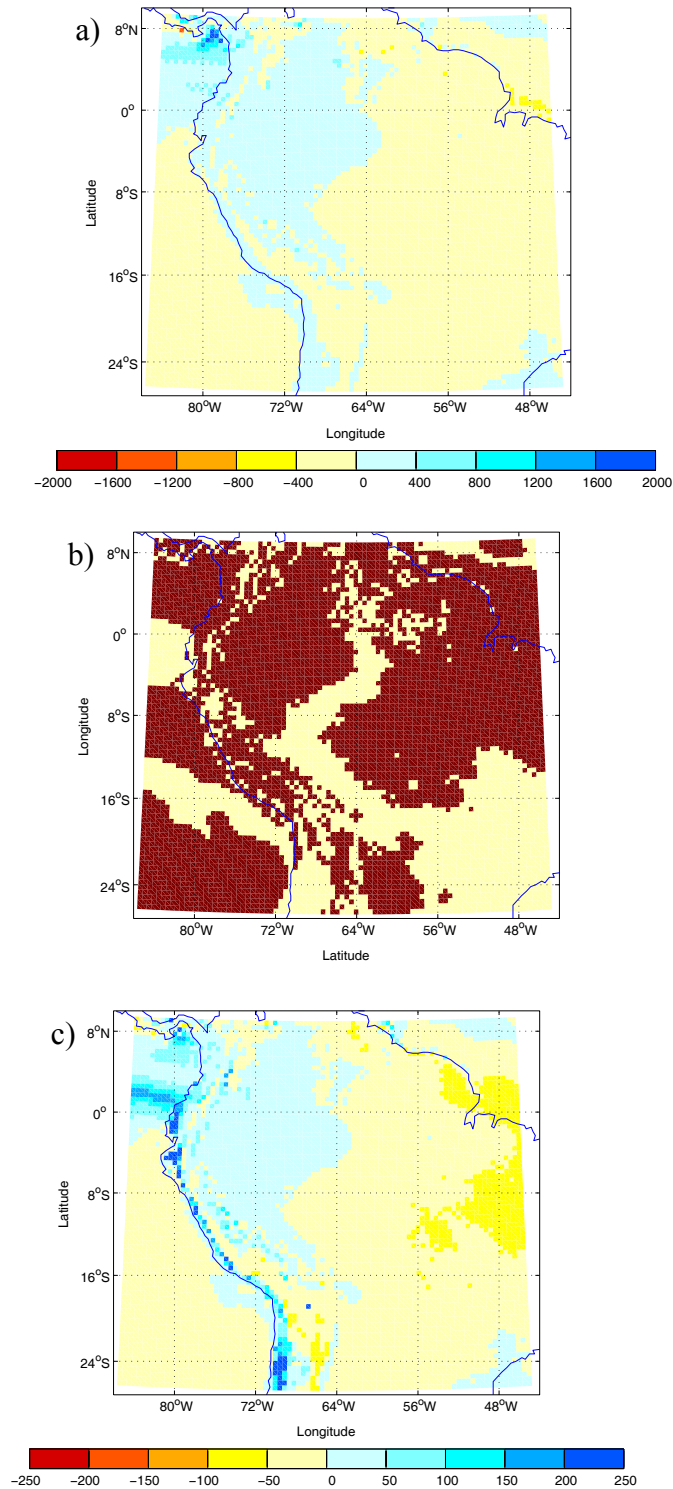
Figure 9. Difference in winter precipitation (in absolute values) between A2 and control run b) Map showing where winter mean precipitation values are significantly different between both scenarios. Areas in dark red are significantly different at 95% of confidence c) The same as a), but for relative difference (percentage).

Differences in winter precipitation reflect a more uniform pattern of reduction in precipitation throughout much of South America, with an increase over the western and a decrease over the eastern Amazon basin. A large increase occurs in the rainy season precipitation over the Pacific Ocean off the coast of Ecuador, Colombia and Panama, significant at 95%. The largest relative increase in precipitation is displayed along the coast south of 0º S, and over the ocean north of 0º, while the largest decrease occurs in the eastern part of the study area, and also in some areas of the Andes south of 20ºS (up to 100%). Again, mean values near the limit between increasing and decreasing precipitation in a N-S transect, are not significantly different between both scenarios, and most of the area south of 16ºS presents differences which are insignificant.

In summary our simulations suggest a decrease of summer precipitation in north-northeastern South America and an increase in a NW-SE diagonal across the interior of the continent, especially south of the Equator, featuring a stronger monsoon system. In winter on the other hand, precipitation shows an increase in northwestern South America and in some places in the north, but decreases in most of the area south of 8 ºS. There, however, differences are mostly insignificant, especially south of 16ºS. The one area that is affected significantly by a decrease in precipitation throughout the year is northeastern Brazil.

Figure 10 shows the difference between summer and winter precipitation in absolute values, for the control and A2 scenario.
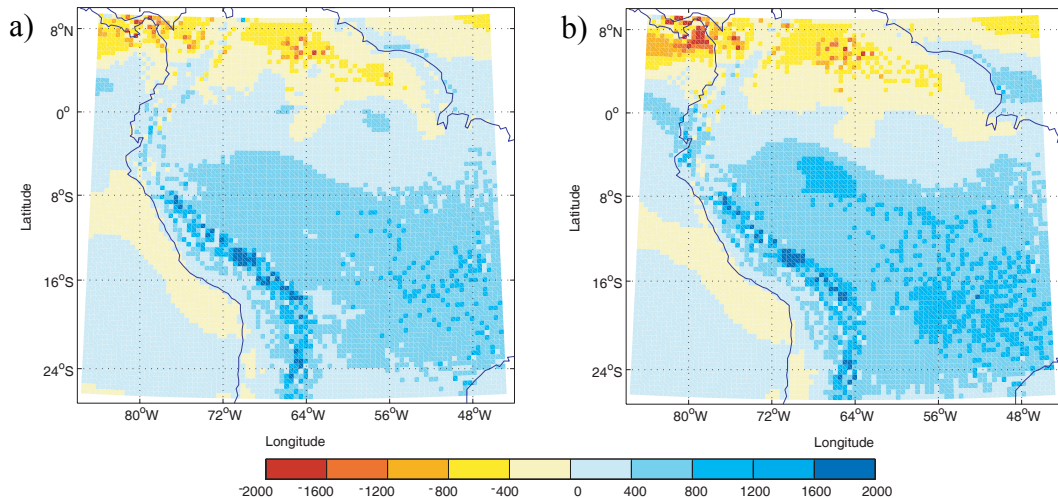
Figure 10. a) Difference between summer and winter precipitation at control scenario. b) The same as a), but for the A2 scenario.

As can be expected, differences between DJF and JJA precipitation are negative for northern South America and positive south of the Equator, reflecting the known precipitation seasonality in these regions. The spatial patterns of difference in precipitation between summer and winter seasons are very similar in both runs. However, two important changes can be appreciated south of 0°; one is the larger positive differences over the continent south of the equator in the A2 run, and the other is the more continuous area of negative differences located south of 20°S in northern-central Chile. Higher positive differences in precipitation between the wet and dry season could be associated with the intensification of precipitation in the wet season and/or a decrease in the dry season in this region. Negative differences located in the Atacama Desert region are associated with increased winter precipitation in that area. The most important change north of the equator is an intensification of the negative difference seen in north-northwestern South America, and especially over the Pacific Ocean near Panama. This pattern can be interpreted as an intensification of precipitation in the wet season (JJA in

this case) and/or a decrease during the dry season. In DJF, precipitation appears to increase during the wet season and decrease during the dry season north and south of the Equator respectively.

Simulated changes in precipitation in the Andes generally agree with observed trends during the 20th century. They are consistent with the tendency for increased precipitation found north of 11º S in Ecuador, and northern Peru in annual and summer values (Vuille et al., 2003). However this trend is clearer and more pronounced north of 8 º S in the model. In addition, simulated changes conform to the decrease in precipitation observed in southern Peru and along the Peru/Bolivia border. Nevertheless, it is important to point out that neither individual observed station trends nor simulated changes in precipitation in the Andes Cordillera are always significant. Moreover, projected changes in precipitation present a mixed pattern with increases and decreases in different areas along the Andes.

Projected changes in precipitation also agree with observed changes in convective activity over the last few decades. Large changes in this variable have taken place between 1974 and 2005, especially during summer. The outgoing longwave radiation (OLR) has decreased over the tropical Andes and to the east over the Amazon basin in the inner tropics, indicating an increase in convective activity. On the other hand, OLR has significantly increased in the outer tropics in the same season, implying less convective activity in that area (Vuille et al., 2008a). These changes are consistent with the observed pattern of change in precipitation, and also are in agreement with the projected changes in rainfall, suggesting that the same observed trends may continue and be especially noticeable in the future along the tropical Andes.

The simulated spatial change in precipitation is in agreement with the notion that the inner tropics are getting wetter, and the outer tropics are getting drier. This fact can be explained through an intensification of the meridional overturning circulation, or the regional Hadley circulation, with an enhanced upward flow in the tropics, balanced by a stronger subsidence and clear skies in the subtropics (Vuille et al., 2008a). This situation is portrayed in a north-south transect at 65º W in South America, where a vigorous vertical ascent has been observed between ~ 10º S and 10º N, balanced by a stronger descending flow in the subtropics in the period 1950-1998 (Vuille et al., 2008a).

Another factor that supports the current positive trend in precipitation in the tropics is the upper and lower atmospheric circulation, characterized by a trend toward divergence and convergence, respectively (Vuille et al., 2008a). These two factors reflect the convective activity in the tropics. In addition, in-situ recorded data, satellite information and reanalysis data suggest that a strengthening of the meridional overturning circulation in the tropics is already taking place (Vuille et al., 2008a).

According to Seidel et al., (2008) a widening of the tropical belt, and specifically of the Hadley circulation, is already occurring associated with global warming, and this poleward expansion is likely to bring even drier conditions to the subtropics and increased moisture to other areas in the future. The intensification of the Hadley cell circulation and changes in divergent winds have not been assessed in the present study.

The larger increase in precipitation simulated to the east of the Andes, is in agreement with the general observed pattern of increase in rainfall along the eastern slopes of the Andes, even at lowlands to the east, such as the one reported along the eastern slopes in Ecuador in the rainy season (Vuille et al., 2000a), and the one found in

northwestern Argentina (Villalba et al., 1998). On the hand it is important to note that the

projected increase in precipitation in the tropics is more noticeable to the east of the

Andes, rather than in the Cordillera itself, where a more mixed pattern, and some

insignificant changes can be found. On the other hand, the decrease in precipitation in

annual and summer values is more noticeable in the Andes than in the interior of

subtropical South America, even though changes are mostly insignificant. For winter

precipitation the decreasing pattern is evident in most of the outer tropics.

3.1.1.3. Near-surface relative humidity

Figure 11 shows the difference in annual mean relative humidity values between

A2 and control scenarios. Again a map showing where these values are significantly

different between both scenarios is included.
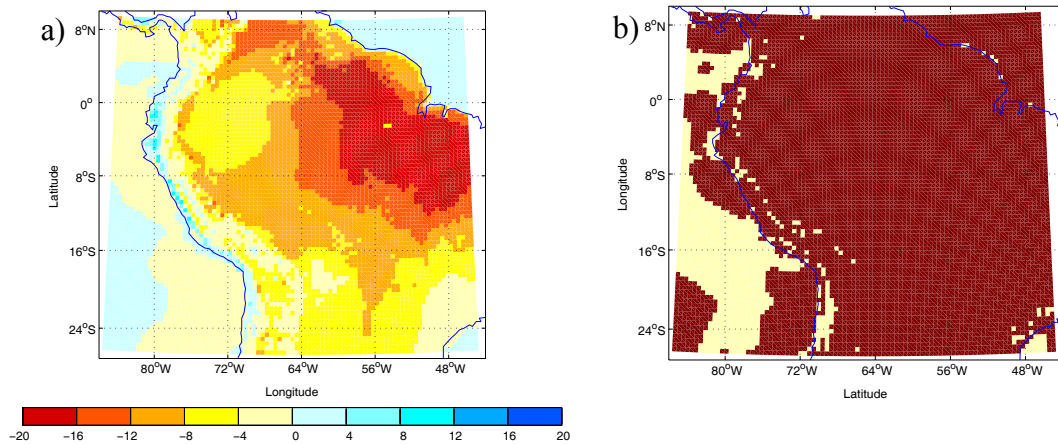
Figure 11. a) Changes in mean annual relative humidity between the A2 and control run (in percent) b) Map showing where annual values are significantly different between both scenarios. Areas in dark red are significantly different at 95% of confidence.

Changes in relative humidity present more or less the same pattern as the mean

annual temperature differences, but with opposite sign (Fig. 3a). The largest decrease in

relative humidity is observed where the highest increase in temperature is located

(northeastern area, including parts of the Amazon basin). For most of the continental area a decrease is projected, while a small increase is simulated over parts of the oceans and for most of the Pacific coastal area and the western Andean slopes (not significant south of 18 º S). These areas match with the ones which show a more modest increase in temperature, and a larger increase in precipitation (Figs. 3a and 7a). In general, most of the continental area shows a pattern where mean annual values are significantly different between both scenarios. The closer relationship between the spatial patterns of temperature and relative humidity suggests that temperature is the main driver of the relative humidity behavior.

In the Andes the areas most affected by a decrease in relative humidity are the northern Andes and the area to the east of the Andes between 8º and 12º S, both coinciding with areas of warming above 4ºC (Fig. 3a). In the Cordillera Blanca and the Altiplano the relative humidity decrease fluctuates between 4 and 8%.

Figure 12 and 13 present summer and winter differences in relative humidity, and their respective maps showing where seasonal mean values are significantly different between both scenarios.
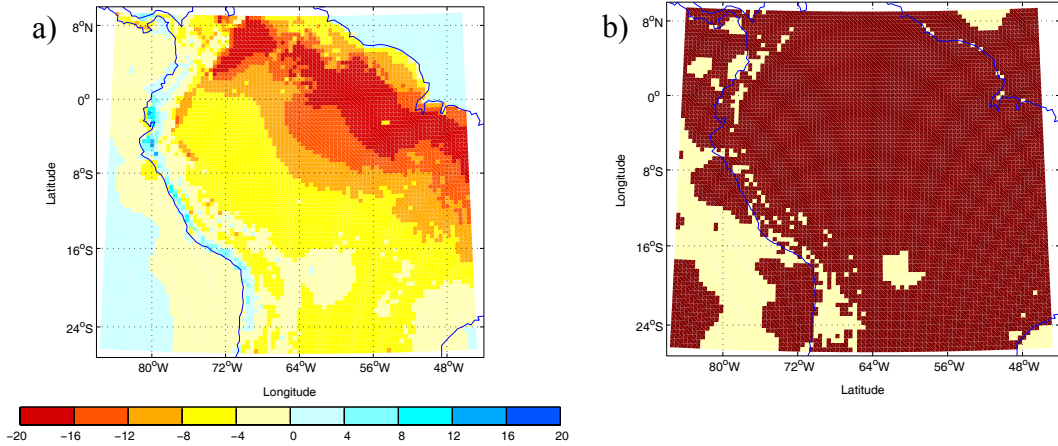
Figure 12. a) Difference in summer relative humidity between the A2 and control run b) Map showing where summer values are significantly different between both scenarios. Areas in dark red are significantly different at 95% of confidence.
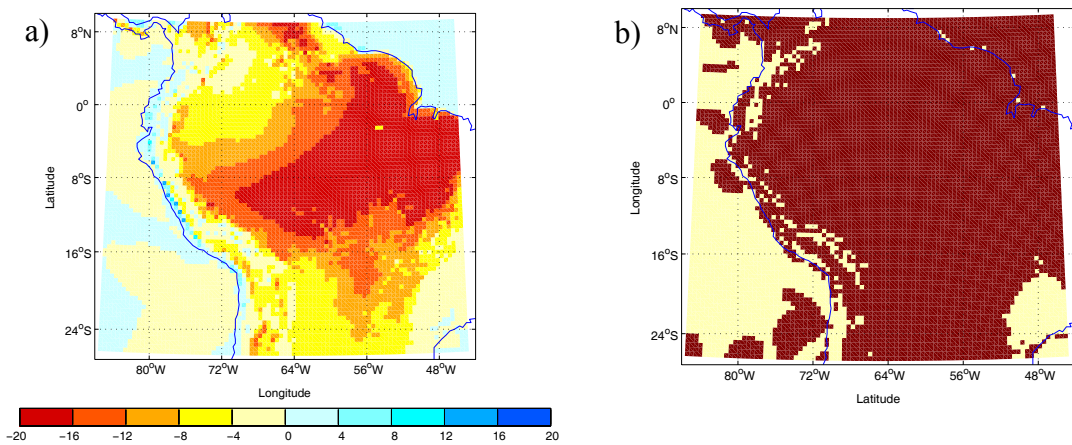
Figure 13. a) Difference in winter relative humidity between the A2 and control run b) Map showing where winter values are significantly different between both scenarios. Areas in dark red are significantly different at 95% of confidence.

The pattern in Figures 12 and 13 is the same as the one presented for summer and winter difference in mean annual temperature, respectively, but with opposite sign (Fig.3b and 3c). The largest increase in relative humidity occurs over the Pacific coastal area between approximately 0º and 20ºS. This pattern is better developed during the summer season when warming is less pronounced in that area. However, summer and

winter differences are largely insignificant between the two scenarios, especially south of

15º S. The increase in relative humidity along the coast of Ecuador and northern Peru ,

significant at 95% of confidence, is also associated with a large increase in precipitation

in both summer and winter in that area.

3.1.1.4. Near-surface specific humidity

Figure 14 shows the difference in annual mean specific humidity between both

scenarios and their statistical significance.
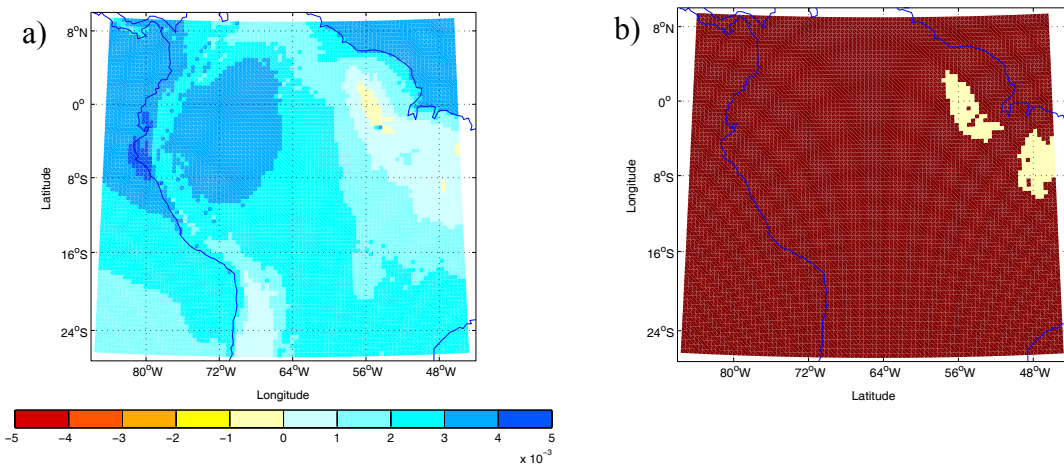
Figure 14. a) Changes in annual mean specific humidity (kg/kg) between the A2 and control scenarios, b) Map showing where annual values are significantly different between both scenarios. Areas in dark red are significantly different at 95% of confidence.

Most regions experience an increase in specific humidity, except for a small area

in the northeast. Limited increases are observed in the surrounding area and in the Andes

south of approximately 18ºS. The region of decrease or insignificant change in the

northeast coincides with the area of largest increase in temperature, the largest decrease

in precipitation, and the largest negative change in relative humidity. In the case of the

Andes, the area south of 18ºS corresponds with an area of high projected warming in the

Altiplano. The area with the highest increments in specific humidity, approximately between 0º and 8ºS along the coast of Ecuador and northern Peru, corresponds with an area of less pronounced warming and the largest increase in relative humidity, and precipitation.

Figures 15 and 16 present summer and winter differences in specific humidity, and their respective significance.
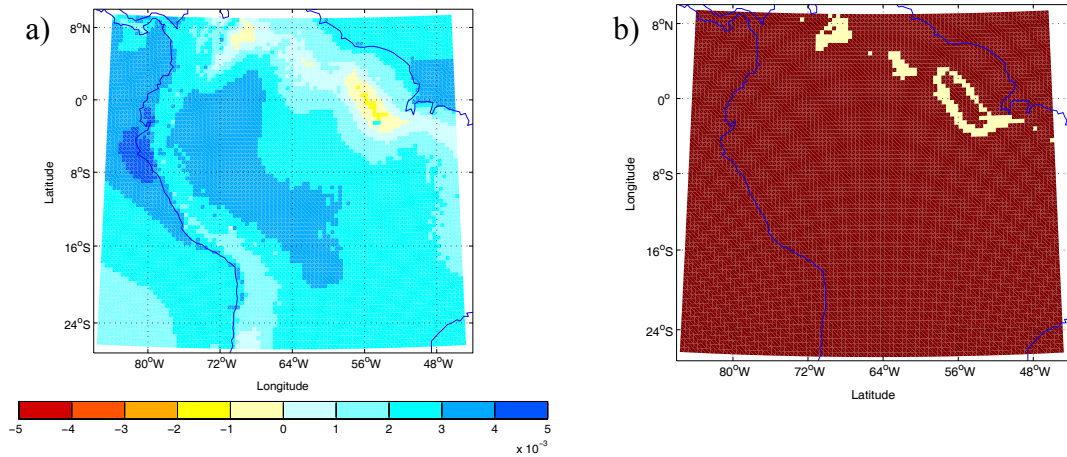
Figure 15. a) Summer difference in specific humidity between the A2 and control scenario. b) Map showing where summer values are significantly different between both scenarios. Areas in dark red are significantly different at 95% of confidence.
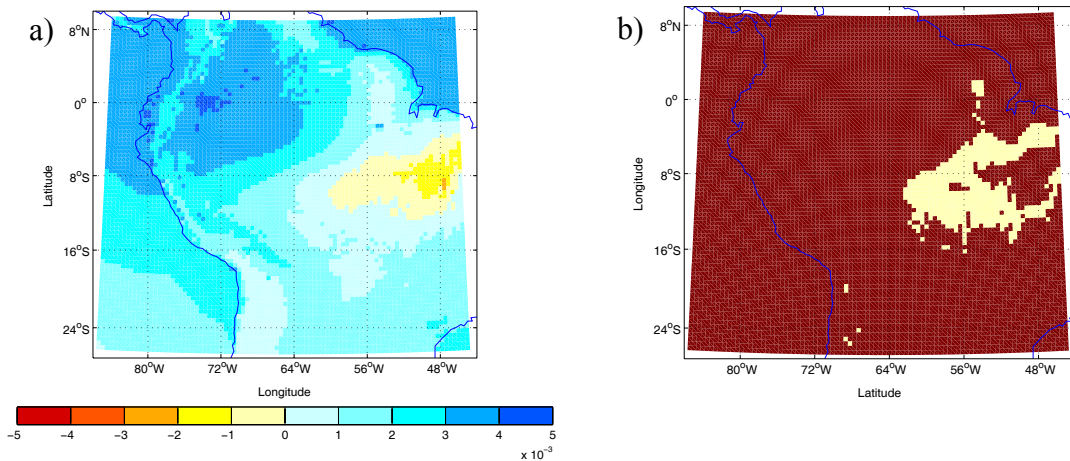
Figure 16. a) Winter difference in specific humidity between the A2 and control scenario. b) Map showing where winter values are significantly different between both scenarios. Areas in dark red are significantly different at 95% of confidence.

The summer pattern better represents what occurs on an annual basis, with the largest decrease and increase in specific humidity in the northeast and along the coast of Ecuador and northern Peru, respectively. In winter the decrease in the east matches the area with the strongest decline in precipitation and large warming in the same season. Moreover, the area with a small increase in specific humidity in the Andes simulated in the annual difference is more noticeable in winter, when the decrease in precipitation is more pronounced.

It is difficult to assess the effects of increasing or decreasing humidity levels on tropical Andean glaciers. According to previous studies (Francou et al., 2003, Vuille et al., 2003, Vuille et al., 2008b), increasing near-surface humidity reduces the vapor pressure gradient between the glacier and the air above, limiting sublimation and increasing the energy consumed by melting. However, this process is only important in the ablation zone of the glacier and when temperatures are at or above freezing (Vuille et al., 2008b). From this point of view the predicted changes in surface relative humidity in the Andes (mostly decreasing, especially along the eastern slope of the Andes), are not likely to contribute significantly to glacier retreat. Nevertheless, it is important to take into account that this process is more relevant on outer tropical glaciers and that future changes in relative humidity appear to be driven by increasing temperature rather than by changes in specific humidity. Higher temperatures will lead to a rise of the freezing line, which in turn will affect the ELA especially of glaciers in the inner tropics. In summary, based on this assessment of changes in mean climate alone, it is not possible to predict what the exact impacts on tropical glaciers will be. Further analyses considering glacier

models are needed to completely understand and assess future changes in glaciers energy and mass balance related to changes in climatic variables.

Generally speaking the Cordillera Blanca and the Altiplano appear to be the areas most affected by warming in the outer tropical Andes. In addition, both regions will be strongly affected by a decrease in precipitation, even though values in the Altiplano are generally not significant. Moreover, in both places, relative humidity is also decreasing by the end of this century (all evaluated for annual, summer and winter values).

The inner tropical Andes appear less affected by a decrease in precipitation and relative humidity, but will face an increase in temperature of more than 3ºC in all seasons. This fact is especially important in the inner tropics, since temperature is more relevant as a direct cause of glacier retreat. Areas in the Andes of Colombia and Venezuela appear to be the ones most affected by an increase in temperature, decrease in precipitation and in relative humidity in the inner tropics.

3.1.2. Analysis of surface climate as a function of altitude and slope

In addition to analyses at a unique level, changes in mean annual surface temperature, precipitation, relative and specific humidity at different altitude levels were analyzed using ranges of 500 m (from 100 to 5000 m). These analyses were developed for the Andes, separately considering the eastern and western slopes. Only altitudes above 100 m and 400 m were considered for the west and east of the Andes, respectively.

3.1.2.1. Temperature at different altitude levels

Figure 17 shows the variation of mean annual surface temperature at different altitude levels for the western and eastern slope and both scenarios (control and A2 scenarios). The standard deviation for each level is also added.
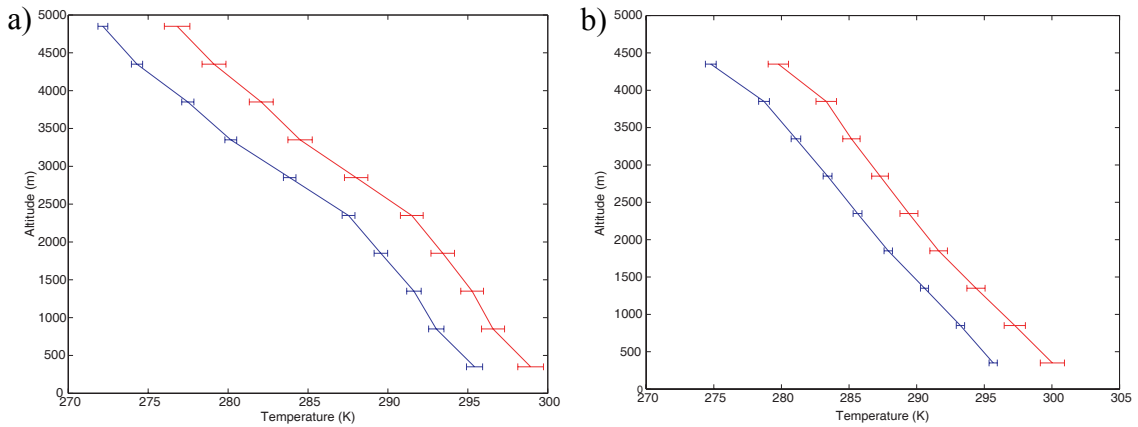
Figure 17. a) Mean annual surface temperature at different altitude levels for the control (blue line) and A2 scenario (red line) along the western slope of the Andes. Horizontal bars correspond to the standard deviation of mean annual temperature at different altitude levels b) The same as a), but along the eastern slope of the Andes.

Both scenarios produce slopes that run parallel to one another. However, there is a change in the slope of the curves below 2500 m.a.s.l. on the western side (Fig. 17a), where temperatures warm less rapidly with decreasing elevation. This change towards lower temperatures and lower lapse rates at lower elevations (below 2500 m) could be caused by the upwelling effect of the Peruvian cold current, which tends to cool temperatures at low altitudes on the western slope of the Andes. Another important point to note is that temperature at the highest altitude in the A2 scenario is well above the freezing level (273.15º K or 0º C), meaning that glaciers, although usually located at somewhat higher altitudes, might be exposed to temperatures above zero and

67

consequently to rain rather than snow, thereby intensifying their retreat (Vuille et al., 2008a).

On the eastern slope temperature also runs parallel between both scenarios without major breaks, except at the highest level where temperatures decrease at a higher rate in both scenarios. Temperatures are warmer on the eastern slope than on the western slope at lower altitudes (below 1000 m) in the control and A2 scenarios. This is consistent with the notion that the influence of cold sea surface temperatures on the western side keep surface temperatures cooler compared to the eastern slope. Above 1000 m, the pattern reverses and temperature is higher on the western slope up to 3000 m, probably caused by the low level inversion. Above this altitude temperature is again higher on the eastern slope. Standard deviations are higher in all cases for the A2 scenario on both slopes.

Figure 18 shows the difference in mean annual temperature between the A2 and control scenario for the western and eastern slope of the Andes.
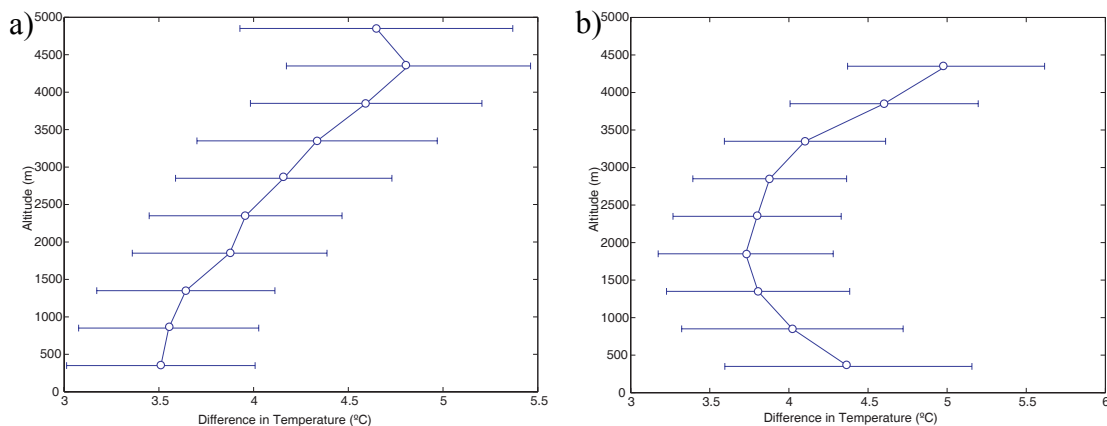
Figure 18. a) Difference in temperature between the A2 and control scenario for the western slope of the Andes. Horizontal bars correspond to the standard deviation of the difference in temperature at different altitude levels and empty circles indicate that annual mean temperature values between both scenarios are significantly different at 95% of confidence. b) The same as a), but for the eastern slope of the Andes.

Along the western slope differences in temperature range from 3.5º C at 500 m increasing at higher elevations to approximately 4.8º C above 4000 m.a.s.l. The temperature change between both scenarios is significant at all altitude levels.

Along the eastern slope the largest differences in temperature (above 4.5º C) are present at the highest altitudes (above 3500 m.a.s.l.). In addition, a large increase in temperature (approximately 4.4º C) is observed at the lowest level (below 500 m.a.s.l), while intermediate values of warming are present at intermediate altitudes between 500 m up to 3500 m.a.s.l. As in the case of the western slope mean temperature values between both scenarios are significantly different at 95% of confidence. The projected temperature change is larger at higher and lower altitudes along the eastern slope compared to the western slope.

The predicted pattern does not entirely agree with the general warming pattern found for observations between 1º N and 23º S by Vuille et al., (2003). In Vuille et al., (2003) observed warming appears to be stronger in the western than in the eastern Cordillera at lower elevations, especially below 1000 m. Above this elevation and up to 2500 m, however, both studies agree that the warming is higher over the western slope. This discrepancy between observed and projected warming might partially be explained by the fact that the present study includes latitudes north of 1º N, which show a larger warming on the eastern than on the western slope. In addition, Vuille et al., (2003) observed a decrease in warming with elevation, while in this study warming is more pronounced at higher altitudes in both slopes of the Andes.

To complement previous figures and have an idea about changes in the lapse rate for the western and eastern slope in both scenarios, Table 2 presents temperature lapse

rates for three different altitude ranges. Altitude ranges correspond to 100/400 m to 2500 m (100 m and 400 m for the western and eastern slope, respectively), 2500 m to 5000 m, and the complete range from 100/400 m to 5000 m. The subdivision into regions above and below 2500 m was chosen because of the well-known change in the lapse rate at approximately 2500 m on the western slope of the Andes.

Table 2. Lapse rates (ºC/100 m) for the western and eastern slope of the Andes in the control and A2 scenario and three altitude ranges. Values below 100 m and 400 m for the western and the eastern slope respectively were ignored.

Altitude ranges (m)	Lapse rates western slope (ºC/100m)		Lapse rates eastern slope (ºC/100m)	
	Control	A2	Control	A2
100/400-2500	0.38	0.36	0.51	0.54
2500-5000	0.58	0.56	0.57	0.49
100/400-5000	0.54	0.51	0.50	0.49

Lapse rates below 2500 m on the western slope are extremely low, probably reflecting the regulating effect of the cold current at lower altitudes in that area. Above 2500 m lapse rates on the western slope increase abruptly and are even higher than the ones for the eastern slope. Moreover, considering the complete altitude range, lapse rates are also higher on the western slope than on the eastern slope for both scenarios. As expected, there is a general trend to lower lapse rate values in the A2 scenario except for the lower level on the eastern slope. Especially noticeable is the significant decrease in lapse rate at higher altitudes along the eastern slope of the Andes.

3.1.2.2. Precipitation at different altitude levels

Figure 19 shows changes in precipitation at different altitudes for the western and eastern slope of the Andes and both scenarios.
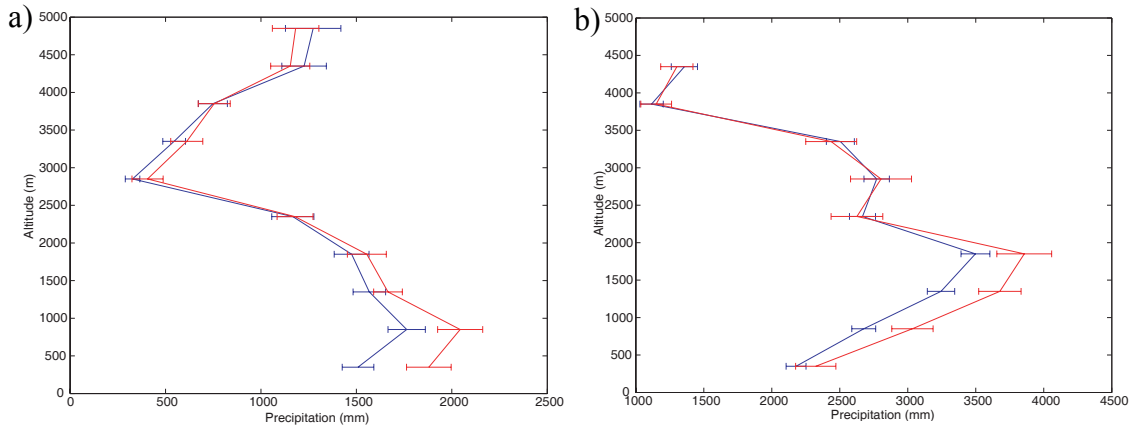
Figure 19. Precipitation at different altitude levels for the control (blue line) and A2 scenario (red line) along the western slope of the Andes. Horizontal bars correspond to the standard deviation of mean annual precipitation at different altitude levels b) the same as a), but for the eastern slope of the Andes. Note different scale in b).

In both scenarios precipitation increases along the western slope up to 1000 m.a.s.l and decreases after that until approximately 3000 m.a.s.l. Above that point precipitation increases, but does not reach values as high as at lower elevation. Differences in precipitation between both scenarios are not as clear as differences in temperature at different altitude levels. Larger differences in absolute values are present at the lowest altitude level. In general, slightly higher precipitation in the A2 scenario is present from the lowest level up to 4000 m.a.s.l.. Above that elevation the situation reverses and precipitation is slightly lower in the A2 scenario.

Along the eastern slope precipitation increases with altitude up to 2000 m.a.s.l, above which point it mostly decreases. The most evident change is present below 2500 m.a.s.l, where precipitation is higher in the A2 scenario compared with the control. Above this altitude differences between scenarios are not that clear. Standard deviations are higher in most cases for the A2 scenario on both slopes.

Figure 20 presents differences in precipitation between the A2 and control
scenario for the western and eastern slope of the Andes.
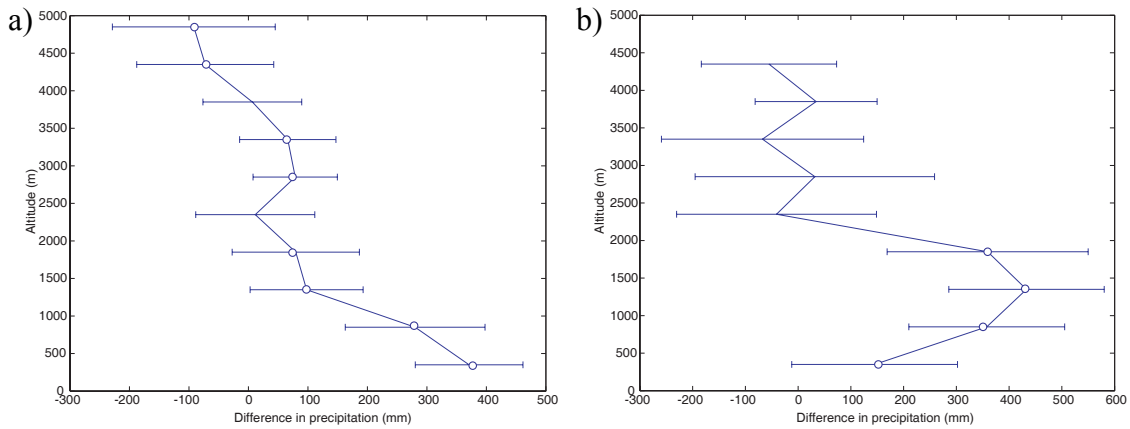
Figure 20. a) Differences in precipitation between the A2 and control scenario for the
western slope. Horizontal bars correspond to the standard deviation of the difference in
precipitation at different altitude levels and empty circles indicate that annual mean
precipitation values between both scenarios are significantly different at 95% of
confidence. b) As in a), but for the eastern slope of the Andes. Note different scale in b).

Figure 20 a) clearly shows the increase in precipitation in the A2 scenario
compared to the control at all altitudes up to 4000 m.a.s.l and the decrease above this
level. Along the eastern slope large absolute positive differences in precipitation between
both scenarios occur below 2000 m.a.s.l. Above 2000 m, all differences are close to zero
and not significant, indicating a lack of dependence on altitude.

In relative terms (percentage, not shown) the increase in precipitation is higher on
the western than on the eastern slope below 1000 m.a.s.l. Above that altitude the situation
reverses and the increase in rainfall is larger along the eastern slope up to 2500 m. Above
2500 m, the situation is mixed with higher increases either along the western or eastern
slope. The major increase in precipitation along the western slope at lower elevations is
reflecting the large increase in precipitation projected for coastal areas of Ecuador and
northern Peru (Fig. 7a).

In summary a general increase in precipitation might be expected, at least up to 2000 m.a.s.l., for both slopes of the Andes. Above that altitude no significant changes (eastern slope) or even a decrease (western slope) are projected. This is fundamentally important to consider, since it shows that glacier mass balance, affected by larger warming at higher altitudes will not benefit from compensating effects of increased precipitation.

3.1.2.3. Relative humidity at different altitude levels

Figure 21 shows changes in relative humidity at different altitudes for the western and eastern slope of the Andes and both scenarios.
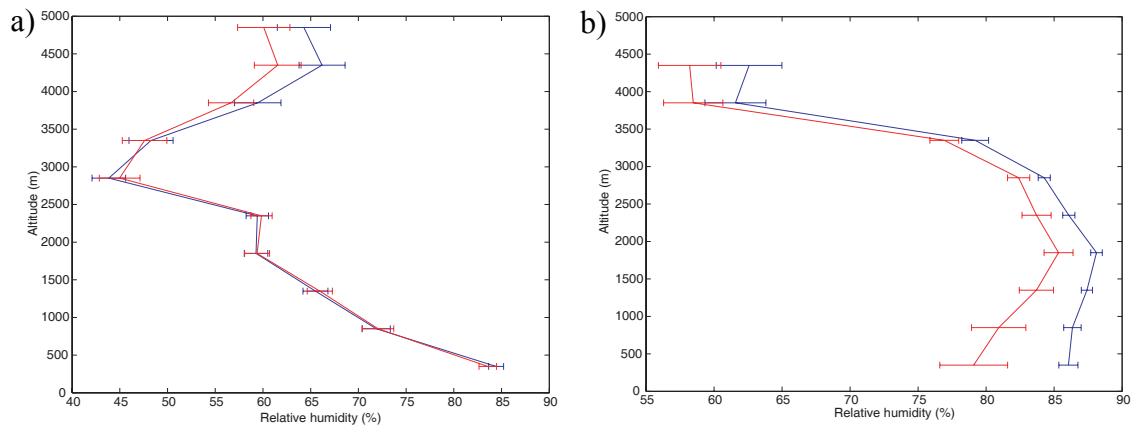

Figure 21. a) Relative humidity at different altitude levels for the control (blue line) and A2 scenario (red line) along the western slope of the Andes. Horizontal bars correspond to the standard deviation of mean annual relative humidity at different altitude levels b) As in a), but for the eastern slope of the Andes. Note different scale in b).

Annual mean relative humidity values decrease with altitude up to 3000 m, and increase above this point along the western slope of the Andes (Fig. 21a). Changes in relative humidity with altitude between both scenarios are minimal up to 3500 m, but above this altitude it is possible to recognize a decrease in the A2 scenario.

Along the eastern slope, annual mean relative humidity values increase up to 2000

m, and decrease above this point. There is a general decrease in relative humidity

projected for all altitude levels in the A2 scenario. In most cases standard deviations are

higher for the A2 scenario on both slopes.

Figure 22 presents differences in annual mean relative humidity between the A2

and control scenario for the western and eastern slope of the Andes.
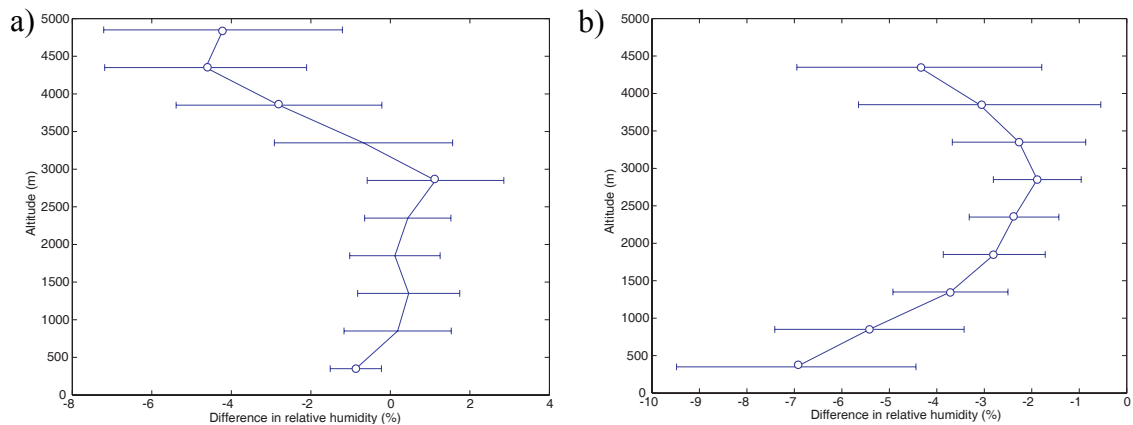
Figure 22. a) Differences in relative humidity between the A2 and control scenario for the western slope. Horizontal bars correspond to the standard deviation of the difference in relative humidity at different altitude levels and empty circles indicate that annual mean relative humidity values between both scenarios are significantly different at 95% of confidence. b) As in a), but for the eastern slope of the Andes. Note different scale in b).

Relative humidity decreases in most levels in the A2 scenario along the western

slope of the Andes (Fig. 22a). Significant changes are limited to the decrease in the

lowest and highest levels (above 3500 m) and a significant increase at 3000 m.

Along the eastern slope on the other hand annual mean values are all significantly

different between both scenarios. The decrease in relative humidity is larger at lower

elevations (approximately 7% below 500 m), smaller at intermediate elevations (3 to

2%), and again larger at higher elevations (close to 4%). The behavior of relative

humidity with altitude closely follows the pattern of temperature with altitude, with a

larger warming (and a corresponding larger decrease in relative humidity) at lower and higher altitude.

In general the decrease in relative humidity is larger along the eastern than the western slope, except for the highest elevations. On both slopes the decrease in relative humidity is especially large and significant at higher altitudes.

3.1.2.4. Specific humidity at different altitude levels

Figure 23 shows changes in specific humidity at different altitudes for the western and eastern slope of the Andes and both scenarios.
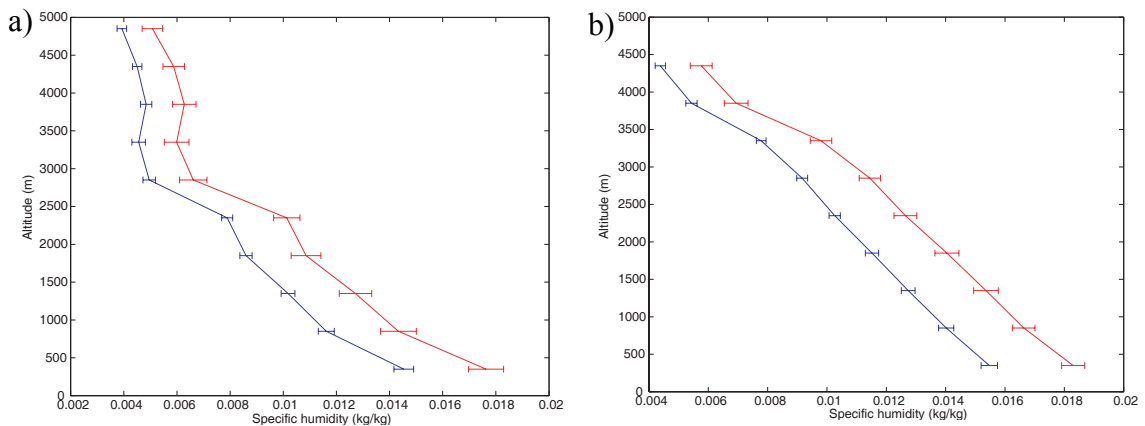

Figure 23. a) Specific humidity at different altitude levels for the control (blue line) and A2 scenario (red line) along the western slope of the Andes. Horizontal bars correspond to the standard deviation of mean annual specific humidity at different altitude levels b) The same as a), but for the eastern slope of the Andes.

As expected, specific humidity decreases with elevation. In addition, there is a persistent increase of this variable at all altitude levels along the western and eastern slope in the A2 scenario. This fact indicates that the air will become much more humid along both slopes of the Andes by the end of this century, basically because of a warmer atmosphere that can hold more water vapor. Standard deviations are higher in all cases for the A2 scenario on both slopes.

Figure 24 presents differences in annual mean specific humidity between the A2 and control scenario for the western and eastern slope of the Andes.
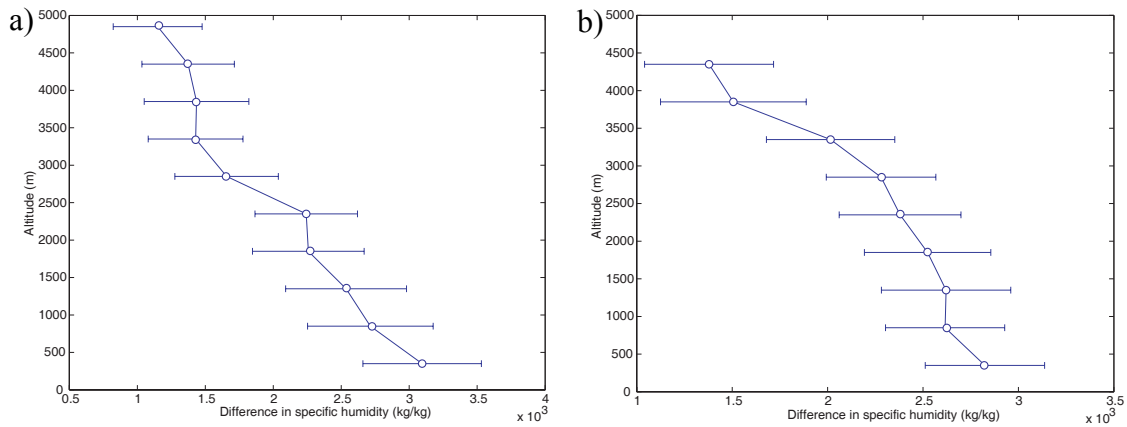

Figure 24. a) Differences in specific humidity between the A2 and control scenario for the western slope of the Andes. Horizontal bars correspond to the standard deviation of the difference in specific humidity at different altitude levels and empty circles indicate that annual mean specific humidity values between both scenarios are significantly different at 95% of confidence. b) The same as a), but for the eastern slope of the Andes. Note different scale in b).

As expected specific humidity increases in the A2 scenario are larger at lower elevations and decrease with altitude. The differences between A2 and control scenario are significant at all altitude levels along the western and eastern slope of the Andes.

The projected relative increase (not shown) is larger along the western than the eastern slope at all altitude levels except for the highest elevation. The relative increase in specific humidity is generally larger at higher altitudes for both slopes of the Andes.

In summary these results suggest that higher elevations will be subject to a larger increase in temperature, a smaller and insignificant increase or even a decrease in precipitation, and a larger decrease in relative humidity despite a larger relative increase in specific humidity when compared to lower altitudes. In addition it appears that the eastern slope might be characterized by a higher increase in temperature, higher relative increase in precipitation, lower decrease in relative humidity and a higher relative

increase in specific humidity than the western slope, at least when considering higher

elevations.

Clearly the increase in specific humidity predicted for the end of the 21st century

is insufficient to increase the relative humidity along different altitudes under the

evaluated warming scenario. This is especially true for the eastern slope of the Andes

where a larger decrease in relative humidity might be expected.

3.1.2.5. Probability Density Function for surface temperature

In order to compare the statistical distribution of annual mean temperature for the

30 years in the control, A2 and B2 scenarios, and to determine the magnitude of its shift

and the change in the width of its distribution, the function "normalpdf" in Matlab was

used to determine the Probability Density Function (PDF). As in the previous section,

results are again subdivided into western and eastern slopes, and only grid cells above

100 and 400 m.a.s.l. were considered for the western and eastern Cordillera, respectively.

In addition, to analyzing changes in distributions at upper levels, the same analysis was

repeated using only grid cells above 4000 m for the control and A2 scenarios.

Figure 25 shows the PDF for the control, A2 and B2 scenario for temperatures

above 100 m on the western slope of the Andes (Figures a) and b)). Figures c) and d)

show the same, but for the eastern slope of the Andes. Bars indicate the actual years in

each distribution.
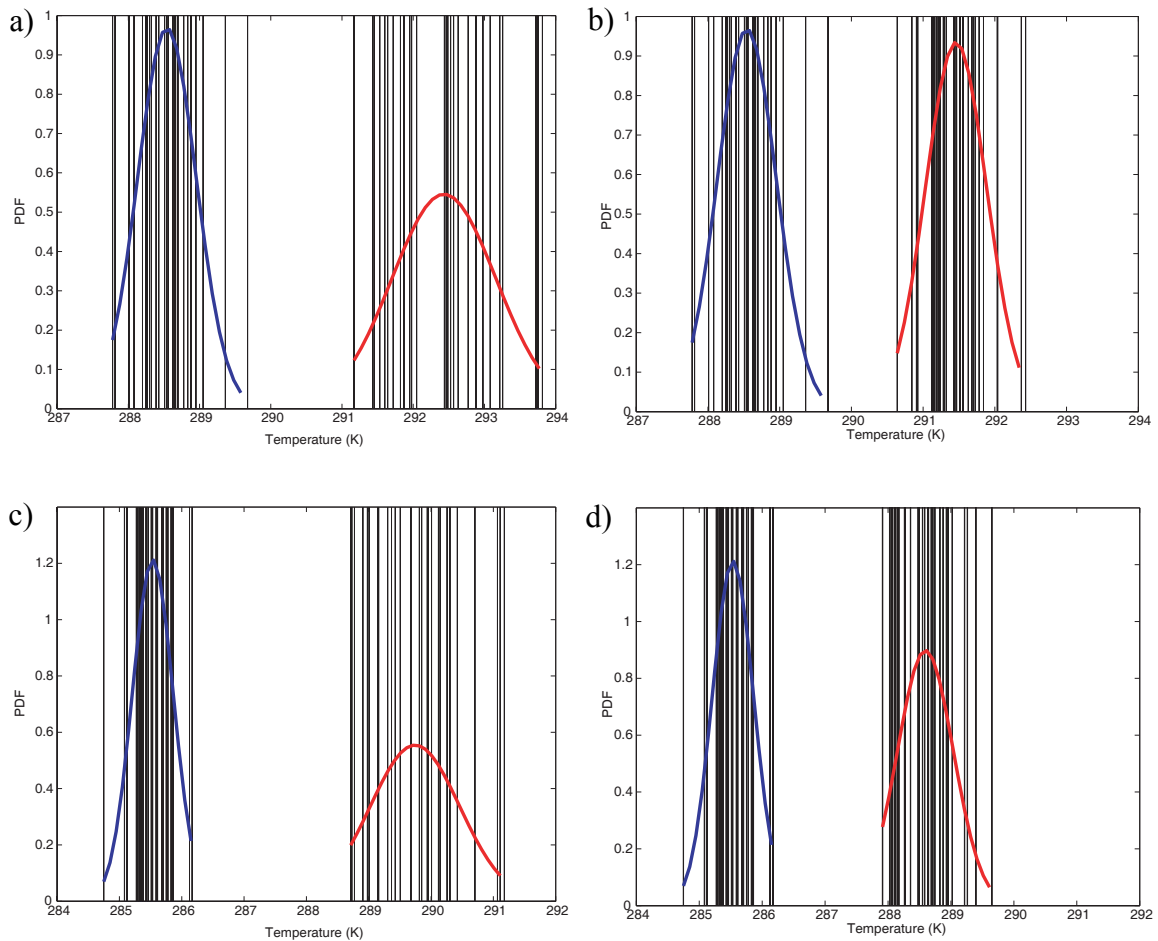
Figure 25. a) PDF for mean annual temperature for the control (blue line) and A2 (red line) scenario, considering grid cells above 100 m along the western slope of the Andes. Bars represent the actual years for each distribution. b) The same as a), but for the B2 scenario. c) The same as a), but considering grids above 400 m along the eastern slope of the Andes. d) The same as c), but for the B2 scenario. Note that the scales for eastern and western slopes are different.

The mean annual temperature for the control run along the western slope corresponds to 288.5º K, and for A2 to 292.4º K, indicating a shift in the mean annual temperature between both scenarios of 3.9º K (Fig. 25a). The standard deviation in the control run corresponds to 0.41º K and the one in A2 to 0.73º K, being 78% larger in the latter. This is evident in the plots of the individual years, with a much more spread out distribution in the A2 scenario.

The mean annual temperature along the western slope in the B2 scenario corresponds to 291.4º K and the shift between B2 and control corresponds to 2.9º K. Hence the B2 mean temperature is one degree less than in the A2 scenario. The standard deviation in B2 corresponds to 0.43º K, only 0.02º K more than in the control run, and 70% less than in the A2 scenario. This is evident in the PDF plot where individual years in the B2 scenario are not nearly as spread out as in the case of the A2.

According to Figure 25 c) mean annual temperature in the control run along the eastern slope of the Andes corresponds to 285.5º K, and to 289.7º K in A2. These values are 3º K and 2.7º K lower when compared to the western slope for control and A2 runs, respectively. The shift in mean annual temperature on the eastern slope corresponds to 4.2º K, 0.3º K more than the shift obtained for the western slope. With regard to the standard deviation, the difference is also much larger, corresponding to approximately 118%. This larger increase reflects the much lower standard deviation on the eastern slope in the control run when compared to the west. Indeed the A2 standard deviations only differ by 0.01º K between both slopes (standard deviation values are 0.33º K and 0.72º K for the control and A2 scenario, respectively).

In the B2 scenario (Figure 25 d), the mean annual temperature corresponds to 288.6º K; 3.1º K higher than in the control run. The standard deviation in B2 is 0.44º K; 0.11º K higher than in the control scenario. Comparing this figure with the previous one indicates that the change in temperature is 1.1º K less in the B2 than the A2 scenario, and that the change in standard deviation is not as pronounced in the B2 run, being 63% larger in the A2 scenario. Table 3 shows a summary of the mentioned values of mean

temperature and standard deviation for control, A2 and B2 scenarios and for both slopes of the Andes.

Table 3. Average temperature (μ) and standard deviation (σ) in each PDF for each scenario and slope of the Andes

	Control		A2		B2	
	μ (°)	σ (°)	μ (°)	σ (°)	μ (°)	σ (°)
Western slope	288.5	0.41	292.4	0.73	291.4	0.43
Eastern slope	285.5	0.33	289.7	0.72	288.6	0.44

In summary annual mean temperature values are higher on the western than the eastern slope in all scenarios, but projected changes are more noticeable along the eastern slope, featuring a larger increase in mean annual temperature and standard deviation. Changes in mean temperature are significant at 95% of confidence in all cases (both slopes and both scenarios), but changes in standard deviation are only significant for the western and eastern cordillera in the A2 scenario. In addition, it is noteworthy that on both slopes the temperature of the warmest year in the control run is well below the temperature of the coldest year in future predictions (A2 and B2 scenarios), suggesting the lack of any analog in the modern record of things to come and indicating a drastic change in the overall mean conditions in the future. The biggest difference between A2 and B2 scenarios on both slopes appears to be the less pronounced change in standard deviation in the B2 run. This suggests that a future B2 climate might be warmer, but with an interannual variability similar to today, very much unlike what is projected for the A2 scenario.

Figure 26 shows the PDF for the western and eastern slope considering only points above 4000 m.a.s.l. and only the A2 scenario.
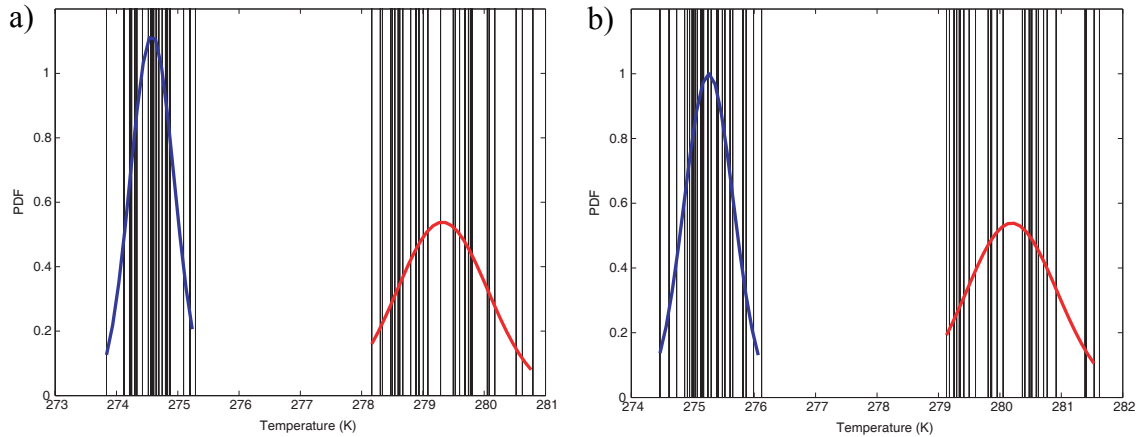
Figure 26. a) PDF for mean annual temperatures for the control and A2 scenario, considering only grid cells above 4000 m along the western slope of the Andes. b) The same as a), but along the eastern slope of the Andes. Note that the scales for eastern and western slopes are different.

According to Figure 26 a) the mean annual temperature on the western slopes is 274.5º K for the control scenario and 279.3º K for A2, yielding a difference of 4.8º K between both runs. The standard deviation corresponds to 0.35º K and 0.74º K for the two scenarios, indicating an increase of 111% in the A2 scenario when compared to the control run. Comparing these results with the previous projections based on data from all altitudes (above 100 m) suggests that changes in A2 will be enhanced at higher altitudes, both with regards to mean and standard deviation.

On the eastern slope (Figure 26 b) mean annual temperature for the control and A2 runs correspond to 275.2º K and 280.2º K, respectively. These values are 0.7º K and 0.9º K higher than the ones on the western slope, respectively. In addition differences between both scenarios are also higher, reaching a value of 5.0º K. The standard deviation for the control and A2 run corresponds to 0.39º K and 0.74º K respectively, indicating an increase of 89.7%. This difference is less than what was obtained for the western slope, mainly due to a higher standard deviation in the control run. Table 4

summarizes mean temperatures and standard deviations for the control and A2 scenario and for both slopes of the Andes.

Table 4. Average temperature (μ) and standard deviation (σ) in each PDF for control and A2 scenario and both slope of the Andes.

	Control		A2	
	μ (°)	σ (°)	μ (°)	σ (°)
Western slope	274.5	0.35	279.3	0.74
Eastern slope	275.2	0.39	280.2	0.74

The change in mean temperature at higher altitudes along the eastern slope is larger than what was obtained for all altitudes (above 400 m). However, the change in standard deviation is larger when considering all altitudes.

Unlike the results based on all elevations, temperature is higher on the eastern than on the western slope at higher altitudes (see also Figure 17). Projected changes in temperature are also slightly larger on the eastern than the western slope, despite a lower standard deviation. Differences in mean temperature and standard deviation are significant for both slopes at 95% of confidence.

3.1.3. Time-latitude diagram of the seasonal cycle of precipitation

To analyze what might be the main changes in the seasonal cycle of precipitation and the monsoon system, Figure 27 presents a time-latitude diagram of precipitation (in mm/day) averaged over longitude 50°-70° W for the control and A2 scenarios as well as their difference. These longitudes chosen are the same as in Vuille and Werner (2005) to facilitate a comparison with their results based on monthly Climate Prediction Center Merged Analysis of Precipitation (CMAP) data and the ECHAM-4 T106 AGCM for the last two decades of the 20th century.
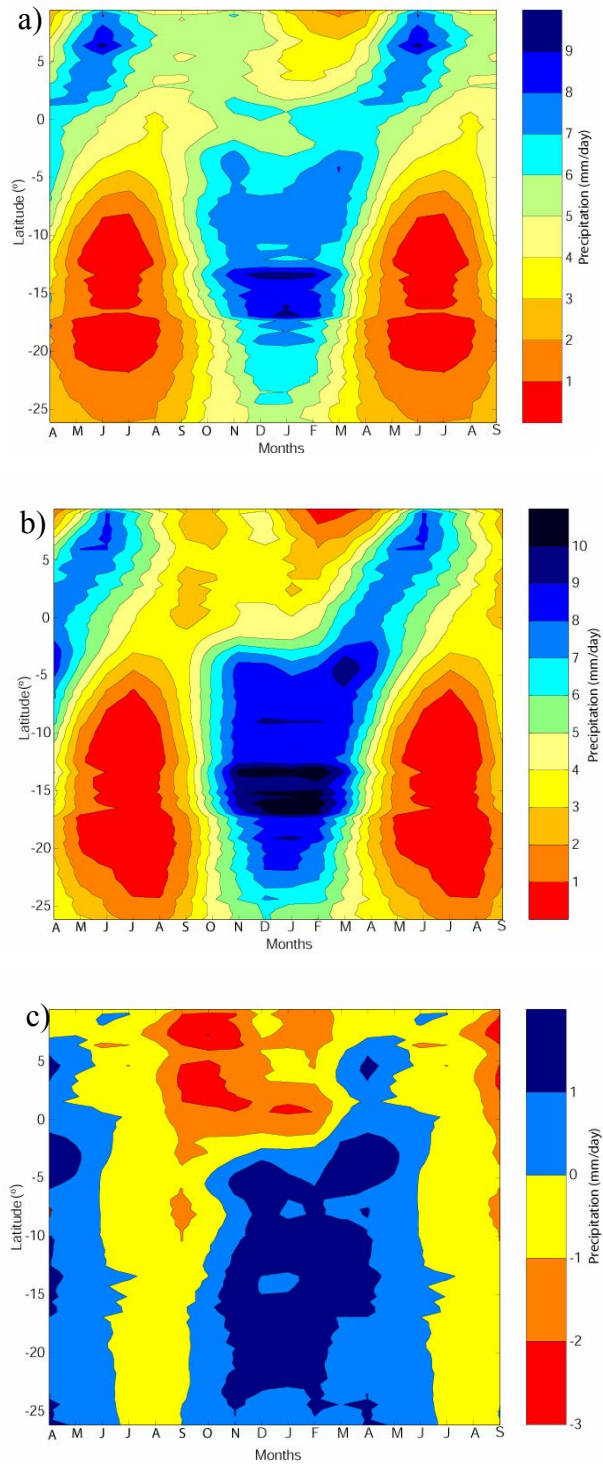
Figure 27. a) Time-latitude diagram of the seasonal cycle of precipitation (in mm/day) averaged over longitude 50º-70º W for the control scenario b) The same diagram as in a), but for the A2 scenario. c) The same as a), but for the difference between the A2 and control scenario.

Figure 27 a) and b) show the typical behavior of the South American summer monsoon (SASM), where a precipitation maximum starts developing over the southern Amazon in late spring. This onset of precipitation south of 0º is rather abrupt at this time of year, while the demise of summer precipitation is characterized by a gradual northward displacement of the zone of maximum precipitation (Vuille and Werner, 2005).

Comparing Figure 27 a) with the one obtained by Vuille and Werner (2005), it indicates that PRECIS, as ECHAM-4, correctly simulates summertime climate over tropical South America, but underestimates precipitation during the SASM season. The apparent distortion present in Figure 27 a) and b) between 12º S and 18º S is due to the enhanced precipitation seasonality of the Andes, which significantly affects the zonal average at those latitudes, but not further north or south.

The comparison of both scenarios indicates a general increase in precipitation in spring-summer-fall south of the Equator, suggesting a strengthening of the South American Summer Monsoon system (Fig, 27c). This pattern is in agreement with the projected changes in summer precipitation discussed in Figure 8. The increase in summer precipitation, combined with the simulated decrease in precipitation in winter along all latitudes, effectively leads to an enhanced amplitude of the seasonal precipitation cycle.

To observe changes along the Andes, especially south of 15º S in Central Andes, Figure 28 shows a similar time-latitude diagram, but averaged over longitudes 64º to 70ºW only.
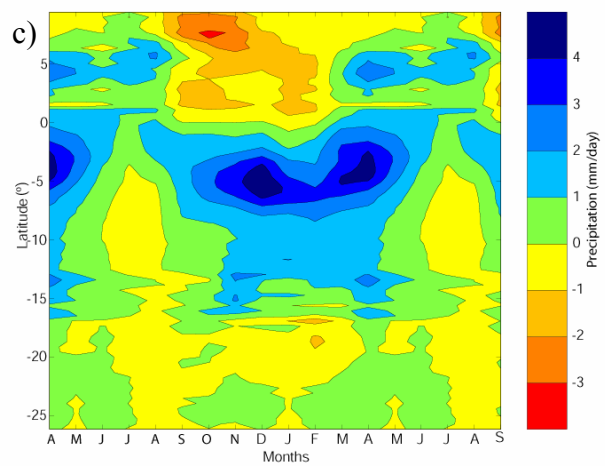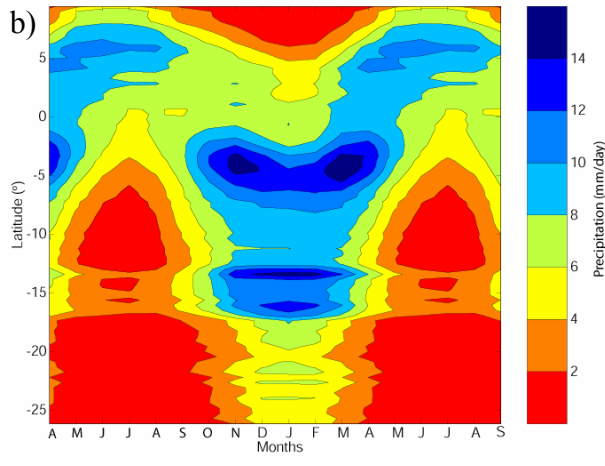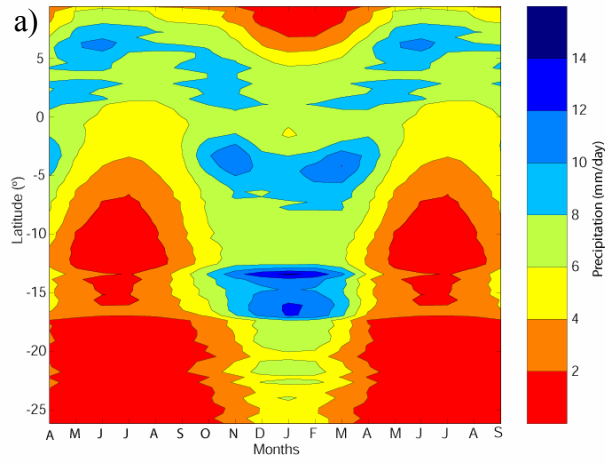
Figure 28. a) Time-latitude diagram of the seasonal cycle of precipitation (in mm/day) averaged over longitude 64º-70º W for the control scenario b) The same diagram as in a), but for the A2 scenario. c) The same as a), but for the difference between the A2 and control scenario.

South of 16º S and up to 22º S the Andes will experience a decrease in precipitation in summer according to the results presented in Figure 28c). This is in contrast with what is expected to the north of this region (the Amazon) where an increase in precipitation is projected, associated with a stronger monsoon system in South America. As it was stated before, the monsoon system also influences precipitation in the Andes; therefore an increase in precipitation could be also expected for that region. However, this is not the case basically because the monsoon is not the only element that influences precipitation in that area (especially in this case the Altiplano area), where westerlies have a high influence blocking and displacing easterlies coming from the Amazon to the Andes. A complete assessment of changes in winds will be presented in section 3.2.2.

3.2. Analysis of variables at different levels in the troposphere

3.2.1. Free tropospheric temperature

Figure 29 shows the difference in annual mean free tropospheric temperature between A2 and the control scenario and between B2 and the control run, based on ten pressure levels in the atmosphere (1000, 925, 850, 700, 600, 500, 400, 300, 250, 200 mb). Pressure levels were transformed into elevations using geopotential height.
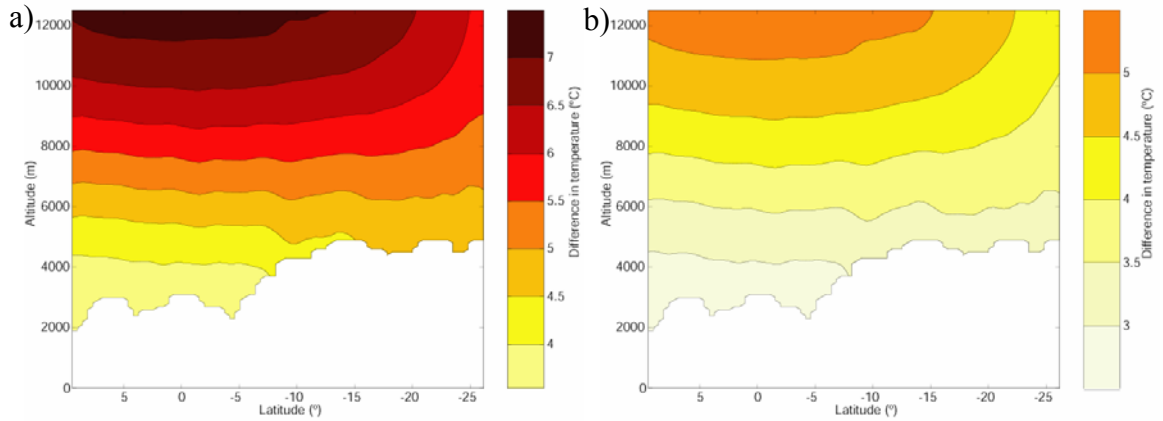
Figure 29. a) Difference in annual mean free tropospheric temperature between the A2 and control scenario. b) The same as in a), but considering the B2 and control scenario.

Annual mean free tropospheric temperature changes in the A2 scenario increase with altitude and vary between 3.5º C at approximately 2,000 m and 7.5º C at approximately 12,000 m (Fig. 29a). Differences between A2 and control run are largest in the inner tropics and decrease with increasing latitude. The larger warming in the tropics likely reflects the latent heat release associated with tropical convection.

Figure 29 b) shows that in the B2 simulation differences in free tropospheric temperature with altitude range between 2.5º to 5.5º C from approximately 2,000 m to 12,000 m. These values are 1º C and 2º C lower than the ones projected by the A2 scenario. The larger difference between low and high altitude temperature change in the A2 scenario implies a larger reduction in the free tropospheric lapse rate. However, the basic patterns of change with altitude are similar between the two scenarios.

Figure 30 shows the difference in summer free tropospheric temperature between the A2 and control scenario, and between the B2 and control run.
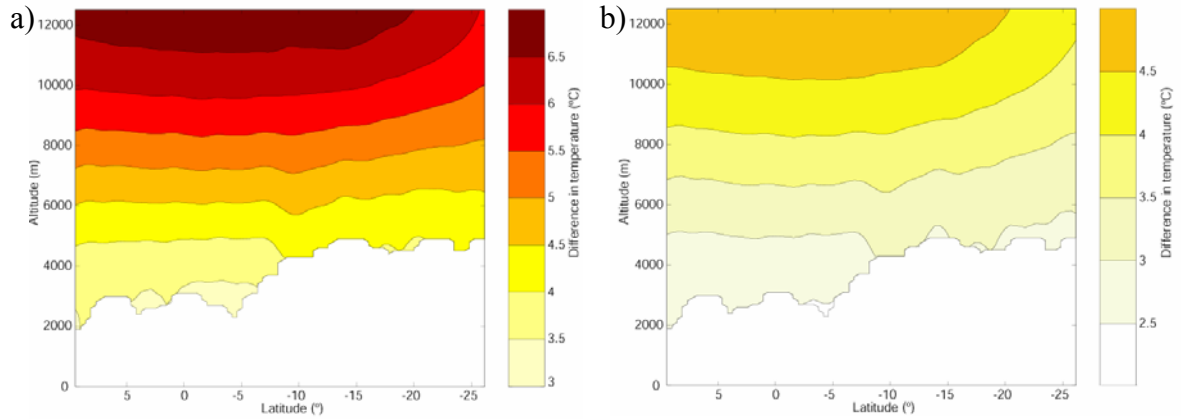
Figure 30. a) Difference in summer free tropospheric temperature between the A2 and control scenario. b) The same as in a), but for the B2 and control scenario.

According to Figure 30 a), differences in temperature range between 3º and 7ºC. These values are 0.5º C lower than those projected using annual values. Summer differences in free tropospheric temperature using the B2 scenario vary from 2º to 5º C, again being 1º and 2ºC lower than the ones projected using the A2 scenario. Similarly the range between the highest and lowest temperature change is again larger for the A2 scenario.

Figure 31 shows the difference in winter free tropospheric temperature between the A2 and control scenario, and between the B2 and control run.
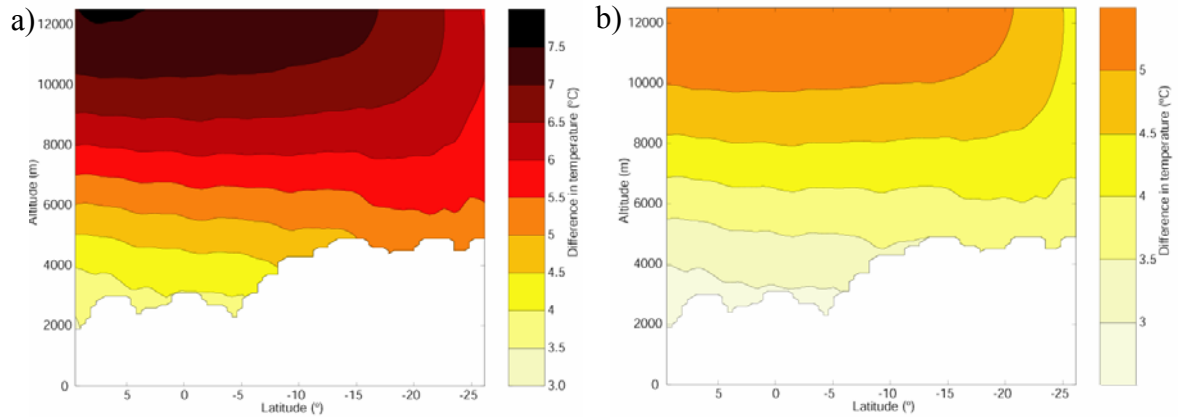
Figure 31. a) Difference in winter free tropospheric temperature between the A2 and control scenario. b) The same as in a), but for the B2 and control scenario.

Differences in winter free tropospheric temperature in the A2 scenario range between 3.5º and 8º C. The warming is on average 0.5 ºC higher than the annual mean values. In the B2 scenario the warming of winter free tropospheric temperature ranges between 2.5º and 5.5 ºC. These values are 1º and 2.5ºC lower than what is projected using the A2 scenario. Again the range between the highest and lowest temperature is smaller in the B2 than in the A2 scenario. At the same elevation the projected warming is larger in winter than in summer. This suggests a smaller amplitude of the seasonal cycle especially in the outer tropics; a condition also observed for surface temperature. In the annual mean as well as for summer and winter seasons the differences between the A2 and B2 scenario are larger at higher than at lower altitude levels. In all cases (annual, summer and winter), changes are significant at 95% of confidence for the A2 and B2 scenario.

According to Thompson (2000), warming in the free troposphere will result in a negative glacier mass balance in all of the tropical Andes due to an increase in glacier melt. Specifically, changes in free-tropospheric temperature will bring about an

adjustment in the equilibrium line altitude of glaciers. Warmer temperatures will also increase the likelihood of rainfall rather than snow in the ablation zone, thereby contributing to a lower glacier albedo. While glaciers in the inner tropics are more sensitive to changes in tropospheric temperature, the sheer magnitude of the changes projected in this study leaves little doubts that the warming would also have a large impact in the outer tropics, where nowadays glaciers are mostly located well above the freezing line.

3.2.2. Geopotential height and wind fields at selected pressure levels

To assess changes in geopotential height and wind fields between the A2 and control scenarios at different pressure levels, wind vectors are plotted together with geopotential height at 850 mb, 500 mb and 200 mb. These three levels were chosen to assess changes relatively close to the surface, at a level close to the Andean peaks and in the upper troposphere. Changes are assessed for summer only as this is the main precipitation season for most of the domain.

Figure 32 shows the geopotential height and the corresponding wind field at 850 mb for the control and A2 run in summer.
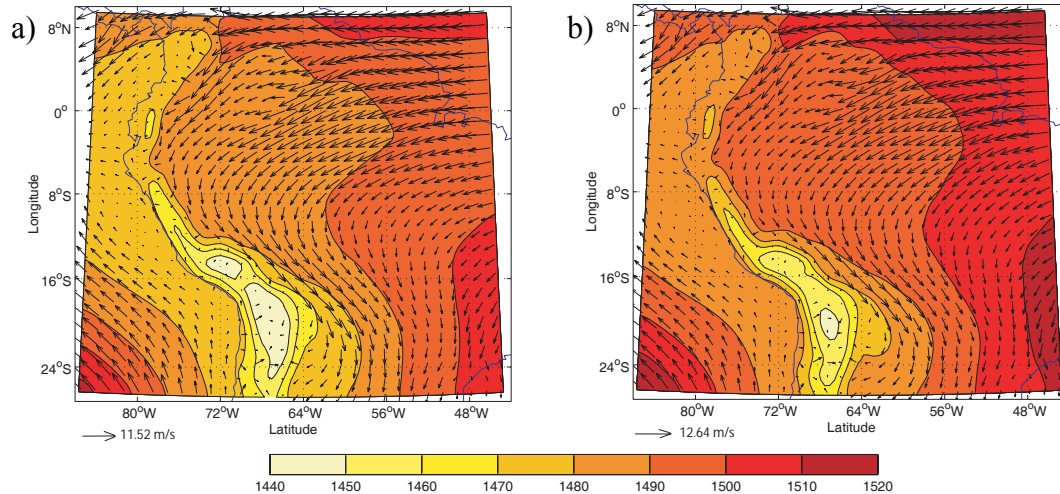
Figure 32. a) Geopotential height (in meters) and wind field at 850 mb for summer in the control scenario. The arrow at the bottom of the figure corresponds to the largest wind vector velocity. b) The same as a), but for the A2 scenario. Note different scale for wind vector in b).

The Andes Cordillera acts as a barrier, separating low level circulation to the west and east of the Andes (Vuille, 1999). Strong easterly winds from the Atlantic Ocean north of 8º S penetrate into the continent and are deflected southward once they reach the Andes Cordillera, fueling the South American Low Level Jet (SALLJ) to the east of the Andes south of 10ºS. In the southeast Pacific winds blow from the southeast to the northwest away from the continent. This offshore flow corresponds to the Southeast Pacific Anticyclone that produces dry and stable conditions, maintained by subsiding air masses and cool SST. The subsidence inversion at about 900 mb (Vuille, 1999) traps moist air and contributes to the arid climate of northern Chile and southern Peru. The geopotential height pattern in the control run features a center of high pressure in the Pacific Ocean, a center of low pressure in the middle of the continent, and likely another high pressure center towards the Atlantic Ocean (not completely shown). In the interior

of the continent, a thermal heat low (Chaco low) develops in summer and conditions in

the lower troposphere are warm and humid (Vuille, 1999; Garreaud and Aceituno, 2001).

In the A2 scenario, the observed pattern is approximately the same as the one

observed in the control run, but with generally higher geopotential height values than in

the control run. Higher values of geopotential height in the A2 scenario are expected

given the expansion of the air column with higher temperatures (Rohli, and Vega, 2007).

Thus, in a warming atmosphere a certain pressure value will be placed at a higher

altitude.

Figure 33 shows the difference in geopotential height and wind field, between the

A2 and control scenario at 850 mb.
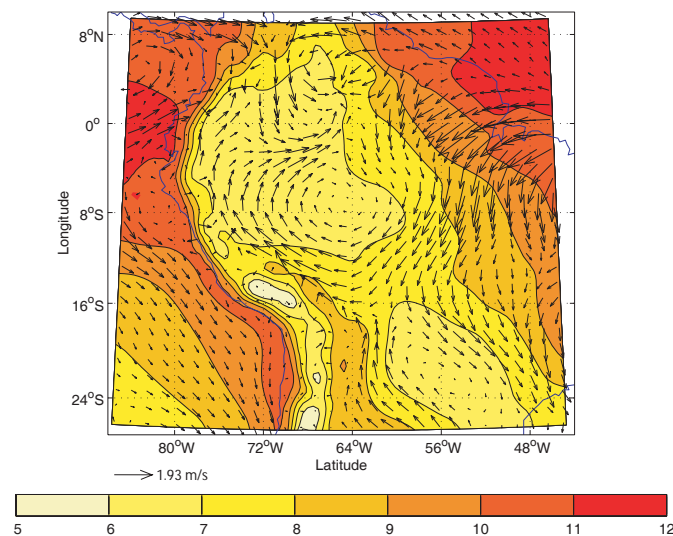
Figure 33. Difference in geopotential height (in meters) and wind field at 850 mb
between the A2 and control scenario for summer (anomalies). The arrow at the bottom of
the figure corresponds to the largest wind vector anomaly.

According to this figure differences in summer geopotential height range from 5

to 12 m with the lowest values in the interior of the continent along a diagonal across

South America from northwest to southeast. In essence this pattern reflects a steepening

of the land-sea pressure gradient, known to significantly influence the summer monsoon strength. The lowest pressure increases (6-7 m) are present over the Amazon basin and in southeastern South America over Paraguay and southern Brazil. The larger increases are present near the coastal areas and over the Pacific and the Atlantic Ocean.

The wind pattern represents a first order response to the pressure changes discussed above. The easterly trade winds are strengthened over NE Brazil due to the steeper land-sea pressure gradient. The low level jet east of the Andes is relaxed, leading to an anomalous cyclonic circulation that might produce wetter conditions in the Amazon.

The weakened southward flow from the Amazon (South American Low Level Jet, SALLJ) may cause drier conditions in southeastern South America (mostly outside the domain of study). However, this deficit appears to be compensated by enhanced low level convergence at the exit region of the SALLJ due to anomalous northward flow east of the Andes and anomalous northeasterly flux over southern Brazil, both converging over the Bolivian lowlands, which could explain the enhanced summer precipitation in this region presented in Figure 8.

The northwesterly wind anomalies off the coast of Chile and southern Peru indicate a weakening of the southeast trades over the SE Pacific. This change may occur in response to warmer SSTs and reduced subsidence and may result in wetter conditions towards the end of the 21st along the western coast of South America south of 8º S. This situation is indeed observed in the precipitation pattern for summer in the study area, and agrees with the southward displacement of the South Pacific anticyclone projected in GCMs and PRECIS for the end of this century (Garreaud and Falvey, 2008). The

poleward shift of the South Pacific anticyclone is also a robust response across the different model simulations that are archived at the Program for Climate Model Diagnosis and Intercomparison (PCMDI) and reported in the Fourth IPCC Assessment Report (AR4, Christensen et al., 2007). The weakening of the anticyclone can also be observed in the wind anomalies for winter (not shown), bringing more humid conditions to the coastal and low Andes area of western South America.

The northwesterly wind anomalies in the South Atlantic Convergence Zone (SACZ), suggest an intensification of this pattern. On intraseasonal timescales the SACZ forms a dipole pattern over southeastern South America (SESA), characterized by enhanced rainfall over the SACZ itself and decreased precipitation over the nearby subtropical plains. The opposite pattern occurs during periods of enhanced LLJ activity, transporting moisture from the Amazon toward SESA (Vera et al., 2006 a). In addition, low-level zonal westerlies over tropical Brazil in summer are related to an active SACZ and moisture divergence over the subtropical plains, denoting a weak South American Low Level Jet (Jones and Carvalho, 2002, Vera et al., 2006a). Although the SALLJ appears weakened in the future and the SACZ appears stronger, it is not possible to assess the intraseasonal variability based on the analysis shown here. In addition the weakened SALLJ does not appear to reduce precipitation at its exit region, mainly because of the low-level convergence in that area that might enhance moisture influx to the subtropical plains. Finally the enhanced onshore flow along the coast of Ecuador is noteworthy and together with a larger warming in that area, might help explain the significant increase in precipitation expected for that area in summer (see Fig 8c).

Figure 34 shows the summer geopotential height and wind field at 500 mb for the control and A2 run.
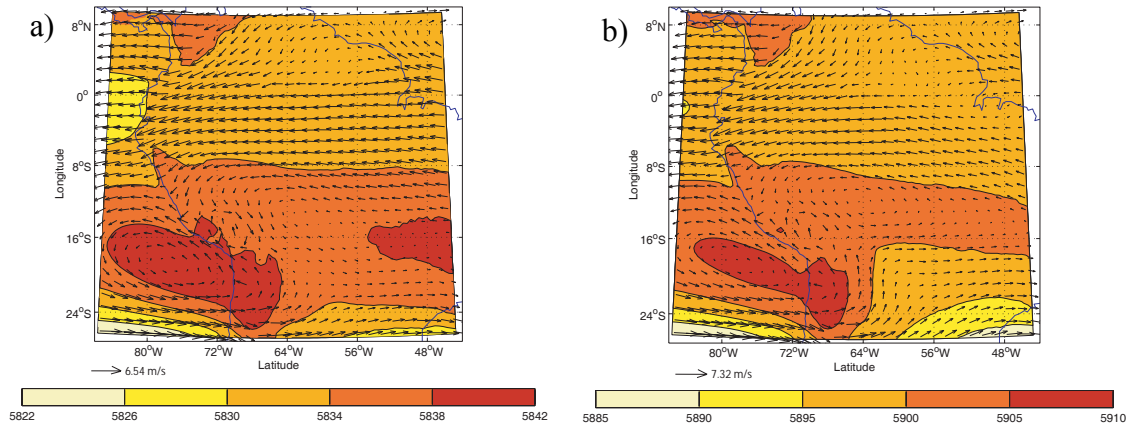
Figure 34. a) Geopotential height (in meters) and wind field at 500 mb for summer in the control scenario. The arrow at the bottom of the figure corresponds to the largest wind vector velocity. b) The same as in a), but for the A2 scenario. Note different scale for both geopotential height and wind vector in b).

The highest values of summer geopotential height are located along the Andes and over the Pacific Ocean mainly south of 16º S. The lowest values are also located over the ocean, but south of 25 ºS. The difference between the lowest and highest values is 20 m. The resulting wind field is characterized by strong easterlies that cross the continent mainly north of 12ºS, by strong westerlies south of 22ºS, and by an anticyclonic vortex around the area of highest geopotential height. This anticyclonic pattern corresponds to the Bolivian High, but it is displaced westward of its regular position in the model.

The geopotential height pattern and wind field in the A2 scenario is similar to the one for the control run, but geopotential height values are much higher. A slightly more meridional circulation over the southeastern part of the domain with and enhanced southerly component is also notable.

Figure 35 shows the difference in geopotential height and wind field between the A2 and control scenario at 500 mb for summer.
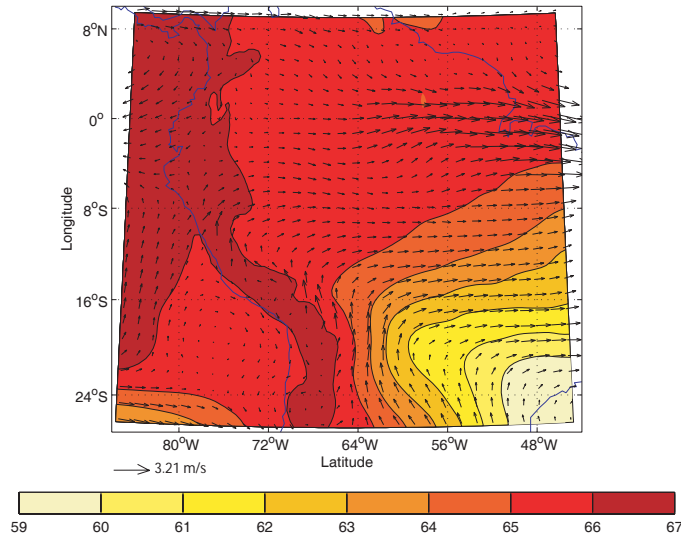
Figure 35. Difference in geopotential height (in meters) and wind field at 500 mb for summer between the A2 and control scenario. The arrow at the bottom of the figure corresponds to the largest wind vector anomaly.

The largest differences (up to 67 m) in summer geopotential height between the A2 and control run occur along the Andes Cordillera and over the Pacific Ocean mainly north of 20º S and west of 80 ºW. The Andean pattern should be interpreted cautiously as it is likely caused by the model topography either intersecting with or distorting geopotential height in the vicinity of the Andes. The smallest geopotential height increase is located over southeastern South America. The resulting east-west pressure gradient leads to a weakening of the easterly winds (westerly anomalies) especially over eastern South America near the equator. The slight imprint of a cyclonic circulation anomaly to the west of the Altiplano suggest a minor weakening of the Bolivian High, which could potentially cause drier conditions over the Altiplano.

Figure 36 shows the summer geopotential height and wind field at 200 mb for the control and A2 run.
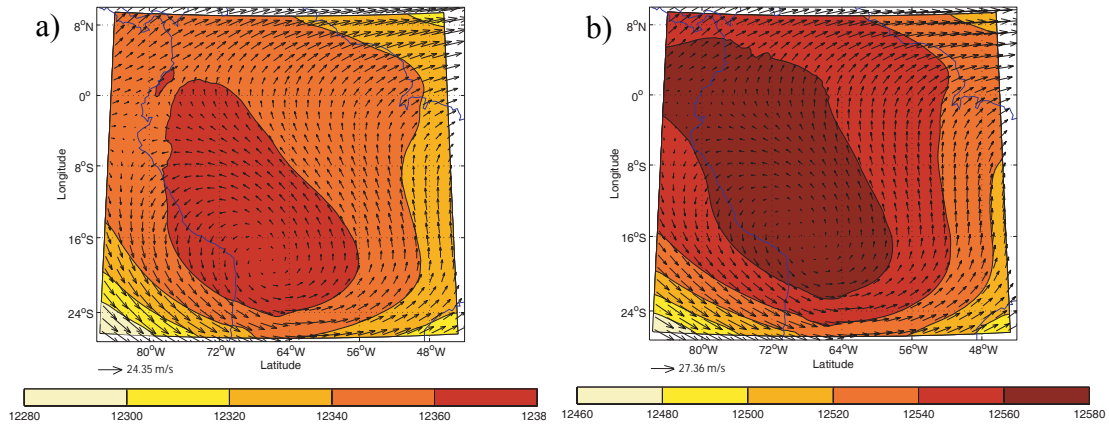

Figure 36. a) Geopotential height (in meters) and wind field at 200 mb for summer in the control scenario. The arrow at the bottom of the figure corresponds to the largest wind vector velocity. b) The same as a), but for the A2 scenario. Note different scale for both wind vectors and geopotential height in b)

The control run shows a well-defined upper level anticyclone (around 18º S and 66 ºW), that corresponds to the Bolivian High, close to its observed climatological location. The difference between the highest and lowest value simulated over the domain is approximately 100 m. The strongest winds are observed at the upper-tropospheric monsoon exit region near the mouth of the Amazon in the area north of 3ºN. Northwesterly winds to the southwest of the Bolivian High over the Pacific Ocean are also strong.

In the A2 scenario the pattern is the same as in the control, but as always higher geopotential height values are present in A2. The difference between the highest and lowest values is also larger in A2 (120 m) than in the control run, suggesting a more vigorous circulation. The Bolivian High appears to be displaced slightly to the north and

west of its original position, indicating a mechanism which could explain potentially drier conditions affecting the Altiplano at the end of this century.

Figure 37 shows the difference in geopotential height and wind field at 200 mb between the A2 and control scenario.
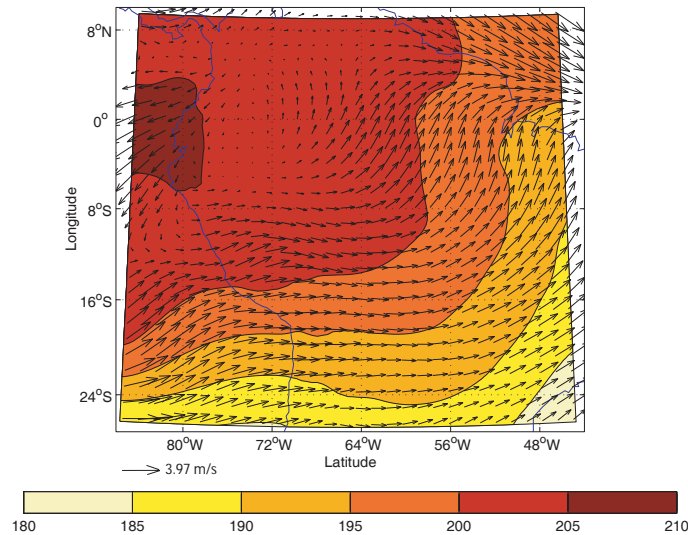

Figure 37. Difference in geopotential height (in meters) and wind field at 200 mb for summer between the A2 and control scenario. The arrow at the bottom of the figure corresponds to the largest wind vector anomaly.

This figure shows that a large increase in geopotential height (up to 210 m) takes place over the coast of Ecuador and northern Peru and over the adjacent equatorial Pacific. The smallest increase occurs over southeastern South America. As a result the NW-SE tilting of the atmosphere is enhanced, which is dynamically consistent with the increased warming near the Equator, where the surplus of heat increases the kinetic energy of the gases, causing molecules of air to expand upward (Rohli and Vega, 2007).

The changes in the wind field are in geostrophic balance with the observed pressure changes. The most important change in the wind field corresponds to the reinforcement of the westerly wind anomalies and the Subtropical Jet south of 16ºS due

to the enhanced meridional baroclinicity (enhanced meridional temperature gradient, see also Figure 30) in the A2 scenario and the associated weakening of the Bolivian high at that latitude. This change in the atmospheric circulation will likely increase the occurrence of dry periods on the Altiplano, since westerly winds in this area tend to inhibit moisture influx from the east (Vuille, 1999). Due to the geopotential gradient, this westward flow continues eastward and strengthens in a northeast direction; ultimately merging with anomalous westerly flow at the monsoon exit region. This anomalous upper-air return flow is a key component of the SASM (Zhou and Lau, 1998) and its strengthening is consistent with the simulated intensification of the SASM as seen in the previous analysis of precipitation (Fig. 27).

In conjunction with the reinforcement of westerly winds, the easterly flow that characterizes the Cordillera Blanca during summer appears to weaken at the end of this century as well, probably also leading to drier conditions in that area.

3.2.3 Summer vertical motion at 500 mb

In order to assess changes in the large-scale ascent and subsidence in summer for the region, Figure 38 presents the vertical velocity at 500 mb for summer in the control and A2 scenario.
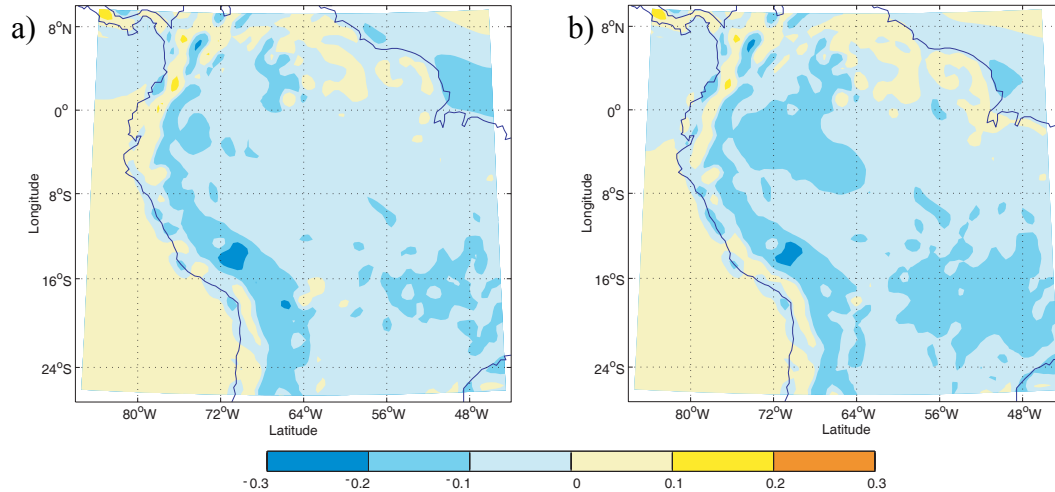
Figure 38. a) Summer vertical velocity (Omega (ω)) at 500 mb in the control scenario. Negative values indicate upward motion and positive values subsidence. b) the same as a), but for the A2 scenario.

Upward motion characterizes most of the Andes region, especially along the eastern slope, and the interior of the continent especially south of the equator. Downward motion or subsidence dominates over the southern Pacific Ocean and contributes to the formation of the subtropical anticyclone, and over the northern part of the continent, where DJF represents the dry season. The pattern in the A2 scenario is very similar, although some areas feature enhanced upward or downward motion in the future.

Figure 39 shows the difference in vertical velocity between the A2 and control scenario and indicates where the A2 vertical velocity values are significantly different from control values at 95% of confidence.
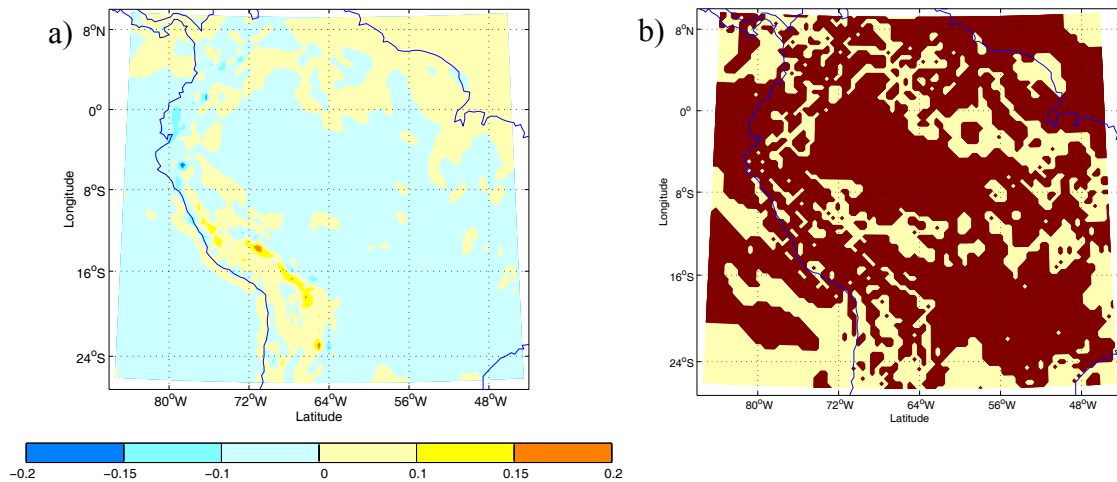
Figure 39. a) Differences in summer vertical velocities at 500 mb, between the A2 and control scenarios. Negative values indicate an enhanced upward flow or decrease in subsidence and positive values indicate a decrease in upward flow or increase in subsidence. b) Map showing where summer values are significantly different between both scenarios. Areas in dark red are significantly different at 95% of confidence.

The upward motion is reduced along the eastern slope of the Andes Cordillera and the Altiplano (positive differences), indicating drier conditions for that area. In northeastern South America, subsidence increases in A2 also leading to drier conditions. Both patterns can be also appreciated in the context of simulated changes in precipitation, as both areas appear affected by a decrease in precipitation in summer (Figure 8). In the case of the Andes this pattern is also consistent with the weakening of the easterlies and strengthening of the westerlies observed at mid and upper levels in the atmosphere (Fig. 37), causing drier conditions in that area. Over the Pacific Ocean, in coastal and Andean areas of Ecuador and northern Peru Figure 39 indicates reduced subsidence or even an increase in motion in the A2 scenario. Again this pattern is in agreement with the large increase in precipitation projected for that area, related to the appearance of strong onshore winds from the ocean, which are forced upslope upon reaching the Andes.

The decreased subsidence over the Pacific Ocean on the other hand does not lead to an increase in precipitation (Figure 8). Along the Pacific coastal area south of 8º S a mixed pattern with predominantly negative changes can be observed, consistent with the simulated increase in summer precipitation shown in Figure 8. Finally, in the interior of South America enhanced upward motion over the NW and SE agrees with the pattern found in Figure 8 for summer surface precipitation, demonstrating a stronger monsoon system in the A2 scenario.

It is important to highlight the agreement between the increase in precipitation found for the monsoon area in South America, the enhanced upward motion at 500 mb in this same region, the strengthening of the upper-tropospheric monsoonal outflow towards North Africa and the anomalous cyclonic flow at 850 mb, all indicating a future strengthening of the SASM..

3.2.4. Total fractional cloud cover

In order to assess probable changes in cloud cover and their effects on climatic conditions in the future, the following figures address expected changes in annual, summer and winter total fractional cloud cover for the A2 scenario.

Figure 40 shows the annual cloud cover in the control and A2 scenario.
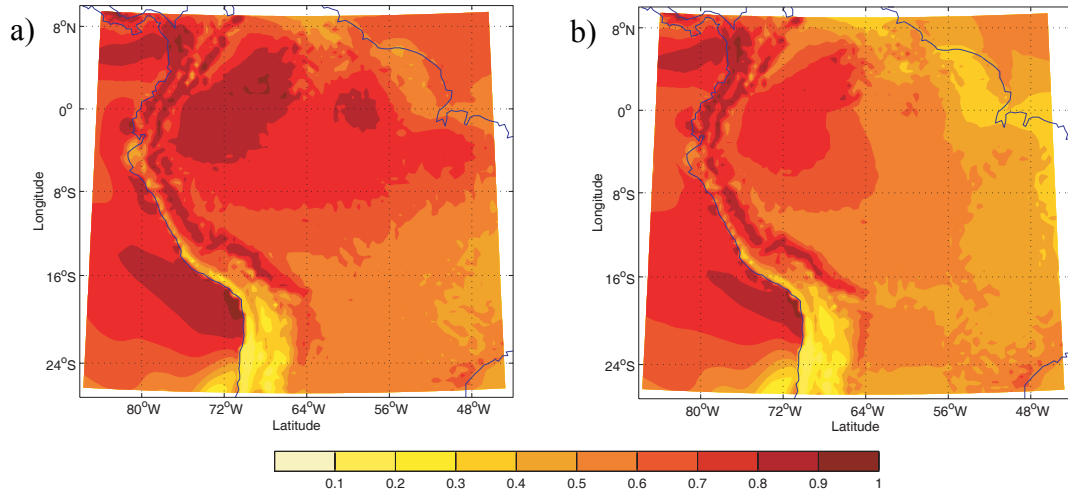
Figure 40. a) Annual total fractional cloud cover for the control scenario b) the same as a), but for the A2 scenario

Areas with the highest cloud cover in the control run are located in the northwestern Amazon basin, along the Andes of Colombia and Ecuador, along the eastern slope of the Andes Cordillera from 9º N to 16º S and off the coast of Colombia, northern Chile and Peru. The lowest values are located over the Atacama desert along the coastal area and Andes Cordillera south of 16º S. Looking at the A2 scenario the main difference is that the cloud proportion over the Amazon basin and northeastern Brazil decreases.

Figure 41 shows the difference in annual cloud cover amount between the A2 and control scenario and a map showing if the mean values are significantly different between the two scenarios.
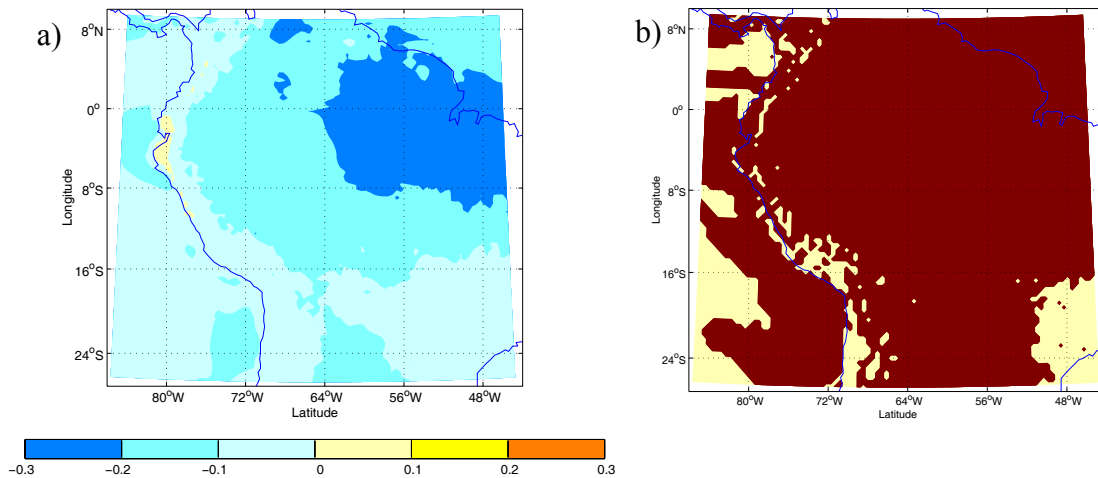
Figure 41. a) Difference in annual total cloud cover between the A2 and control scenario. b) Map showing where mean values are significantly different between A2 and control scenarios at 95% of confidence. Areas in dark red correspond to areas where mean values are significantly different between both scenarios.

Annual mean cloud cover decreases almost everywhere in the A2 scenario. The only areas which see an increase are the coast of Ecuador and northern Peru and some isolated areas in the Andes of Colombia. The largest decrease in cloud cover is located over northeastern South America, the same region where the largest decrease in precipitation (up to 50% decrease), the largest increase in temperature, the largest decrease in relative humidity and the smallest increase in specific humidity are projected.

The decrease in total fractional cloud cover over northeastern South America could help explain the large warming in that area due to higher receipts of solar radiation. On the other hand, the small area in coastal Ecuador and northern Peru with a projected increase in cloud cover corresponds with the region of largest relative increase in precipitation in South America. Most of the differences are significant, except for some areas along the Andes Cordillera, over the Pacific Ocean, and in southeastern South America.

A decrease in cloud cover over the Andes (albeit not significant everywhere) would suggest an increase in short-wave radiation received at the glacier surface. Due to the expected decrease in precipitation in the outer tropics (especially in the Altiplano area) and the increase in temperature in the inner tropics (causing more precipitation to fall as rain rather than snow), glacier albedo is expected to decrease as well, which would effectively enhance absorption of shortwave radiation. However, long-wave incoming radiation may be reduced as well due to the reduction in cloud cover, so the effects on net radiation at the glacier surface are not entirely clear,

It is important to note the discrepancy between the expected reduction in cloud cover over the interior of South America and the increase in annual mean precipitation (Figure 7) predicted for that area (including SESA). One possible explanation is that the intensity of rainfall may become stronger, which is not necessarily reflected in the total fractional cloud cover. For one, not all clouds produce precipitation. Hence the total cloud cover may be reduced, but probably the relative proportion of different types of clouds (convective / stratiform) that are present have also changed. A more detailed analysis of various cloud types in A2 and control run would be necessary to conclusively answer this question.

The notion of more intense precipitation agrees with a projection of extreme events using two AOGCMs that predict more intense wet days per year over a large portion of SESA and central Amazonia (Hegerl et al., 2004). It is also consistent with a projection using a multi-model ensemble for the end of the 21st century based on the SRES A1B scenario, where the increase of precipitation intensity was found to be largest in the tropics and south-central South America (Meehl et al., 2005). This expected pattern

of changes in precipitation intensity is associated with increased water vapor availability in a warmer future, leading to increased precipitation within any given event (Meehl et al., 2005).

Figure 42 shows the total summer cloud cover amount for the control and A2 scenario.
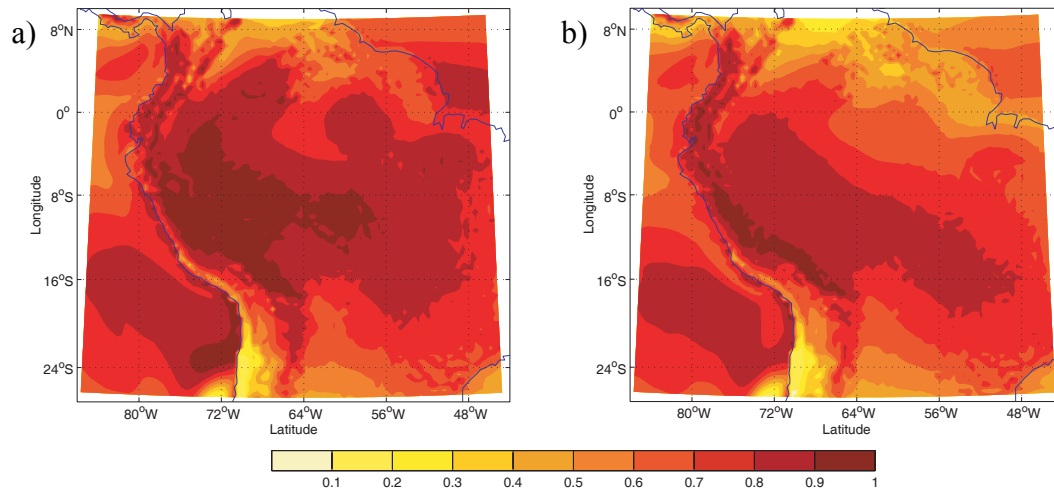
Figure 42. a) Summer total fractional cloud cover in the control scenario. b) The same as a), but for the A2 scenario.

The highest cloud cover values (between 0.9 and 1.0) in the control scenario are located over the southwestern Amazon basin that includes parts of Brazil, Peru and Bolivia, in some areas of the Andes of Bolivia, Peru, Ecuador and Colombia, and over the ocean along the coast of southern Peru and northern Chile. The high proportion of cloud cover over the interior of South America reflects the mature phase of the monsoon system. The lowest values are located over northern South America and along the coastal area and the Andes south of 20º S. In the case of the A2 scenario values above 0.9 are limited to areas along the eastern slopes of the Andes.

Figure 43 shows the difference in summer fractional cloud cover between the A2 and control scenario and a map showing if the mean values are significantly different between the two scenarios.
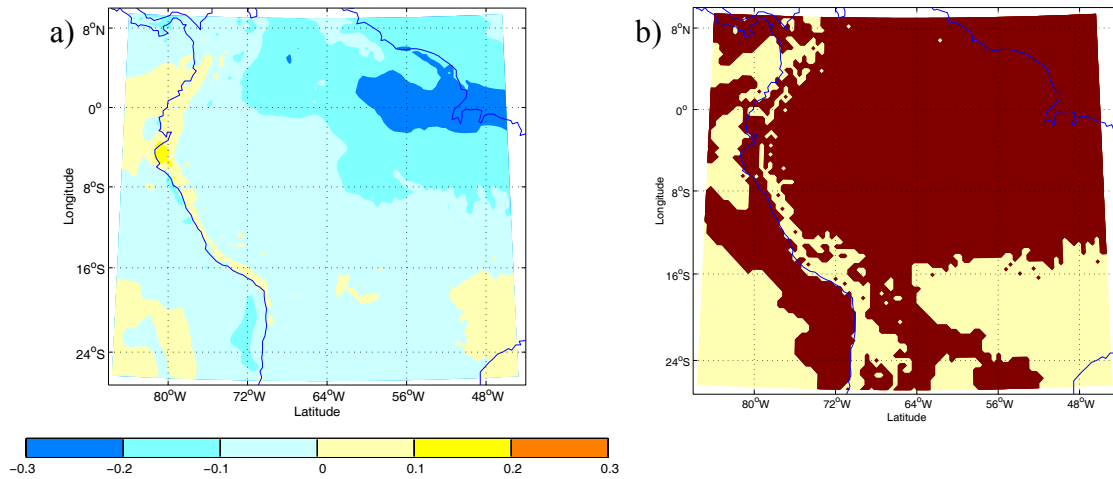

Figure 43. a) Difference in summer total fractional cloud cover between the A2 and control scenario. b) Map showing where mean values are significantly different between A2 and control scenarios at 95% of confidence. Areas in dark red correspond to areas where mean values are significantly different between both scenarios.

Most of the study area is dominated by a decrease in summer cloud cover, with the most negative values over northeastern South America where summer precipitation decreases up to 100% (Fig. 8c). However, there are some areas where summer cloud cover increases in the A2 scenario, for example along the coast of Ecuador and northern Peru where a significant increase in precipitation is simulated. Summer cloud cover also increases along the western slope of the Andes and coastal areas between 6º N and 20º S (which also show an increase in precipitation), over some areas of the Pacific Ocean and over southeastern Brazil where the SACZ is located. In the latter region an increase in precipitation is also simulated. However, the last two areas mentioned mainly present insignificant differences.

107

Again, for reasons discussed above, the decrease in cloud cover in the interior of South America does not reflect the increase in summer precipitation and the enhanced upward motion in the mid-troposphere expected for that region (Figures 8 and 39, respectively).

Figure 44 shows the total fractional cloud cover amount for winter for the control and A2 scenario.
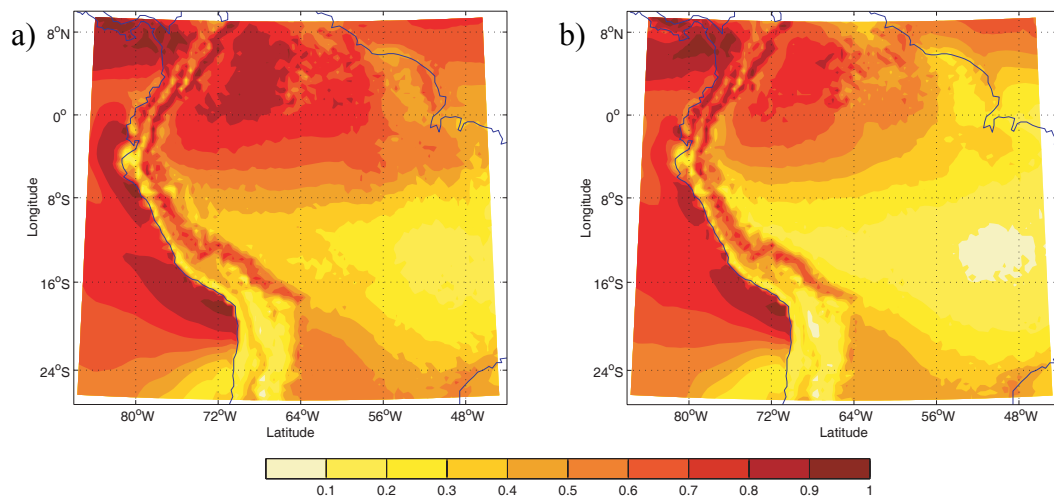
Figure 44. a) Winter total fractional cloud cover for the control scenario. b) The same as a), but for the A2 scenario.

Winter cloud cover in the control run is characterized by low cloud cover in the interior of the continent between 8º and 20º S. The Central Andes are also largely cloud-free. Higher amounts of cloud cover are located over northern South America, reflecting the seasonal march of precipitation in South America.

Figure 45 shows the difference in total winter cloud cover amount between the A2 and control scenario and a map showing if the mean values are significantly different between the two scenarios.
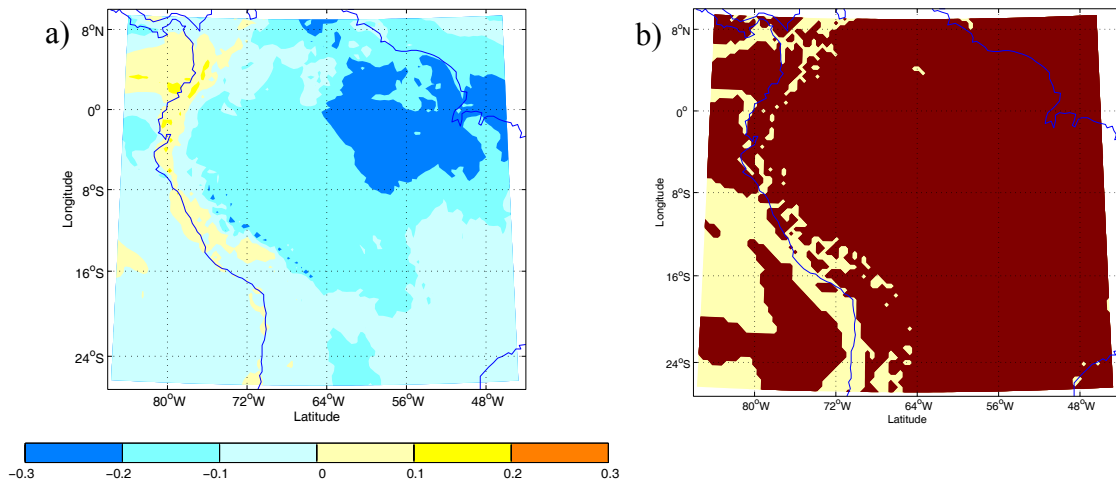
Figure 45. a) Difference in winter total fractional cloud cover between the A2 and control scenario. b) Map showing where mean values are significantly different between A2 and control scenarios at 95% of confidence. Areas in dark red correspond to areas where mean values are significantly different between both scenarios.

Again a decrease in cloud cover characterizes most of the continent in winter. Increased cloud cover is observed over the Andes and coastal areas north of 16 ºS, although in some areas the difference is not significant. The change in winter cloud cover largely matches the one presented for winter precipitation (Figure 9), except for the mismatch between increase in precipitation and decrease in cloud cover projected for the northwestern Amazon basin. This conundrum is basically the same as discussed previously for summer and annual mean values and might again be explained by an increase in precipitation intensity.

3.2.5. Pressure-longitude cross sections of zonal wind and vertical velocity.

Figure 46 shows pressure-longitude cross-sections of zonal wind and vertical velocity from 55º to 85º W, at 16ºS (the Altiplano region) for summer in the control and A2 scenario.

109
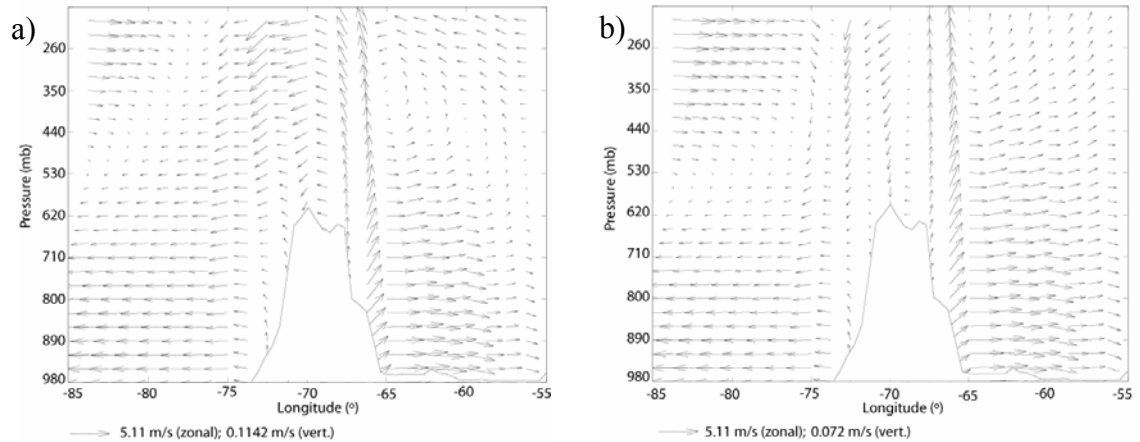
Figure 46. Pressure-longitude cross section of zonal wind and vertical motion at 16ºS for DJF in the control scenario. b) as in a) but for the A2 scenario. Note different scale for vertical motion in b).

The upslope flow along the eastern slope of the Andes advects moisture from the continental lowlands towards the Altiplano (Fig. 46a). Strong easterly zonal flow dominates aloft the Cordillera. In the A2 scenario, the basic pattern is similar but the upper-air easterlies are considerably weaker and there is reduced upward motion over the central and eastern part of the Altiplano.This is much more evident in Figure 47, which shows the differences in zonal wind and vertical velocity between the A2 and control scenarios.
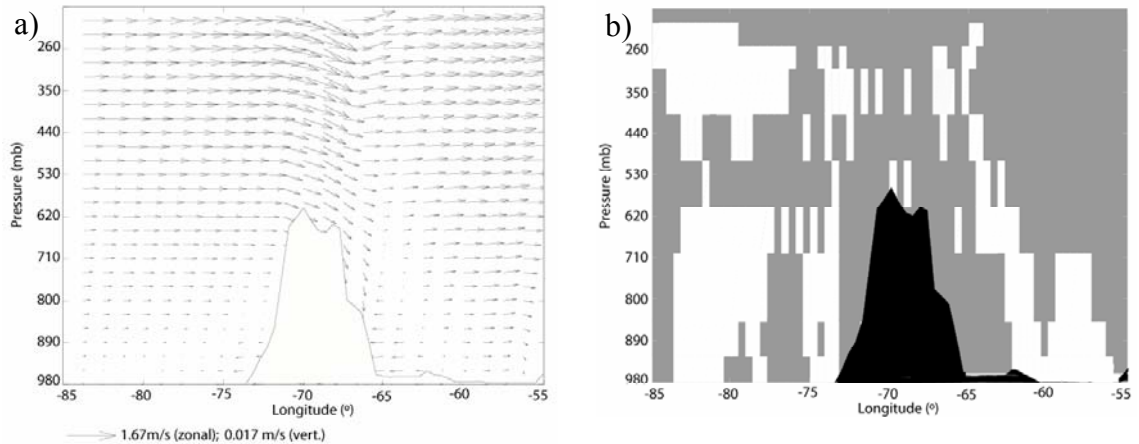
Figure 47. a) Pressure-longitude cross section of the difference in zonal wind and vertical motion between the A2 and control scenario at 16ºS and for DJF. b) Cross section showing where mean values in zonal wind and/or vertical velocity are significantly different between A2 and control scenarios at 95% of confidence. Areas in grey correspond to significant changes between both scenarios

Clearly the easterlies in the upper troposphere are weakened in A2 as manifested by the anomalous westerlies observed throughout the cross-section. The upslope flow to the east of the Andes is also weakened, likely due to the entrainment of the near-surface flow due to downward mixing of westerly momentum from higher levels. The circulation changes portrayed in Figure 47 clearly suggest drier conditions in the Altiplano region at the end of this century.

Hence it appears as if the projected decrease in precipitation in the Altiplano under the A2 scenario might mainly be occurring in response to changes in the zonal wind field (even when changes are not significant in all areas). Despite the projected intensification of the South American Monsoon, the Altiplano region might face drier conditions because the stronger westerlies might inhibit enhanced moisture influx from the east (Garreaud et al., 2003).

To test if this change in zonal circulation is also valid further north, the same analysis was repeated over the Cordillera Blanca at approximately 9º S. In this Cordillera the relationship between glacier mass balance and precipitation is stronger and more widespread than with temperature (Vuille et al., 2008b). Therefore, looking at probable changes in atmospheric circulation that can have an impact on precipitation is of fundamental importance in this mountain range with the highest percentage of tropical glaciers in the world.

Figure 48 shows the pressure-longitude cross section of zonal wind and vertical velocity at 9º S for summer in the control and A2 scenario.
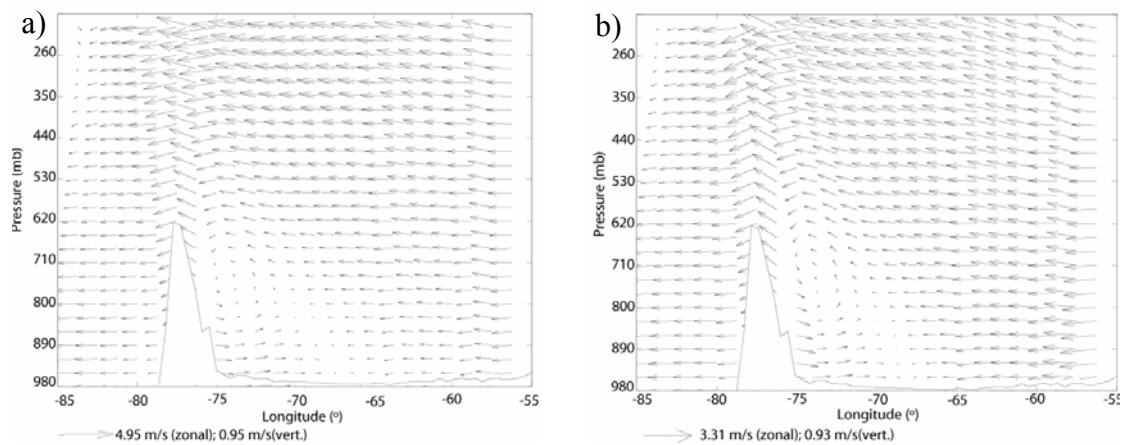
Figure 48. Pressure-longitude cross section of zonal wind and vertical velocity at 9ºS for DJF in the control scenario. b) as in a) but for the A2 scenario. Note different scale for both zonal and vertical components in b).

As seen in the control run, winds at all levels are easterlies, except in near-surface levels to the east of the Andes, where westerlies related to the SALLJ dominate. This pattern is consistent with the observed conditions that characterize the Cordillera Blanca in summer. The circulation is dominated by upper-level cold easterlies which, through downward mixing, enhance moisture advection in the near surface, thereby causing wet

conditions in the high Andes (Vuille et al., 2008b). In the A2 scenario, the pattern is

similar, but of different magnitude.

Figure 49 shows the differences in zonal and vertical components between the A2

and control scenarios in the Cordillera Blanca.
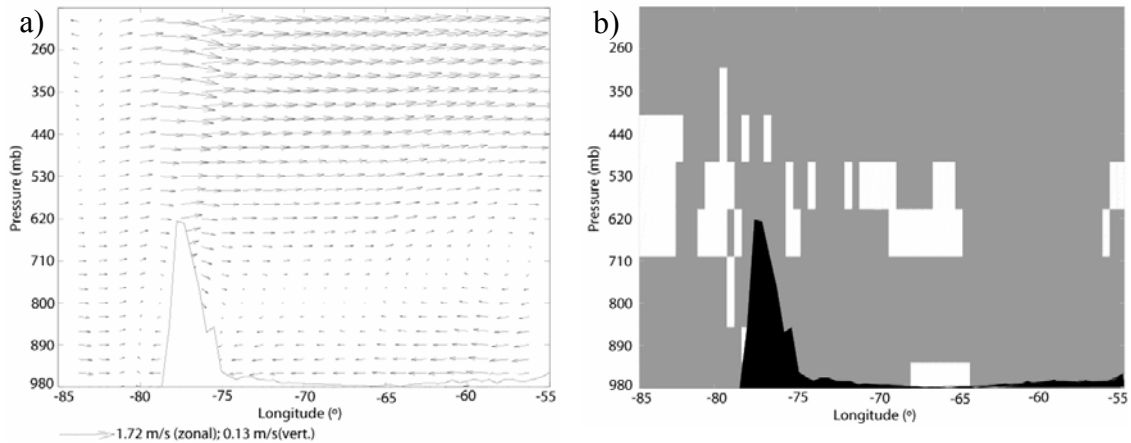
Figure 49. a) Pressure-longitude cross section with differences in zonal wind and vertical velocity between the A2 and control scenarios for Cordillera Blanca. b) Cross section showing where mean values in zonal wind and/or vertical velocity are significantly different between A2 and control scenarios at 95% of confidence. Areas in grey correspond to significant changes between both scenarios.

As already observed over the Altiplano, the easterly flow at different altitudes

weakens in the A2 scenario, thereby reducing the influx of humid air to the Cordillera

Blanca. Hence conditions might equally be expected to become drier at the end of this

century.

The present and future mechanisms operating in both the Altiplano and the

Cordillera Blanca seem to be very similar, where the easterlies provide the main

mechanism for moisture influx, responsible for wet conditions in the Andes. In both

locations a weakening of these winds appears to be the scenario we can expect for the

future.

Looking at the wind mechanism and its projected change in the Altiplano and Cordillera Blanca, it is important to point out that this is the same mechanism through which ENSO influences these two areas and the corresponding glacier mass balance on interannual timescales. According to Vuille et al., (2008b), mechanisms linking ENSO with glacier mass balance are similar in both regions. Thus, changes in the meridional temperature gradient between tropical and mid-latitudes, related to ENSO SST anomalies, interrupt the upper tropospheric flow inducing westerlies and easterlies in El Niño and La Niña years, respectively. This irregular upper-tropospheric flow is the main factor responsible for the reduced and increased moisture influx from the east and consequently for the anomalously dry (El Niño) and wet (La Niña) conditions. Nevertheless, this mechanism is stronger to the south, over the Altiplano Region, and does not influence Cordillera Blanca during all ENSO events. Hence, in the case of Cordillera Blanca there is not such a close linear relationship between ENSO and glacier mass balance as over the Altiplano region.

CHAPTER 4

DISCUSSION

4.1. Comparison of results with other climate predictions in South America

In this section projected changes in different climatic variables resulting from this study are compared with the ones obtained by other authors for South America. Most of the future climate projections developed so far for this area have been based on GCMs (Bradley et al., 2004; Bradley et al., 2006; Boulanger et al., 2006; Boulanger et al., 2007; Vera et al., 2006c; Li et al., 2006). In addition, there are two studies based on RCMs for tropical-subtropical South America, one coupled with a potential vegetation model (Cook and Vizy, 2008) and another one that uses the regional climate model PRECIS, but has only been assessed for Chile at a 25 km x 25 km resolution (Fuenzalida et al., 2007). A third study based on RCMs by Garreaud and Falvey (2008), is not considered here, because it is mostly focused in north-central Chile to the south.

Results from this study show a much larger warming than what was presented by Boulanger et al. (2006), who predict an increase in mean annual temperature of only up to 4 ºC in tropical areas for the end of the 21st century. Their projection used one simulation each of seven different atmospheric-ocean global circulation models based on the A2 scenario. The discrepancy between Boulanger et al. (2006) and this study might in part be due to the lower resolution of GCMs, which does not allow a more regional definition of changes. However, both studies agree in the location of the places that could see the largest warming such as the Colombia-Venezuela regions and the Central Amazon. In addition, both studies agree in that the warming of the tropical Pacific could reach between 3º and 4º C.

As in the case of annual differences, comparing seasonal results with the ones obtained by Boulanger et al., (2006), also shows much larger warming in the present study. However, some results obtained here, such as the strong warming found in parts of the Colombia-Venezuela region in DJF, and the much stronger and widespread warming in winter (especially in the Amazon) than in summer are in agreement between both studies. This last factor would contribute to a smaller amplitude of the seasonal cycle of temperature as projected by both studies. On the other hand, important discrepancies also exist. For example the strongest warming observed in northeastern Brazil in all seasons in the present study is not observed in Boulanger et al. (2006). On the other hand Boulanger et al., (2006) project the largest warming to occur along the coasts of Chile and Peru, which is not the case in the present study. Finally in Boulanger et al., (2006) the warming in some cases seems to be equal or stronger in the summer than in the winter along the Andes region.

With regard to precipitation, the increase in mean annual precipitation along the coast of Ecuador and the decrease in precipitation in northern South America (parts of Colombia and Venezuela) in the A2 scenario are consistent with what was simulated by Boulanger et al., (2007) for the end of this century. In their study, such as in the case for temperature, Boulanger et al., (2007) used one simulation from each of seven different AOGCMs based on the A2 scenario. They also mentioned that the decrease of annual precipitation over Colombia and Venezuela could have an extension over the mouth of the Amazon; a situation that is in agreement with what has been found in this report. It is important to note that the models used in Boulanger et al., (2007) strongly disagree about

the evolution of precipitation over the Amazon region, which precludes corroborating the increase in precipitation in the interior of South America found in the present study.

Predicted changes in summer and winter precipitation do not correspond with the ones simulated by Boulanger et al., (2007), mainly because their results show a precipitation increase in austral summer in northern South America, an increase in austral winter precipitation in NE Brazil, a weaker summer monsoon and a decrease in precipitation in the area of influence of the SALLJ, all of which are not projected in the present study.

Despite the discrepancies in seasonal predictions of precipitation with Boulanger et al., (2007), our results are in agreement with the ones obtained by Vera et al., (2006c) using seven IPCC AR4 models based on the A1B scenario at the end of this century. Both studies basically agree in the prediction of an increase in precipitation in the wet season and a decrease in the dry season, in the increase of summer precipitation over the Andes of Ecuador and Peru and in SESA, and in the widespread pattern of decrease in precipitation in winter. Results obtained by Vera et al., (2006c) are also mixed for the Amazon basin.

It is important to mention that in general climate models provide better simulations for temperature patterns, while they have low skill in simulating precipitation (Boulanger et al., 2007). Models strongly differ from each other and from observations, and therefore the projections obtained should be viewed as suggestive of possible projections based on the models available to date, which might change in the future as models improve.

Li et al., (2006) used 11 GCMs from the IPCC AR4 to predict rainfall in South America under the A1B scenario, including the HadCM3 model. There is only partial agreement between HadCM3 results in Li et al. (2006) and this study. HadCM3 projects a decrease in rainfall by 2101-2130 during the wet and transition seasons for the Amazon with the largest values in the central and eastern tropical basin, unlike PRECIS which only project such a decrease for northeastern South America and not for the entire Amazon. In addition, the HadCM3 projects a one to three month increase in the length of the dry season, which, although not completely evaluated in this study, was not observed in the Hovermuller diagram for part of the Amazon region (Figure 27). This difference in simulated precipitation changes over the western Amazon is a clear discrepancy between PRECIS and its driving model, indicating that the regional model may indeed add useful new information to the prediction due to the ability to simulate meso-scale processes, not resolved in the GCM. It is important to consider although that the periods of time are different, a factor that could be contributing to the divergence between both studies.

According to Li et al. (2006) the HadCM3 model predicts an El Niño-like sea surface temperature change and warming in the northern tropical Atlantic; a condition that would lead to enhanced atmospheric subsidence and reduced cloud cover over the Amazon. As discussed in more detail below, expected changes in climate in this study also resemble El Niño-like conditions, but with drier conditions mostly concentrated in the eastern Amazon (northeastern South America) rather than in the entire basin. The change in precipitation simulated in this study is in agreement with studies that noted that western Amazon rainfall is relatively insensitive to interannual variations in SST, and

that this region may be more sensitive to local forcings (Enfield, 1996 and Fu et al., 2001).

In another study where Rojas et al., (2006) analyzed changes in precipitation in the A2 scenario (2070-2100) for the monsoon region using six coupled GCMs for the AR4, some coherent patterns were found that agree with the ones obtained here. All models predict an increase in precipitation over SESA and most of them simulate a larger amplitude of the annual cycle, with more precipitation in the wet season, but less precipitation in the dry season for the monsoon and Amazon region. The only exception to this pattern is again HadCM3, which predicts a drier Amazon and monsoon region.

In relation to future temperature changes reported in the fourth assessment report (AR4) of the IPCC (Christensen et al., 2007), the mean warming projected by a coordinated set of 21 climate model simulations archived at the Program for Climate Model Diagnosis and Intercomparison (PCMDI), ranges between 1.8 º and 5.1º C for the Amazon region at the end of this century for the A1B scenario (2080-2099 compared to 1980-1999). The maximum temperature change projected using global climate models is below the one found in the present study for the A2 scenario, but this is not surprising given the more moderate emission path projected in A1B. The difference with the B2 simulation is maybe not the one expected, because the maximum warming for B2 is also above 5º C, but the proximity in these values could be explained by the difference in resolution . In addition, both projections agree that the warming in central Amazonia tends to be larger in winter than in summer, but they do not agree on changes in the seasonal cycle of temperature in the Altiplano, which is projected to increase in AR4,

while the present study projects a larger warming in winter than in summer and hence a decrease of the seasonal cycle.

The fourth assessment report of the IPCC (Christensen et al., 2007), and this study both predict an increase of rainfall in Ecuador and northern Peru and a decrease at the northern end of the continent and in southern northeast Brazil. The multi-model mean precipitation response for the A1B scenario projects a decrease over northern South America, as well as over large areas of northern Brazil, and an increase over Colombia, Ecuador, Peru, around the equator and SESA (Christensen et al., 2007). Except for the case of Colombia where the present study projects a decrease in mean precipitation in some areas, both studies match in their results. In addition, the multi-model projects an increase in monsoon precipitation in the Amazon basin in DJF and decrease in winter, which is also in agreement with what was obtained in the present study.

In relation to projected changes in free tropospheric temperature, the pattern of change is very similar to the projected change simulated by the mean of eight different GCMs of the IPCC AR4 using the A2 scenario (Bradley et al., 2006). This result was obtained by calculating changes in mean annual free-air temperatures between 1990 to 1999 and 2090 to 2099 along a transect from Alaska to southern Chile. In both projections the rate of warming increases with altitude, but the highest temperature (>7 ºC in both models) is reached at a lower altitude in the projection using the GCMs than in the one using PRECIS. This situation may be related to the fact that the time periods are different and probably the results based on the GCM projections are more extreme as they only include the last ten years of each century. However, looking at the temperature change surrounding the highest mountains peaks in the area depicted in Bradley et al.,

(2006) and in an update provided by Vuille et al., (2008a), temperature changes are quite similar and at most half a degree higher in the mentioned GCM-based studies than in the present report.

Looking at summer and winter free-air temperature change projections and comparing them with the ones obtained using seven GCM simulations with 2x CO_2 levels (Bradley et al., 2004) shows that the amount of warming is much lower in the latter study (up to 4º C rather than up to 7.5 ºC in this study) due to the different CO_2 scenarios used. However, warming seems to be higher in austral winter (JJA) than in summer (DJF) in both projections.

Cook and Vizy (2008) used the fifth-generation Pennsylvania State University-National Center for Atmospheric Research Mesoscale Model (MM5) asynchronously coupled with a potential vegetation model to study changes in tropical-subtropical climate and vegetation in South America. Their simulation is for the 2081-2100 period forced by the A2 emission scenario and they predict a reduction of the areal extent of the Amazon rain forest of 69%. Most of the rain forest is replaced by savanna and grasslands in the Central Amazon (north of about 15 º S) and in southern Bolivia, northern Paraguay and southern Brazil, respectively. According to the authors, the decrease in the area of rain forests is primarily related to moisture availability, especially with a decrease in rainfall and/or a lengthening of the dry season. Annual rainfall is projected to decrease especially in southeastern Brazil and the SACZ, which weakens and shifts to the southwest. This pattern does not agree with the one projected with PRECIS where a strengthening of the SACZ can be expected. In addition, the increase in mean annual precipitation close to the equator in the eastern part of the continent and the pronounced

drying of the ITCZ over the Pacific close to the continent, and drying over the adjacent land surface do not agree with the present study either. However, some agreements correspond to the increase in annual rainfall in central South America close to the equator and a pronounced drying of the ITCZ over the Atlantic and adjacent areas over the continent. A weaker SALLJ is also projected by Cook and Vizi (2008), associated with enhanced moisture convergence and precipitation in the central equatorial Amazon; a situation that agrees with the present study.

It is important to point out that the drying and dieback of the Amazon vegetation projected by Cook and Vizi (2008) do not occur when a simulation is only driven by increased CO_2 levels or by SST forcing, where in fact a slight expansion of the rain forests occurs. However, when only the future lateral boundary conditions from the GCM that drives the RCM are used, the response is that of drying, indicating that large-scale hydrodynamic changes are forcing the regional changes in climate and vegetation. This suggests that differences in the driving GCM between Cook and Vizi (2008) and the present study might be the cause for some of the disagreements in projections of annual precipitation changes. As the weakening of the tropical circulation is a common feature for future climate projections for all AR4 models (Vecchi and Soden, 2007) including the one used in Cook and Vizi (2008) and the HadCM3, it is probable that other features (e.g. SST) could be the cause of some of the different patterns in expected rainfall.

Predicted changes in northern Chile using the PRECIS model (Fuenzalida et al., 2007) agree with the present study and show an increase in summer and winter temperature between 3º and 5º C and 4º and > 5º C, respectively in Chile and part of the Altiplano in Bolivia (between 17º and 27º S). Predicted changes in precipitation were

difficult to accurately compare due to the mixed pattern obtained for precipitation in the present study and because in Fuenzalida et al., (2007) expected changes in places where precipitation was very low were not shown. However, based on the information available it appears that the increase in summer precipitation projected for parts of the Altiplano is in agreement with what has been found in the present study (Figure 8). The decrease in winter precipitation found for some places in the Andes in Fuenzalida et al., (2007) is also consistent with results obtained for that season in the present study. Finally, both studies simulate decreased precipitation over the adjacent Pacific Ocean.

4.2. Review of some expected climatic changes in South America and the Andes region

According to the projected climate changes for South America, a stronger monsoon might be expected in summer, as suggested by changes in precipitation, in mid-tropospheric vertical velocity and in the intensity of the outflow that returns to North Africa. However, this stronger monsoon is not evident when looking at changes in total fractional cloud cover, which indicates that changes in precipitation amount might be mainly a reflection of enhanced precipitation intensity. An increase in precipitation in the monsoon area would partly affect the Amazon basin, especially towards the western basin; however large parts of the basin might be affected by a decrease in precipitation, especially towards eastern and northeastern Brazil.

It is important to note that the Amazon area where the largest decrease in precipitation is projected (eastern and southeastern Amazon in winter) corresponds to the zone with the most active deforestation. This factor could be especially threatening for

the survival of tropical forests in the future, due to intensified ecosystem feedbacks such as forest die-back and the reduced transpiration in remaining forests (Malhi et al., 2008).

On the other hand, the projected increase in precipitation in some parts of the Amazon region does not take into account if the rate of deforestation in the Amazon, which is among the highest in the world (annual average rate of 0.48%, Vera et al., 2006a) is expected to increase and spread to the entire Amazon basin in the future. Deforestation in tropical areas leads to a decrease in precipitation due to a decrease in evapotranspiration, but changes in atmospheric moisture convergence can modify that effect (Vera et al., 2006a, Christensen et al., 2007). However, most model simulations of Amazonian deforestation impacts indicate reduced moisture convergence, which would effectively amplify the decrease in rainfall associated with deforestation (Christensen et al., 2007). According to Vera et al., (2006a) precipitation can also decrease due to stomatal closure due to rising CO_2 levels in a future scenario. This stomatal closure would act to suppress transpiration and amplify surface warming (Cox et al., 2004).

Research about the future climate and vegetation patterns in tropical and subtropical South America contain significant uncertainty (Cook and Vizy, 2008). One of the reasons is the complexity of the system, where surface and atmospheric processes are strongly connected. The other reason is the highly regional character of the climate over these areas (Cook and Vizy, 2008). Furthermore, there is no agreement in the literature about future climate changes in tropical South America in this century (Cook and Vizy, 2008) and large sources of uncertainty such as SST changes in the tropical Pacific and Atlantic Oceans, clouds and land surface feedbacks (Li et al., 2006) remain. Due to the complexity of the system, and because the potential for abrupt changes in biogeochemical

systems in the Amazon remains as a source of uncertainty (Christensen et al., 2007), it is difficult to assess with certainty what would happen in terms of future precipitation in that area. An earth system model, capable of simulating changes in vegetation associated with climate and its feedbacks, changes in vegetation caused by human activity, and chemical processes, plus CO_2 feedbacks, would be needed to provide the necessary information to address future changes with more confidence.

In addition, seasonal prediction over tropical South America presents two main challenges: the first one is for the regions where the mean state of the climate is modulated by external forcing (such as SST). Here effective forecasting tools are needed to predict the future state of the oceans, as SST simulations for example still vary greatly among models. The second challenge is over regions where ocean conditions have little influence on climate. Here coupled models that include the ocean, atmosphere and surface feedbacks are needed (Nobre et al., 2006).

Climatic changes at high altitudes in the Andes (above 4000 m) will be amplified for some variables and subdued for others. There are also pronounced differences between projected changes on the eastern and western side of the Andes, with different ramifications for glaciers. Warming is expected to be higher at upper elevations along the eastern slope than along the western slope of the Andes. Changes in precipitation seem more favorable for glacier survival along the eastern side (precipitation increase, but not significant). On the other hand, less of a decrease in relative humidity and a larger increase in specific humidity are projected for the eastern slope of the Andes at higher elevations than for the western slope. Based on a qualitative description of these projections alone, it is not possible to conclude whether changes on either slope of the

Andes will have a more significant impact on glacier energy and mass balance. A more detailed analysis, combining these results with a tropical glacier-climate model will be needed to answer these questions.

In addition to these expected changes at higher elevations it is also important to consider that predicted warming is higher for the eastern than the western slope at all elevations and that the variability is also predicted to increase more in the east. This larger projected warming for the eastern slope is relevant because most glaciers in Ecuador and Bolivia are located along the eastern Cordillera and the largest tropical ice cap (Quelccaya) is also located in the eastern branch of the Andes (Vuille, 2007). In addition, ELAs are generally lower on the eastern slope due to the east-west precipitation gradient. Therefore ELA's are closer to the freezing level and will be more immediately affected by significant warming than glaciers in the west, with ELAs often situated well above the freezing level.

The decrease in precipitation expected for the Altiplano and Cordillera Blanca regions appears to be mainly caused by weaker easterly winds and strengthened westerlies leading to drier overall conditions in those areas. Less precipitation might affect glaciers in these regions due to the decrease in albedo. In the inner tropics on the other hand a decrease in precipitation is less imminent and even an increase may occur in some regions. But the enhanced free-tropospheric warming at altitude will lead more precipitation to fall as rain rather than snow, equally affecting glacier mass balance in a negative way.

At lower altitudes expected changes are subdued along the western slope of the Andes, mainly because warming is less pronounced, but a significant increase in

precipitation, less of a decrease in relative humidity and a larger increase in specific humidity might be expected. The enhanced precipitation might be related to the presence of strong onshore wind anomalies along the coast of Ecuador and northern Peru, as well as to the projected weaker or probably southward displaced subtropical anticyclone that will allow more humid conditions to develop along the tropical west coast of South America.

Some of the expected climatic changes, such as a decrease in precipitation in the Altiplano, northeastern South America and parts of the Amazon (east-central Amazonia), or the increase over SESA and the coastal areas of Ecuador and Peru are similar to present day precipitation anomalies during El Niño events. Although more El Niño-like conditions might be expected, models do not agree whether this phenomenon is going to be more frequent in the future. Furthermore, the ability to simulate changes in the frequency or structure of natural modes of low frequency variability such as ENSO has not been adequately tested in climate models, and the assessment of future changes in ENSO behavior is further complicated by decadal and longer time-scale variability of future climate predictions (Nobre et al., 2006). Current model projections do not demonstrate a systematic response of El Niño to global warming, and although changes in the mean state of the Pacific Ocean provide the basis to understand its response, the intensity, character and frequency of this phenomenon depends on different physical processes whose reactions to global warming are not well represented by current models (Vecchi et al., 2008).The IPCC AR4 also concludes that there are currently no consistent indications of apparent future changes in ENSO amplitude or frequency (Meehl et al., 2007).

There are still large systematic errors in simulating current tropical climate and its variability, and as was pointed out before, large differences exist between models related to future changes in El Niño amplitude. Most climate models either show a tendency toward a more El Niño-like state or no tendency at all and it has been suggested that global warming would increase the likelihood of strong El Niños (Hansen et al., 2006). Given the lack of reliable predictions of future ENSO behavior, and since theory, models and observations diverge in their representation of the Pacific response to global warming (Vecchi et al., 2008), it is not possible to assess how ENSO changes might affect the climate of tropical South America in the 21st century (Christensen et al., 2007). Clearly further work is needed to first improve ENSO predictions in modern climate model simulations.

Land cover changes are another area of uncertainty which was not addressed in this study. Again there is a high level of uncertainty about how land cover will change in the future, and current land process models are not able to simulate all the potential impacts of human land cover conversion (Christensen et al., 2007).

The factors mentioned above add uncertainty to future climate predictions over South America. The complex interactions between regional and remote factors that contribute to the climate of South America, make it difficult to account for all the changes that might occur in the future and could affect climate (Nogues-Paegle et al., 2002). It is therefore vitally important to develop more and better predictions including regional climate models, so that changes at a more local scale can be assessed with a higher degree of certainty. Probably the use of model ensembles can improve future

projections, but it is important to keep in mind that climate variability may be artificially damped when using these ensembles.

Furthermore, a whole range of additional and complementary analyses could contribute to better understand probable future changes in climate. These analyses, not developed in this thesis because of time constraints, include: 1) the development of precipitation PDFs in different scenarios to assess changes in mean precipitation and its variability along the Andes, 2) the analysis of daily or pentad precipitation per season to analyze changes in the onset and demise of the monsoon system. This is a key analysis because a delayed onset of precipitation (snowfall) and the associated prolonged exposure of dirty ice has been identified as one of the main culprits of enhanced ice wastage due to enhanced absorption of solar radiation through ice-albedo feedbacks (Francou et al., 2003), 3) the analysis of the divergent wind and velocity potential in the upper-troposphere to confirm potential changes in the intensity of the monsoon system (Trenberth et al., 2000), and 4) the analysis of changes in specific humidity at different levels in the troposphere to assess their likely effects on glaciers, among others.

CHAPTER 5

CONCLUSIONS

The main conclusions of this study are the following:

- A mean annual warming ranging from 2º to 8º C might be expected for tropical South America under the A2 scenario, with the largest values in northeastern South America. In this same area the most pronounced decrease in precipitation, the most significant decrease in relative humidity, the lowest increase in specific humidity and the largest decrease in fractional cloud cover might also be expected.

- The largest warming projected for northeastern South America can partially be explained by the pronounced decrease in cloud cover in that area. Hence warmer temperatures in that area may partially reflect greater incoming short-wave radiation.

- Expected mean annual warming in the Andes ranges from 2º to 7ºC for the A2 scenario, with the highest values predicted for the Cordillera Blanca.

- Warming is expected to be enhanced in northern South America in austral summer and south of the equator in winter, thereby decreasing the seasonal amplitude of temperature in the outer-tropics.

- The expected pattern of warming is the same under the A2 and B2 scenarios but the magnitude changes with temperature being up to 3º C warmer in the A2 than in the B2 run.

- No area in the Andes will remain below freezing in summer under the A2 scenario. This is of concern given the close coupling of ELA and 0°C isotherm in

the tropics (Greene et al., 2002) and the role temperature plays in determining the rain-snow line and hence glacier albedo. However, one needs to keep in mind that the 50 km resolution of the simulation used here does not fully resolve individual mountains and therefore underestimates the elevation of the highest peaks.

- An increase in precipitation might be expected for the monsoon area and along the coast of Ecuador and northern Peru in summer, while precipitation may be reduced over most of the continent in winter under the A2 scenario.

- Precipitation along the Andes presents a mixed pattern with both regions of increase and decrease. In general, however, rainfall is projected to decrease in the outer-tropics and to increase in the inner- tropics, consistent with an observed intensification of the meridionally overturning atmospheric circulation.

- Relative humidity will mostly decrease across tropical South America, except for a region along the Pacific coast. Specific humidity will increase across the continent, driven the moistening of the atmosphere under global warming. Temperature and relative humidity changes show very similar spatial patterns indicating that the decrease in relative humidity is coupled to the observed temperature increase and that specific humidity increases less than would be predicted based on the Clausius Clapeyron relationship under conditions of constant relative humidity.

- The largest temperature increase can be expected at higher elevations on both slopes of the Andes. In the free troposphere the largest warming is expected to occur at higher levels, with a stronger temperature increase in winter than in summer, thereby decreasing the seasonal amplitude in the outer-tropics.

- A stronger warming at higher altitudes is of concern for glaciers in the inner-tropics, because the ELA is located very close to the 0ºC isotherm and therefore higher temperatures will lead to more precipitation falling as rain rather than snow, thereby decreasing the albedo and contributing to a negative glacier mass balance. However, the magnitude of warming projected in this study will also have an effect on glaciers in parts of the outer-tropics, where today temperature is not a yet limiting factor for their vertical extent.

- The eastern slopes will be characterized by a stronger warming, less of a decrease in relative humidity and a larger increase in specific humidity at higher elevations, when compared with the western slopes of the Andes.

- It is not possible based on the results from this study to conclude what the likely effects of changes in humidity on glaciers will be. The relationships between this variable and glaciers are complex and vary depending on scale, glacier location, season and atmospheric level (free troposphere versus surface humidity) considered. To accurately assess future effects of humidity on glaciers will require linking these results with a tropical glacier-climate model.

- Even though temperature is in general warmer along the western Cordillera than to the east at all elevations, changes in mean annual temperature and temperature variability (by means of PDF) are higher along the eastern slope for the A2 and B2 scenarios. This will effectively reduce the east-west temperature gradient across the Andes.

- Changes in the PDF on both slopes of the Andes demonstrate that there is no overlap between mean annual temperatures of the control run and at either of the

two future scenarios (A2 and B2). This shows that the highest temperatures in the control run are much lower than the lowest temperatures projected for a future scenario. In addition, changes in variability (a wider distribution) are expected for the A2 scenario but not for B2.

- Expected changes along the western slope at lower altitudes seem to be less extreme in terms of warming or more moderate in terms of humidity with a significant increase in precipitation expected for that area. The largest relative increase in annual precipitation in South America is projected for the coastal area and Andes of Ecuador and northern Peru and for the western cordillera to the south. This increase in precipitation may be related to the weakening of the South Pacific High over that area.

- Projected changes in low-level circulation for South America for the A2 scenario are a weaker South Pacific High, stronger onshore winds towards Ecuador and northern Peru and stronger winds over the SACZ. The SALLJ appears to weaken, yet low level convergence at its exit region is enhanced, leading to increased precipitation in SESA.

- Projected changes in circulation at upper levels for South America are a weaker Bolivian High, weakened easterlies and stronger westerlies responsible for drier conditions in the Cordillera Blanca and the Altiplano region, and a strengthened return flow towards North Africa that reinforces the notion of a stronger summer monsoon in South America.

- The notion of a stronger summer monsoon appears to be inconsistent with the decrease in total fractional cloud cover projected for that region in summer.

However this discrepancy may be explained by a higher intensity of rainfall in that area as opposed to more frequent precipitation events.

- While this study focused primarily on variables which are relevant for glacier mass and energy balance, it is important to recognize that climatic change documented in this study may also negatively affect social and economic activities and other ecosystems in tropical South America. For example, to only name a few, the expected reduction in precipitation in the central-eastern Amazon could exacerbate the loss of tropical forests due to an increased chance of fire occurrence and replacement by other uses; the decrease in the seasonal amplitude of temperature could increase the risk of occurrence or spread of existing endemic diseases, and the increase in temperature can lead to the altitudinal migration of species, which in certain cases may lose their optimal range of climatic conditions for survival.

- Most of the expected changes such as higher precipitation over Ecuador and northern Peru, lower precipitation over northeastern South America, higher precipitation over SESA, and reduced precipitation over the Altiplano associated with stronger westerlies, are very much distinctive features of the El Niño phenomenon. Although there is a clear connection between expected changes and El Niño features, it is not possible to say that more El Niño events will characterize future climate in South America, mainly because predictions related to El Niño are not assessed in the PRECIS model but also because there is still little agreement among models about the future characteristics of ENSO.

- It is important to note that this study constitutes the first attempt to simulate climate change by means of a regional climate model for the tropical Andes. In addition, this is only the second study developed to date predicting climate in tropical South America using an RCM. Predicted climatic changes only constitute an approximation of what might happen in the future in this region, and certainly, the validation of the model constitutes a key process to assess the ability of PRECIS to predict future climate in tropical South America.

- Comparing projections from PRECIS with other simulations for tropical South America, some similarities are found with the multi-model simulation of the AR4, projecting an increase in summer precipitation for the monsoon area and a decrease over northern South America and northern Brazil. The increase in free-tropospheric temperature with altitude is also a common pattern found in PRECIS and coupled GCMs. Finally, the discrepancy found for precipitation changes over the western Amazon between PRECIS and its driving model might reinforce the idea that this region is more susceptible to local forcings than to large-scale changes forced by SSTs.

- More analyses such as an assessment of changes in mean annual precipitation distribution, changes in humidity at different levels in the atmosphere and evaluation of the onset and demise of the monsoon, among others, are needed to completely assess expected changes in climate in tropical South America and the Andes Region.

- Many uncertainties remain from the projection of future conditions through PRECIS (e.g. future greenhouse gas concentrations, response of climate, regional

climate change), and one of the main weaknesses of the model is the lack of biophysical feedbacks between the atmosphere and the prescribed vegetation and soil properties. The incorporation of biological responses is fundamental to predict future climate in the region that holds the largest forested area, but also one of the most threatened ecosystems in the world.

- Finally, more studies using regional climate models are needed to have a more comprehensive understanding of expected climatic changes in South America and especially along the Andes. Moreover, the evaluation and understanding of their potential effects on different ecosystems constitutes the key step to implement possible adaptation and mitigation strategies to face future climate changes.

BIBLIOGRAPHY

Boulanger, J.P., F. Martinez, and E.C. Segura (2006), Projection of future climate change conditions using IPCC simulations, neural networks and Bayesian statistics. Part 1: Temperature mean state and seasonal cycle in South America *Clim. Dyn., 27*, 233-259.

Boulanger, J.P., F. Martinez, and E. C. Segura (2007), Projection of future climate change conditions using IPCC simulations, neural networksand Bayesian statistics.Part 2: Precipitation mean state and seasonal cycle in South America, *Clim. Dyn., 28,* 255-271.

Bradley, R.S., F. Keimig, and H. Diaz (2004), Projected temperature changes along the American cordillera and the planned GCOS network, *Geophys. Res. Lett., 31*, L16210, doi:10.1029/2004GL020229.

Bradley, R.S., M. Vuille, H. Diaz, and W. Vergara, (2006), Threats to water supplies in the Tropical Andes. *Science, 312* (5781), 1755-1756.

Chen, J., B.E. Carlson, and A.D. Del Genio, (2002), Evidence for strengthening of the tropical general circulation in the 1990s. *Science, 295*, 838–841.

Christensen, J.H., B. Hewitson, A. Busuioc, A. Chen, X. Gao, I. Held, R. Jones, R.K. Kolli, W.-T. Kwon, R. Laprise, V. Magaña Rueda, L.Mearns, C.G. Menéndez, J. Räisänen, A. Rinke, A. Sarr and P. Whetton (2007), Regional Climate Projections, in *Climate Change 2007:The Physical Science Basis. Contribution of Working Group I to the Fourth Assessment Report of the Intergovernmental Panel on Climate Change* edited by Solomon, S., D. Qin, M. Manning, Z. Chen, M. Marquis, K.B. Averyt, M. Tignor and H.L. Miller. 847-940 pp., Cambridge University Press, Cambridge, United Kingdom and New York, NY, USA.

Coppola, E., and F. Giorgi (2005), Climate change in tropical regions from high-resolution time-slice AGCM experiments, *Q. J. R. Meteorol. Soc. 131*, 3123-3145.

Cook, K., and E. Vizy (2008), Effects of twenty-first century climate change on the Amazon rain forest, *J. of clim., 21*, 542-560.

Diaz, H.F., J.K. Eischeid, C. Duncan, and R. Bradley (2003), Variability of freezing levels, melting season indicators and snow cover for selected high elevation and continental regions in the last 50 years, *Clim. Change, 59*, 33-52.

Favier, V., P. Wagnon, and P. Ribstein (2004), Glaciers of the outer and inner tropics: A different behavior but a common response to climatic forcing. *Geophys. Res. Lett., 31*, L16403, doi:10.1029/2004GL020654.

Figueroa, S., P. Satyamurty, and P. Silva Dias (1995), Simulation of the summer circulation over the South American region with an ETA coordinate model, *J. Atmos. Sci., 52*, 1573-1584.

Francou, B., E. Ramirez, B. Caceres, and J. Mendoza (2000), Glacier evolution in the tropical Andes during the last decades of the 20th century: Chacaltaya, Bolivia and Antizana, Ecuador, *Ambio*, *29* (7), 416-422.

Francou, B., M. Vuille, P. Wagnon, J. Mendoza, and J.E. Sicart (2003), Tropical climate change recorded by a glacier in the central Andes during the last decades of the 20th century: Chacaltaya, Bolivia, 16°S. *J. Geophys. Res., 108*(D5), 4154, doi: 10.1029/2002JD002959.

Francou, B., M. Vuille, V. Favier,and B. Cáceres (2004), New evidence for an ENSO impact on low latitude glaciers: Antizana 15, Andes of Ecuador, 0°28'S. *J. Geophys. Res., 109*, D18106, doi:10.1029/2003JD004484.

Fuenzalida, H., P. Aceituno, M. Falvey, R. Garreaud, M. Rojas, and R. Sanchez (2007); Study on climate variability for Chile during the 21st century. Technical Report prepared for the National Environmental Committee. Santiago, Chile. In Spanish. Available on-line at http://www.dgf.uchile.cl/PRECIS (August 2007)

Garreaud, R., (1999), Multi-scale analysis of the summertime precipitation over the Central Andes, *Mon. Wea. Rev. 127,* 901-921.

Garreaud, R., (2000), Intraseasonal variability of moisture and rainfall over the South American Altiplano, *Mon. Wea. Rev. 128*, 3337-3346.

Garreaud, R., M. Vuille, and A.C. Clement (2003), The climate of the Altiplano: Observed current conditions and mechanisms of past changes, *Palaeogeogr. Palaeoclimatol. Palaeoecol., 194*, 5-22.

Garreaud, R. D., and P. Aceituno (2007), Atmospheric circulation over South America: Mean features and variability, in *The Physical Geography of South America,* edited by T. Veblen, K. Young and A. Orme, 45-59 pp., Oxford University Press.

Garreaud, R. and M. Falvey (2008), The coastal winds of western South America in future climate scenarios, *Int. J. Climatol.*, in review.

Giorgi, F. and X. Bi (2005a), Updated regional precipitation and temperature changes for the 21st century from ensembles of recent AOGCM simulations, *Geophys. Res. Lett., 31*, L21715, doi:10.1029/2005GL024288.

Giorgi, F. and X. Bi (2005b), Regional changes in surface climate interannual variability for the 21st century from ensembles of global model simulations, *Geophys. Res. Lett., 32*, L13701, doi: 10.1029/2005GL023002.

Greene, A., R. Seager and W. Broecker (2002), Tropical snowline depression at the Last Glacial Maximum: Comparison with proxy records using a single-cell tropical climate model, *J. Geophys. Res.,* 107(D8), 4061, 10.1029/2001JD000670.

Hansen, J., M. Sato, R. Ruedy, K. Lo, D. Lea, and M. Medina-Elizade (2006), Global temperature change, *Proceedings of the National Academy of Sciences PNAS, 103*(39), 14288–14293.

Hegerl, G.C., F.W. Zwiers, P.A. Stott, and V.V. Kharin (2004), Detectability of anthropogenic changes in annual temperature and precipitation extremes. *J. Clim., 17,* 3683–3700.

Horel, J. and G. Cornejo-Garrido (1986), Convection along the coast of Northern Peru during 1983: Spatial and temporal variations in cloud and rainfall, *Mon. Wea. Rev., 114,* 2091-2105.

Houghton, J. (2004), *Global warming, The complete briefing.* 3rd ed., 351 pp., Cambridge University Press, Cambridge, UK..

Intergovernmental Panel on Climate Change (2000), Emission scenarios, a special report of working group III. Summary for Policy makers.20 pp.

IPCC (2001), Climate Change 2001: The Scientific Basis. Contribution of Working Group I to the Third Assessment Report of the Intergovernmental Panel on Climate Change, edited by Houghton, J.T.,Y. Ding, D.J. Griggs, M. Noguer, P.J. van der Linden, X. Dai, K. Maskell, and C.A. Johnson, 881pp., Cambridge University Press, Cambridge, United Kingdom and New York, NY, USA.

Jones, R.G., M. Noguer, D. Hassell, D. Hudson, S. Wilson, G. Jenkins and J. Mitchell (2004), Generating high resolution climate change scenarios using PRECIS. 40 pp., Met Office Hadley Centre, Exeter, UK. April 2004.

Juen, I., G. Kaser, and C. Georges (2007), Modeling observed and future runoff from a glacierized tropical catchment (Cordillera Blanca, Perú), *Global Planet. Change,* 59, 1-4, 37-48.

Kalnay, E., and Coauthors (1996), The NCEP/NCAR 40-year reanalysis project. *Bull. Amer., Meteor., Soc., 77*(3), 437- 471.

Kaser, G., and C. Georges (1999), On the mass balance of low latitude glaciers with particular consideration of the Peruvian Cordillera Blanca, *Geografiska Annaler, 81*A(4), 643-651.

Kaser, G. (1999), A review of the modern fluctuations of tropical glaciers, *Global Planet. Change, 22*, 93-103.

Kaser, G. (2006), Modern glacier fluctuations in tropical high mountains, in *Tropical glaciers,* edited by Kaser, G and H. Osmanton, International Hydrology Series. UNESCO. 61-146 pp. Cambridge University Press.

Lenters, J.D., and K. H. Cook (1997), On the origin of the Bolivian High and related circulation features of the South American climate, *J. Atmos. Sci., 54*, 656-677.

Li, W., R. Fu, and R. Dickinson (2006), Rainfall and its seasonality over the Amazon in the 21st century as assessed by the coupled models for the IPCC AR4, *J. Geophys. Res., 111*, D02111, doi: 10.1029/2005JD006455.

Liebmann, B., G. Kiladis, C.Vera, A. Saulo, and L. Carvalho (2004), Subseasonal variations of rainfall in South America in the vicinity of the low-level jet east of the Andes and comparison to those in the South Atlantic convergence zone, *J. Clim., 17*, 3829–3842.

Madden, R., and P. Julian (1972), Description of global-scale circulation cells in the Tropics with a 40-50-day period, *J. Atmos. Sci., 29,* 1109-1123.

Malhi, Y, J. Roberts, R. Betts, T. Killeen, W. Li, and C. Nobre.(2008), Climate Change, Deforestation, and the Fate of the Amazon, *Science, 319* (5860), 169 - 172.

Marengo, J., B. Liebmann, V. Kousky, N. Filizola, and I. Wainer (2001), On the onset and end of the rainy season in the Brazilian Amazon basin, *J. Clim.,, 14*, 833-852.

Marengo, J. (2004), Interdecadal and long term-variations of rainfall in the Amazon basin, *Theor. Appl. Climatol., 78*, 79-96.

Mcgregor, G. and S. Nieuwolt (1998), *Tropical Climatology, An introduction to the climates of the low latitudes*. 339 pp., John Wiley & Sons. England.

Meehl, G.A., J.M. Arblaster, and C. Tebaldi (2005), Understanding future patterns of increased precipitation intensity in climate model simulations, *Geophys. Res. Lett., 32*, L18719, doi:10.1029/2005GL023680.

Meehl, G.A., T.F. Stocker, W.D. Collins, P. Friedlingstein, A.T. Gaye, J.M. Gregory, A. Kitoh, R. Knutti, J.M. Murphy, A. Noda, S.C.B. Raper, I.G. Watterson, A.J. Weaver and Z.-C. Zhao (2007), Global Climate Projections, in *Climate Change 2007: The Physical Science Basis.Contribution of Working Group I to the Fourth Assessment Report of the Intergovernmental Panel on Climate Change* edited by Solomon, S., D. Qin, M. Manning, Z. Chen, M. Marquis, K.B. Averyt, M. Tignor and H.L. Miller.747-846 pp., Cambridge University Press, Cambridge, United Kingdom and New York, NY, USA.

New, M., M. Hulme and P. Jones (2000), Representing twentieth-century space-time climate variability. Part II: Development of 1901-1996 monthly grids of terrestrial surface climate, *J. Clim., 13*, 2217-2238.

NOAA, (2007), Patterns of greenhouse warming. GFDL climate modeling research highlights 1(6).

Nogués-Paegle, J, C. Mechoso, R. Fu, H. Berbery, W. Chao, T. Chen, K. Cook, A. Diaz, D. Enfield, R. Ferreira, A. Grimm, V. Kousky, B. Liebmann, J. Marengo, K. Mo, D. Neelin, J. Paegle, A. Robertson, A. Seth, C. Vera, and J.Zhou (2002), Progress in Pan American CLIVAR research: Understanding the South American Monsoon, *Meteorologica 27,* 3-30.

Pal, J.S., F. Giorgi, X. Bi, N. Elguindi, F., Solmon, X. Gao, S. Rauscher, R. Francisco, A. Zakey, J. Winter, M. Ashfaq, F. Syed, J. Bell, N. Diffenbaugh, J. Karmacharya, A. Konare, D. Martinez, R da Rocha, L. Sloan, and A. Steiner (2007), Regional climate modeling for the developing world – The ICTP RegCM3 and RegCNET, *Bull. Amer. Meteor. Soc., 88*, 9: 1395-1409.

Parry, M.L., O.F. Canziani, J.P. Palutikof and Co-authors (2007), Technical Summary, in *Climate Change 2007: Impacts, Adaptation and Vulnerability. Contribution of Working Group II to the Fourth Assessment Report of the Intergovernmental Panel on Climate Change edited by,* M.L.Parry, O.F. Canziani, J.P. Palutikof, P.J. van der Linden and C.E. Hanson, pp. 23-78, Cambridge University Press, Cambridge, UK.

Quintana-Gomez, R.A. (1997), Changes in maximum and minimum temperatures at high elevation stations in the central Andes of South America. *Proc. AMS Meeting on Climate Variations,* J112-J113.

Quintana-Gomez, R.A. (2000), Trends of maximum and minimum temperatures in Ecuador and homogeneity evaluation during 1961-90, paper presented at 6th International Conference Southern Hemisphere Meteorology and Oceanography, Santiago Chile, 292-293.

Rahmstorf, S., A. Cazenave, J. Church, J. Hansen, R. Keeling, D. Parker, R. Somerville (2007), Recent climate observations compared to projections, *Science 316,*709.

Ramirez, E., B. Francou, P. Ribstein, M. Desclitres, R. Guerin, J. Mendoza, R. Gallaire, B. Pouyaud, and E. Jordan (2001), Small glaciers disappearing in the tropical Andes: a case study in Bolivia: Glaciar Chacaltaya (16°S), *J. Glaciol., 47*(157): 187-194.

Rauscher, S, A. Seth, B. Liebmann, J. Qian, and S. Camargo (2007), Regional Climate Model–Simulated Timing and Character of Seasonal Rains in South America, *Mon. Wea. Rev., 135*, 2642-2657.

Roads, J., S. Chen, S. Cocke, L. Druyan, M. Fulakeza, T. LaRow, P. Lonergan, J. Qian, and S. Zebiak (2003), International Research Institute / Applied Research Centers (IRI/ARCs) regional model intercomparison over South America, *J. Geophys. Res., 108* (D14), 4425, doi:10.1029/2002JD003201.

Rohli, R. and A. Vega (2007), *Climatology*. 466 pp., Jones and Bartlett Publishers. USA.

Rojas, M., A. Seth, and S. Rauscher (2006), Relationship between precipitation and moisture flux changes in the SRES A2 scenario for the South American Monsoon region. *CLARIS News 3*, 14-20.

Ropelewski, C. and M. Halpert (1987), Global and regional-scale precipitation patterns associated with the El Niño/Southern Oscillation, *Mon. Wea. Rev. 115*, 1606-1626.

Schaer, C., P. Vidale, D. Luethi, C. Frei, C. Haeberli, M. Liniger, and C. Appenzeller (2004), The role of increasing temperature variability in European summer heatwaves, *Nature 427*, 332-336.

Solman, S., M. Nunez, and M. Cabre, (2007), Regional climate change experiments over southern South America I: present climate. *Clim. Dyn.,* doi 10.1007/s00382-007-0304-3

Thompson, L.G. (2000), Ice core evidence for climate change in the Tropics: implications for our future, *Quaternary Science Review 19*(1-5), 19-35.

Trenberth, K. (1997), The definition of El Niño, *Bull. Amer. Meteor. Soc., 78*, 2771-2777.

Trenberth, K., D. Stepaniak, and J. Caron (2000), The global monsoon as seen through the divergent atmospheric circulation, *J. Clim., 13,* 3969-3993.

Vecchi, G.A., B. Soden, A. Wittenberg, I. Held, A. Leetmaa, and M. Harrison (2006), Weakening of tropical Pacific atmospheric circulation due to anthropogenic forcing, *Nature 441*, 73-76.

Vecchi, G.A. A. Clement, and B. Soden (2008), Examining the tropical Pacific's response to global warming. *Eos Trans., AGU, 89*(9), 26 February 2008..

Vera, C., W. Higgins, J. Amador, T. Ambrizzi, R. Garreaud, D. Gochis, D. Gutzler, D. Lettenmaier, J. Marengo, C. Mechoso, J. Nogues-paegle, P. Silva dias, and C. Zhang (2006a), Toward a Unified View of the American Monsoon Systems, *J. Clim. 19*, 4977-5000.

Vera, C., J. Baez, M. Douglas, C. Emmanuel, J. Marengo, J. Meitin, M. Nicolini, J. Nogues-paegle, J. Paegle, O. Penalba, P. Salio, C. Saulo, M. Silva dias, P. Silva dias and E. Zipser   (2006b), The south american low-level jet experiment, *Bull. Amer.Meteor. Soc.*, January 2006: 63-77.

Vera, C., G. Silvestri, B. Liebmann, and P. Gonzalez (2006c), Climate change scenarios for seasonal precipitation in South America from IPCC-AR4 models, *Geophys. Res. Lett., 33*, L13707, doi:10.1029/2006GL025759.

Vergara, W, A. Deeb, A. Valencia, R. Bradley, B. Francou, A. Zarzar, A. Grünwaldt, and S. Haeussling (2007), Economic impacts of rapid glacier retreat in the Andes, *Eos Trans., AGU, 88*(25), 19 June 2007.

Vuille, M and C. Ammann (1997), Regional snowfall patterns in the high arid Andes, *Clim. Change 36* (3-4):413-423.

Vuille, M., D. Hardy, C. Braun, F. Keimig, and R. Bradley (1998), Atmospheric circulation anomalies associated with 1996/1997 summer precipitation events on Sajama Ice Cap, Bolivia, *J. Geophys. Res., 103*, 11,191-11,204.

Vuille, M. (1999), Atmospheric circulation over the Bolivian Altiplano during dry and wet periods and extreme phases of the Southern Oscillation, *Int. J. Climatol. 19,* 1579-1600.

Vuille, M., and R. Bradley (2000), Mean annual temperature trends and their vertical structure in the tropical Andes, *Geophys. Res. Lett., 27,* 3885-3888.

Vuille, M., R. Bradley, F. Keimig (2000a), Climate variability in the Andes of Ecuador and its relation to tropical Pacific and Atlantic sea surface temperatures anomalies, *J. Clim., 13*, 2520-2535.

Vuille, M., R. Bradley and F.Keimig (2000b), Interannual climate variability in the Central Andes and its relation to tropical Pacific and Atlantic forcing, *J. Geophys. Res.,105*, 12,447-12,460.

Vuille, M., R. Bradley, M. Werner, and F. Keimig (2003), 20th century climate change in the tropical Andes: observations and model results, *Clim. Change., 59*(1-2): 75-99.

Vuille, M., and M. Werner (2005), Stable isotopes in precipitation recording South American summer monsoon and ENSO variability - observations and model results, *Clim. Dyn., 25*, 401-413, doi:10.1007/s00382-005-0049-9.

Vuille, M. (2007), Climate Change in the tropical Andes -- Impacts and consequences for glaciation and water resources. Part I: The scientific basis. A report for *CONAM* and the *World Bank.* University of Massachusetts, Amhest, MA.USA.

Vuille, M., B. Francou, P. Wagnon, I. Juen, G. Kaser, B.G. Mark and R.S. Bradley, (2008a), Climate change and tropical Andean glaciers – Past, present and future. *Earth Science Review*, in press.

Vuille, M., G. Kaser, and I. Juen (2008b), Glacier mass balance variability in the Cordillera Blanca, Peru and its relationship with climate and the large scale circulation, *Global Planet. Change*, in press.

Vincent, L.A., T.C. Peterson, V.R.Barros, M.B.Marino, M. Rusticucci, G. Carrasco, E. Ramirez, L.M. Alves, T. Ambrizzi, M.A. Berlato, A.M. Grimm, J. Marengo, L. Molion, D.F. Moncunill, E. Rebello, Y. Anunciaciao, J. Quintana, J.L. Santos, J. Baez, G. Coronel, J. Garcia, I. Trebejo, M. Bidegain, M. Haylock, and D. Karoly, (2005), Observed trends in indices of daily temperature extremes in South America, 1960-2000, *J. Clim. 18*, 5011-5023.

Wagnon, P., P. Ribstein, G. Kaser, and P. Berton (1999), Energy balance and runoff seasonality of a Bolivian glacier, *Global Planet. Change 22*, 49-58.

Wagnon, P., P. Ribstein, B. Francou, and J. Sicart (2001), Anomalous heat and mass budget of Glaciar Zongo, Bolivia, during the 1997-98 El Niño year, *J. Glaciol. 47,* 21-28.